

# Noise-induced phenomena of signal transmission in excitable neural models

---

DISSERTATION  
ZUR ERLANGUNG DES AKADEMISCHEN GRADES  
DOKTOR DER NATURWISSENSCHAFTEN (DR. RER. NAT.)  
IN DER WISSENSCHAFTSDISZIPLIN THEORETISCHE PHYSIK

EKKEHARD ULLNER



INSTITUT FÜR PHYSIK  
FAKULTÄT MATHEMATIK UND NATURWISSENSCHAFTEN  
UNIVERSITÄT POTSDAM

Mai 2004



# Inhaltsverzeichnis

<b>1</b>	<b>Introduction</b>	<b>1</b>
1.1	The neural FitzHugh-Nagumo model . . . . .	3
1.2	Effects of noise in neural systems . . . . .	9
1.2.1	Coherence Resonance . . . . .	9
1.2.2	Stochastic Resonance . . . . .	10
1.2.3	Noise-induced transitions . . . . .	12
1.2.4	Theoretical treatment of systems with multiplicative noise . . . . .	14
1.3	Aims, motivation and structure of the thesis . . . . .	16
<b>2</b>	<b>New resonance phenomena in excitable systems</b>	<b>19</b>
2.1	Vibrational resonance and vibrational propagation . . . . .	21
2.1.1	Vibrational resonance in an excitable electronic circuit . . . . .	21
2.1.2	Vibrational resonance in the FitzHugh-Nagumo model . . . . .	24
2.1.3	Resonant vibrational propagation . . . . .	31
2.2	Canard-enhanced Stochastic Resonance . . . . .	34
2.2.1	The model with Canard dynamics . . . . .	36
2.2.2	Enhancement of Stochastic Resonance . . . . .	39
<b>3</b>	<b>Noise-induced signal processing in systems with complex attractors</b>	<b>47</b>
3.1	The model . . . . .	49
3.2	Classic Stochastic Resonance in an isolated FitzHugh-Nagumo model . . . . .	50
3.3	Frequency-dependent Stochastic Resonance in two coupled oscillators . . . . .	52
3.4	Frequency-dependent Stochastic Resonance in a chain of three oscillators . . . . .	54
<b>4</b>	<b>Noise-induced excitability and related effects</b>	<b>61</b>
4.1	Phase transition to excitability generated by multiplicative noise . . . . .	61
4.1.1	The model with noise-induced excitability . . . . .	62
4.1.2	Analytical description of the noise-induced phase transition . . . . .	63

4.1.3	Manifestation of the noise-induced phase transition in the time series . . . . .	64
4.1.4	The bifurcation diagram . . . . .	65
4.1.5	Phase diagrams . . . . .	67
4.1.6	Discussion of the short-time evolution . . . . .	69
4.1.7	Influence of linear coordinate transformation . . . . .	71
4.2	Stochastic Resonance in noise-induced excitable systems . . . . .	73
4.3	Signal propagation in a two-dimensional lattice of local coupled noise-induced excitable FitzHugh-Nagumo models . . . . .	78
<b>5</b>	<b>Conclusions and outlook</b>	<b>85</b>
	<b>Acknowledgements</b>	<b>91</b>
	<b>Bibliography</b>	<b>93</b>

## Appendix

**A Noise-Induced Excitability in Oscillatory Media**

**B Vibrational resonance and vibrational propagation in excitable systems**

**C Oscillatory amplification of stochastic resonance in excitable systems**

**D Frequency-dependent stochastic resonance in inhibitory coupled excitable systems**

## List of abbreviations and notations

CR	Coherence Resonance
FHN	FitzHugh-Nagumo
HF	high-frequency
ISI	interspike interval
ISIH	interspike interval histogram
LF	low-frequency
NIE	noise-induced excitability
NIT	noise-induced transition
SR	Stochastic Resonance
VP	vibrational propagation
VR	vibrational resonance
$A$	amplitude of a periodic signal
$B$	amplitude of a high-frequency periodic signal
$D$	diffusion coefficient, coupling strength
$Q$	linear response measure
$Q_{th}$	linear response measure with respect to a reduced time series without subthreshold dynamic
$T$	period duration
$T_{hf}$	high-frequency signal period
$T_s$	signal period
$a, b, c, d, g$	time-independent parameters
$n$	integer number
$s(t)$	periodic signal
$t_e$	excursion time
$u(t), v(t), x(t), y(t)$	variables
$x_0, y_0$	fixed point coordinates
$y_{nc,x}, y_{nc,y}$	nullclines with respect to the $x$ or $y$ variable
$\langle \cdot \rangle$	average
$\beta, \gamma$	time-independent parameters
$\delta(\cdot)$	Dirac function $\delta(x) = \{1 x = 0; 0 x \neq 0\}$
$\varepsilon$	small parameter
$\zeta_i(t), \xi_i(t)$	Gaussian white noise
$\sigma_a^2$	additive noise intensity
$\sigma_m^2$	multiplicative noise intensity
$\omega$	circle frequency
$\Omega$	high circle frequency
$\Omega_c$	Canard resonance circle frequency
$\Theta(\cdot)$	Heaviside function $\Theta(x) = \{1 x > 0; 0 x \leq 0\}$



# Kurzfassung

Meine Dissertation behandelt verschiedene neue rauschinduzierte Phänomene in anregbaren Neuronenmodellen, insbesondere solche mit FitzHugh-Nagumo Dynamik.

Ich beschreibe das Auftreten von vibronischer Resonanz in anregbaren Systemen. Sowohl in einer anregbaren elektronischen Schaltung als auch im FitzHugh-Nagumo Modell zeige ich, daß eine optimale Amplitude einer hochfrequenten externen Kraft die Signalantwort bezüglich eines niederfrequenten Signals verbessert. Weiterhin wird der Einfluß von additivem Rauschen auf das Zusammenwirken von stochastischer und vibronischer Resonanz untersucht. Dieser Effekt der vibronischen Resonanz kann auf räumlich ausgedehnte anregbare Systeme in Form einer verbesserten Ausbreitung eines niederfrequenten Signals durch eine optimale hochfrequente Kraft erweitert werden. Weiterhin untersuche ich Systeme, die sowohl oszillierende als auch anregbare Eigenschaften beinhalten und dadurch zwei interne Frequenzen aufweisen. Diese Frequenzen zeigen sich zum einen in den Grenzyklen der Standardspikes und zum anderen in denen von Oszillationen mit kleiner Amplitude unterhalb der Anregungsschwelle (Canard-Orbits). Ich zeige, daß in solchen Systemen der Effekt der stochastischen Resonanz deutlich erhöht werden kann, wenn eine zusätzliche hochfrequente Kraft in Resonanz mit den kleinen Oszillationen unterhalb der Anregungsschwelle hinzugenommen wird. Es ist beachtenswert, daß diese Verstärkung der stochastischen Resonanz eine geringere Rauschintensität zum Erreichen des Optimums benötigt als die standartmäßige stochastische Resonanz in anregbaren Systemen.

Ich untersuche Frequenzselektivität bei der rauschinduzierten Signalverarbeitung von Signalen unterhalb der Anregungsschwelle in Systemen mit vielen rauschunterstützten stochastischen Attraktoren. Diese Attraktoren entstehen durch eine Kopplung über die Variable mit der langsamen Dynamik zwischen identischen anregbaren Oszillatoren. Diese Art der Kopplung sorgt für mehrere nebeneinander existierende gemittelte Perioden, die verschieden zu denen eines isolierten Oszillators sind. Diese neuen Attraktoren mit den abweichenden gemittelten Perioden weisen auch unterschiedliche Phasenbeziehungen zwischen den einzelnen Elementen auf. Ich zeige, daß die Signalantwort des gekoppelten Systems unter verschiedenen Rauscheinwirkungen deutlich verbessert oder auch reduziert werden kann durch das Treiben einzelner Elemente in Resonanz mit diesen neuen Resonanzfrequenzen, die mit passenden Phasenbeziehungen korre-

spondieren.

Weiterhin konnte ich einen rauschinduzierten Phasenübergang von einem selbstoszillierenden System zu einem anregbaren System nachweisen. Dieser Übergang erfolgt durch eine rauschinduzierte Stabilisierung eines deterministisch instabilen Fixpunktes der lokalen Dynamik, während die gesamte Phasenraumstruktur des Systems erhalten bleibt. Die räumliche Kopplung ist erforderlich, um Fluktuationen zu unterdrücken (über die Bildung von Klustern, wenn lokale Kopplung vorhanden ist). Dadurch führt die gemeinsame Wirkung von Kopplung und Rauschen zu einem neuen Typ von Phasenübergängen und bewirkt eine Stabilisierung des Systems. Das sich daraus ergebende rauschinduziert anregbare Regime zeigt charakteristische Eigenschaften von klassisch anregbaren Systemen, wie stochastische Resonanz und Wellenausbreitung. Dieser rauschinduzierte Phasenübergang ermöglicht dadurch die Übertragung von Signalen durch ansonsten global oszillierende Systeme und die Kontrolle der Signalübertragung durch Veränderung der Rauschintensität. Insbesondere eröffnen diese theoretischen Ergebnisse einen möglichen Mechanismus zur Unterdrückung unerwünschter globaler Oszillationen in neuronalen Netzwerken, welche charakteristisch für abnorme medizinische Zustände, wie z.B. bei der Parkinson'schen Krankheit oder Epilepsie, sind. Die Wirkung von Rauschen würde dann wieder die Anregbarkeit herstellen, die den normalen Zustand der erkrankten Neuronen darstellt.

# Abstract

My thesis is concerned with several new noise-induced phenomena in excitable neural models, especially those with FitzHugh-Nagumo dynamics. In these effects the fluctuations intrinsically present in any complex neural network play a constructive role and improve functionality.

I report the occurrence of Vibrational Resonance in excitable systems. Both in an excitable electronic circuit and in the FitzHugh-Nagumo model, I show that an optimal amplitude of high-frequency driving enhances the response of an excitable system to a low-frequency signal. Additionally, the influence of additive noise and the interplay between Stochastic and Vibrational Resonance is analyzed. This effect can be extended to spatially extended excitable media, taking the form of an enhanced propagation of the low-frequency signal. Further, I study systems which combine both oscillatory and excitable properties, and hence intrinsically possess two internal frequencies, responsible for standard spiking and for small-amplitude oscillatory limit cycles (Canard-orbits). I show that in such a system the effect of Stochastic Resonance can be amplified by an additional high-frequency signal which is in resonance with the oscillatory frequency. This amplification needs much lower noise intensities than for conventional Stochastic Resonance in excitable systems.

I study frequency selectivity in noise-induced subthreshold signal processing in a system with many noise-supported stochastic attractors which are created due to slow variable diffusion between identical excitable elements. Such inhibitory coupling permits the coexistence of several average periods distinct from that of an isolated oscillator and of several phase-relations between elements. I show that the response of the coupled elements at different noise levels can be significantly enhanced or reduced by forcing some elements into resonance with these new frequencies which correspond to appropriate phase-relations.

A noise-induced phase transition to excitability is reported in oscillatory media with FitzHugh-Nagumo dynamics. This transition takes place via noise-induced stabilization of a deterministically unstable fixed point of the local dynamics, while the overall phase-space structure of the system is maintained. Spatial coupling is required to prevent oscillations through suppression of fluctuations (via clustering in the case of local coupling). Thus, the joint action of coupling and noise leads to a different type of phase transition and results in a stabilization of the system. The resulting noise-induced regime is shown to display properties

characteristic of excitable media, such as Stochastic Resonance and wave propagation. This effect thus allows the transmission of signals through an otherwise globally oscillating medium. In particular, these theoretical findings suggest a possible mechanism for suppressing undesirable global oscillations in neural networks (which are usually characteristic of abnormal medical conditions such as Parkinson's disease or epilepsy), using the action of noise to restore excitability, which is the normal state of neuronal ensembles.

# Chapter 1

## Introduction

Random fluctuations influence our life in nearly every situation, and so noise plays an important role in the understanding and description of nature. Robert Brown observed in 1827 that small pollen grains suspended in water display a very irregular motion which gained fame as the *Brownian Motion* [1]. He could not exclude any specifically organic origin of this motion. It was a long time before Einstein in 1905 and independently in 1906 Smoluchowski published a statistical explanation of the Brownian Motion. They recognized that the motion evoked by frequent impacts on the pollen grain of the permanently moving molecules of the surrounding water is so complicated that its effect on the pollen grain can only be described in a probabilistic way. They abstracted numerous impacts from the water molecules to a stochastic force. The desire to reduce the complexity of a real system embedded in a complex environment is often the origin of a stochastic formulation of a problem which is usually more elegant and practicable. An actual example of a simplifying effect of stochastic models arose in the climate research. The description of ocean and atmosphere dynamics needs thousands of deterministic equations, whereas including noise can reduce the number of equations. The possible reason for the Permian extinction has been discussed and explained in Ref. [2] with help of the stochastically driven escape of a potential well.

There exist different sources of noise in real systems [3–5]. In chemical reactions noise results from temperature fluctuations and finite-size effects, in lasers quantum fluctuations are the dominant random effect, while in climate models the numerous impacts from annual and other cycles might be looked upon as rapid fluctuations on the long time scale, e.g. ice ages. In neurons, the stochasticity originates from different sources. The random synaptic input from other neurons is the most important one, but a random switching of ion channels and the quasi-random release of neurotransmitter by the synapses also contribute to the stochasticity in neurons.

From everyday experience most people know noise only as a nuisance. Random fluctuations cause disorder or hinder the transmission of information. Nor-

mally, one tries to reduce the influence of noise on experiments, e.g. by cooling or by filtering the random fluctuations or by averaging over many repetitions of the experiment. In contrast to the usual role of noise as a nuisance, under certain conditions noise can also play a constructive (“ordering”) role in nonlinear systems far from equilibrium. The growing interest in such noise-induced effects originates from the increasing number of noise-induced phenomena discovered in natural systems.

An instructive example of a noise-induced enhancement of signal processing concerns the sensory nervous system of a paddlefish [6]. The paddlefish is able to detect the electrical signals of the muscle activity of its planktonic prey *daphnia* and feeds itself by capturing *daphnia*. In a laboratory experiment the paddlefish was swimming in an aquarium and the number of captured *daphnia* per time unit was counted. Additionally two electrodes were put in the aquarium to supply electrical noise which mimics the environmental noise in a natural habitat. At a certain finite electrical noise intensity the paddlefish caught a maximum number of planktonic prey. Hence, the noise helps the paddlefish to detect the position of the planktonic prey. This influence of noise on the sensory nervous system of a paddlefish is manifestation of the stochastic behavioral resonance effect in a natural biological system.

The effect of noise in brain activity evokes special interest. Despite (or maybe because of) the many noise sources in such a neural network, the brain acts very reliably and needs only a very small amount of energy (about 12 W according to Ref. [7]). A growing number of scientific results suggests that noise plays a constructive role in brain activity. For instance, a noise-induced effect has been demonstrated in the visual processing area of the human brain [8]. In this experiment a periodic light signal was sent to one eye, whereas the other eye was subjected by noise, represented by light with fluctuating intensity. The result was that the noise improved the processing of the periodic signal sent to the first eye.

Next I describe the modeling of neural activity with a simple reaction-diffusion model.

## 1.1 The neural FitzHugh-Nagumo model

Excitable systems attract large interests and can be found in many natural systems and realistic models, for instance, in laser systems, neural networks, chemical reactions and climate dynamics, to mention only the most important fields of research [9–19]. All excitable media have in common a threshold of excitation and the three states: a “rest” state, an “excited” (or “firing”) state and a “recovery” (or “refractory”) state. The rest state can be simply an equilibrium (or fixed) point or a small-amplitude subthreshold limit cycle. Small perturbations below the threshold of excitation result in small-amplitude linear response near the rest state [Fig. 1.1(a)]. Sufficient large perturbations beyond the threshold enable the system to leave the rest state, going through the firing and recovery state before it reenters the rest state again [Fig. 1.1(b)]. The strongly nonlinear behavior results in a large difference in the response to small changes in the input and is accomplished by a large excursion through the phase space, the so-called spike. A larger input impulse does not change the dynamics and the response significantly [Fig. 1.1(c)]. The system is very refractory during a spike and does not respond upon further perturbations, which means that it takes a certain recovery time before another excitation can initiate a second spike [Fig. 1.1(d) and (e)].

Excitable media, a typical example of nonlinear systems far from equilibrium, implies a reset mechanism, i.e. a continuous energy supply and a feedback loop. Such a non-equilibrium state can be realized e.g. by external pumping in a laser system, by a permanent matter flow in chemical reactions or by ion pumping across a cell membrane in neurons which leads to a potential difference across them.

Hodgkin and Huxley [20] have shown that these excitable properties can be modeled by a four-dimensional nonlinear differential equation. Later it was demonstrated by FitzHugh [21] and others that two nonlinear differential equations suffice for a qualitative study and understanding of excitability. They suggested the FitzHugh-Nagumo (FHN) model which is at the center of interest in this work. Excitability can be also observed in even simpler models, e.g. one-dimensional systems with a reset rule like integrate-and-fire models or phase models. Such models are used to study specific aspects of excitability. Behavior is made more complicated and richer by coupling of many excitable systems. Depending on the strength and the type of coupling very different spatiotemporal phenomena can be observed, e.g. pulse and spiral propagation, periodic pattern in space and/or time, scroll waves, localized spots, and spatiotemporal chaos.

Since the focus of this work is the FHN neural model, I give a rough sketch of the rather complicated neural dynamics. Detailed explanation of neural models are given for instance in Refs. [22–24]. A typical neuron consists of three parts: the soma or cell body, the dendrites and the axons, which are both extending branches of the soma. A key feature is the difference in the electrical potential

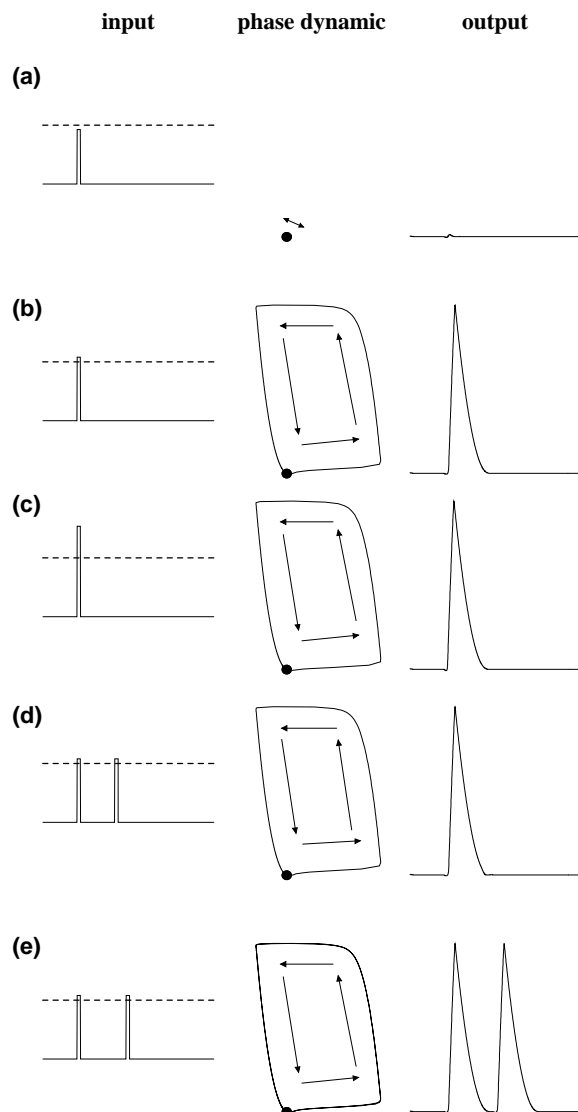


Figure 1.1: Features of excitable systems which may be found in the FitzHugh-Nagumo model. The left column depicts the different signals, which cause very different results in the dynamics in the phase space (middle column) and in the output (right column). The stable state is represented by the full circle in the middle plots. (a) An input below the threshold (dashed line) leads to a small motion around the stable state; (b) an input beyond the threshold initiates an escape from the rest state and leads to a large-amplitude excursion of the system's variables (spike); (c) further increase of the input amplitude does not influence the form of the spike significantly; (d) the system is insensitive during a spike, i.e. a second perturbation in the refractory time does not evoke a second spike; (e) but after this time, the system is accessible again and a second signal leads to a second spike.

in the different parts of the neuron and in the surroundings, which leads to a voltage across the nerve membrane. The nerve membrane is a lipid bilayer and is almost a barrier for ions and acts consequently as a capacitor. The gates in the membrane (ion pumps and ion channels) control the ion flow across them and hence support or change the voltage. Input from other neurons (in the order of  $10^4$ ) enters the neuron across the synapses located on the branches of the dendritic tree in the form of miniature current pulses. Depending on the nature of the synapse (excitatory or inhibitory), the current pulse is either positive or negative. These are summed across the tree, yielding a net input current which induces variations of the potential difference across the cell membrane in the soma hillock (spike initiating zone). If this potential reaches a threshold, a sharp voltage pulse (an action potential or spike) is generated in the axon. Once a spike sets in, the shape of it does not depend on the details of the stimulation. The neuron demonstrates an all-or-nothing behavior response to current stimulation. The spike-generation of neurons includes all the above-mentioned properties of excitable media. This spike rapidly propagates along the axon to send a signal to other neurons [25].

The first model of neurons was suggested by Hodgkin and Huxley [21] to describe the spike-generation in the giant axon of squids. It predicts the voltage-dependent conductances influenced by two sorts of ion channels selective for sodium and potassium, respectively. The FitzHugh-Nagumo (FHN) model was proposed in Ref. [21, 26] as a simplification of the famous model by Hodgkin and Huxley [21] and is a simple example of two-dimensional excitable dynamics. It describes qualitatively rather than quantitatively the response of an excitable nerve membrane to external stimuli. Important features are the inclusion of a refractory mechanism and the existence of different refractory states, as well as states of enhanced and depressed excitability depending on the external stimulation.

A general form of the FHN model is given by

$$\varepsilon \frac{dx}{dt} = f(x) - y, \quad (1.1)$$

$$\frac{dy}{dt} = \gamma x - \beta y + a + s(t) + \xi(t), \quad (1.2)$$

where  $x(t)$  is the activator variable (representing the membrane potential in the neural case) and  $y(t)$  is the inhibitor variable (related to the conductivity of the potassium channels existing in the neuron membrane [18]). Here  $s(t)$  is a periodic signal and  $\xi(t)$  is a Gaussian white noise with zero mean and correlation  $\langle \xi(t)\xi(t') \rangle = \sigma_a^2 \delta(t-t')$ . In neural models, the time-scale factor  $\varepsilon$  is much smaller than one ( $\varepsilon \approx 0.01$ ) and implies that  $x(t)$  is the fast and  $y(t)$  is the slow variable. The nonlinear function  $f(x)$  is one of the nullclines (curves with  $\dot{x} = 0$ ,  $\dot{y} = 0$  respectively) of the deterministic system and a common choice of this function is

$$f(x) = x - \frac{x^3}{3}. \quad (1.3)$$

The deterministic FHN model exhibits excitable behavior when the activator nullcline (i.e.  $\dot{x} = 0$ )  $y_{nc,x} = f(x)$  intersects only once with the linear nullcline of the inhibitor variable (i.e.  $\dot{y} = 0$ )  $y_{nc,y} = \frac{\gamma}{\beta}x + \frac{a}{\beta}$  and the intersection point is a stable fixed point (resting state) on the left branch of the cubic nullcline. For the sake of reduction of the parameters, I chose  $\beta = 0.0$  and  $\gamma = 1.0$ , i.e. I consider a perpendicular inhibitor nullcline in the  $x$ - $y$  phase plane [Fig. 1.2]. The intersection point between the two nullclines (a fixed point) reads then  $x_0 = -a$ ,  $y_0 = \frac{a^3}{3} - a$ . The transition between excitable and oscillatory regimes occurs by changing  $a$  via a supercritical Hopf bifurcation. An excitable behavior can be found for  $|a| > 1$ , because the fixed point  $(x_0, y_0)$  is stable. For  $|a| < 1$  the fixed point becomes unstable and hence a self-oscillating behavior appears. I note that for  $\beta \neq 0.0$  even a bistable regime can be created. However, I shall not extend the discussion about the bifurcation analysis because it is not necessary for the following investigations. For detail see e.g. Refs. [21, 27].

In the excitable regime, sufficiently strong perturbations (i.e. beyond the excitation threshold), either in  $x$  or  $y$ , lead to a far-reaching excursion in the phase plane [Fig. 1.2]. At first a fast motion in the  $x$ -direction to the right branch of the cubic nullcline takes place followed by a slow motion along this right branch until the local maximum is reached (“firing” of a neuron). Then a fast motion in the negative  $x$ -direction appears back to the left branch subsequently followed by a slow one along the left branch (“refractory state”) to the rest state. The single spike in the deterministic FHN [Fig. 1.2 (left column)] is initiated by a suitable initial condition, caused, for instance, by an external stimulus. If sufficiently strong noise ( $\sigma_a^2 > 0$ ) is present, the excitation process occurs permanently when the system reaches the rest state after firing a spike and passing the refractory state [Fig. 1.2 (right column)]. The sequence of action potentials (time series of activator variable  $x$ ) resembles the spontaneous activity of a neuron.

When an additive signal ( $s(t) = A \cos(\omega t)$ ) is present, the evoked spikes will be correlated with this signal. For weak subthreshold signals, noise is absolutely necessary to stimulate spikes and an optimal noise intensity maximizes the correlation between the signal and the response, the manifestation of Stochastic Resonance (SR) in the neural FHN model (see chapter 1.2.2).

Some approximations and limitations are needed for the motivation of a pure additive signal ( $I(t) = s(t) + \xi(t)$ ) in Eq. (1.2) for a neuron. The input signal of a neuron is a summation of the stimuli (spikes) from all synaptic connections. The following assumptions are needed:

- The input is nearly balanced between excitatory and inhibitory current, i.e. the mean value of the total current  $\langle I(t) \rangle$  is small with respect to the excitation threshold.
- The spikes from different synapses are statistically independent.

The first assumption can be realized by a suitable ratio of numbers and/or ampli-

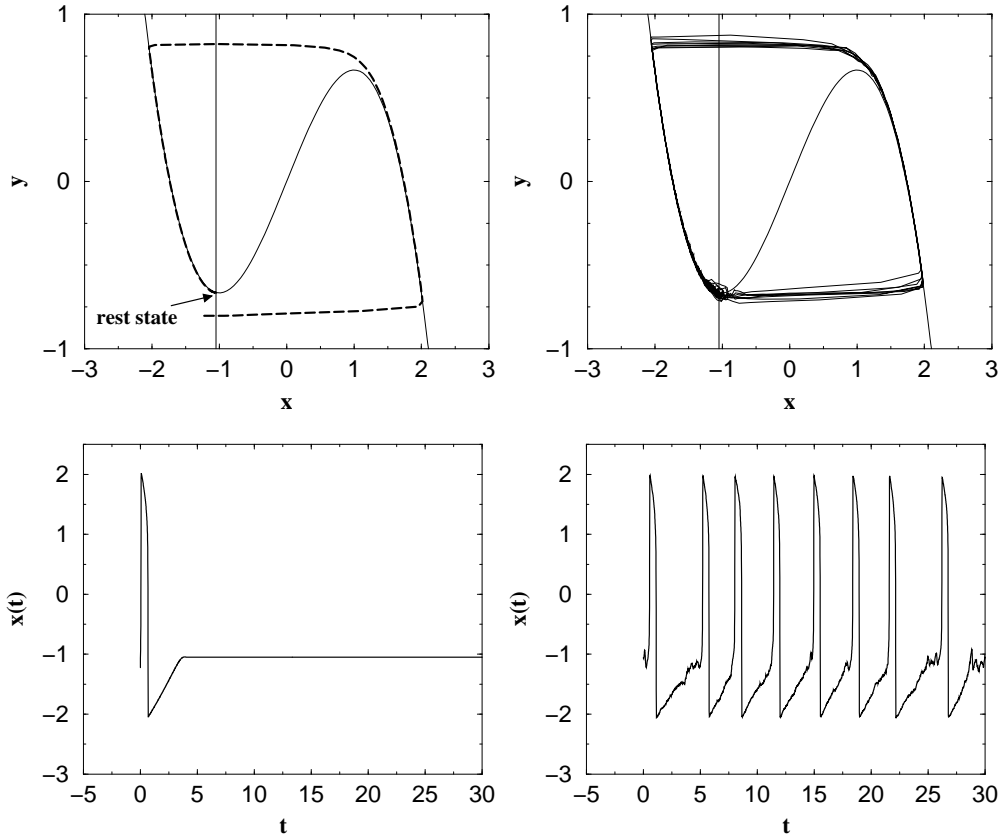


Figure 1.2: Dynamics of the FHN model in the phase plane with the nullclines (top row) and the corresponding time series of the activator variable (bottom row) according to Eqs. (1.1), (1.2) and (1.3) with parameters  $\varepsilon = 0.01$ ,  $a = 1.05$ ,  $\beta = 0.0$ ,  $\gamma = 1.0$ . The cubic line illustrates the activator nullcline and the perpendicular straight line the inhibitory one in the phase plane. The left column depicts a spike in the deterministic FHN evoked by an appropriate initial condition. Right: a stochastic realization for  $\sigma_a^2 = 0.01$  and  $s(t) = 0$ .

tudes of the two spike types (excitatory/inhibitory) [28]. The second one is only an approximation [29]. A subgroup of input neurons may generate a signal by a common time-dependent spike rate. We consider an input current consisting of a summation of spike trains with a periodically modulated rate. Due to the high number of neurons the resulting input signal is a rather continuous random process with periodically modulated variance. This is an example for a noise-encoded signal. There is no reason to expect that the number of activator and inhibitor input neurons are balanced. In this case the resulting input current is a random process with both signal-dependent mean and variance, hence an additive signal appears in addition to the noise-encoded signal. Beside the input subgroup many other neurons stimulate the neuron under consideration and per-

form a massive input from the neural background [24]. That is the contribution of incoherently firing neurons, which are functionally far from the input subgroup and from each other. Their firing rate can be assumed as temporally constant. A pure additive signal can be achieved if only excitatory (or inhibitory) neurons with time-dependent rates are present in the input area and a large number of excitatory and inhibitory neurons with constant rate compose the background contribution. The second group cares for the balance between the two types of stimuli, as in the first assumption above. Under these conditions we obtain a total input current that is a noise with constant intensity but time-dependent mean value. Only in this situation can one separate noise and signal. Such a resulting input is similar to that assumed for receptor neurons. For a more detailed explanation see e.g. Refs. [24, 30].

In the next section I outline the most relevant noise-induced effects.

## 1.2 Effects of noise in neural systems

Here I review two noise-induced effects in which noise plays the constructive role and increases the level of ordering or synchrony in the system and the noise-induced phase transition in which noise leads to a qualitative changing of the system properties.

### 1.2.1 Coherence Resonance

*Coherence Resonance* (CR) is a noise-induced effect and describes the occurrence and optimization of periodic oscillatory behavior due to noise perturbations [Fig. 1.3]. It has been found that at a certain noise intensity the system responds with a maximal periodicity, i.e. with an enhanced coherence in the output. Both an increase and a decrease of the noise amplitude away from this optimal value lead to a decreasing of the coherence. CR has been observed in excitable systems like the Hodgkin-Huxley model [31], the FitzHugh-Nagumo systems [32], leaky integrate-and-fire models [33], the Plant/Hindmarsh-Rose neural model [34], and in dynamic systems which besides show jumps between several attractors [35]. Besides the neural context, CR can be found in climate [17] and laser models [36, 37].

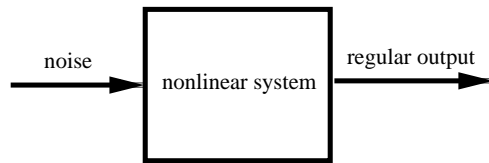


Figure 1.3: Coherence Resonance principle: proper noise intensity optimizes the periodicity of the system output.

Although CR is not in the center of this work, a sketch of the CR in excitable systems helps to understand the generation of the eigenfrequency in the variations of the Stochastic Resonance effects considered here. The CR effect requires an internal time-scale which is provided by excitable systems with the excursion time  $t_e$  (firing plus recovery time), i.e. the time which is needed by the system for a full round trip (spike) from the leaving of the rest state to the reentering of it (see chapter 1.1). Additionally, the CR is determined by the activation time  $t_a$  as the second time-scale. This is the time needed for the escape from the rest state. The statistics of these two times are quite different: while the activation time depicts a strong dependence on the noise intensity and approximately obeys Poissonian statistics, the excursion time corresponds to the decay times of the unstable states (firing and recovery state) and hence it depends much less on the noise intensity than the activation time. The activation and excursion time results in the interspike interval  $T$ . For increasing noise intensity the activation

time decreases rapidly to almost zero, hence the interspike interval is determined by the excursion time which is approximately noise independent for small and intermediate noise intensity. For this optimal noise intensity the system responds with a very regular (coherent) spiking behavior. A well-pronounced peak in the spectrum appears. Further increasing the noise intensity leads to a random variation of the excursion time and the interspike intervals become more random and the coherence decreases again. In summary, the CR effect rests upon the competition between the excursion time with a weak noise dependency and the strong noise-dependent activation time, which in the optimal coherent regime is just negligibly small. Detailed discussions of CR can be found e.g. in Refs. [19, 32].

With the help of this sketch of the mechanism and features of CR, I describe in the next section the manifestation of the Stochastic Resonance effect in excitable systems.

## 1.2.2 Stochastic Resonance

*Stochastic Resonance* (SR) is probably the most famous and established effect among noise-induced phenomena. SR describes the improved synchronization of the system output with the input due to an intermediate and optimal noise intensity [Fig. 1.4].

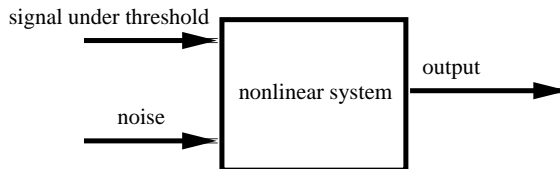


Figure 1.4: Stochastic Resonance principle: proper noise intensity optimizes the signal transmission.

This noise-induced effect can be easily illustrated by the example of the excitable system and will be discussed with the help of the FHN model according to Eqs. (1.1), (1.2) and (1.3) in chapter 1.1 with the parameters noted there. If the periodic signal  $s(t) = A \cos(\omega t)$  is strong, the response will follow this forcing, i.e. the spikes evoked will be correlated to the signal phase. This can be easily understood in the FHN model for very slow driving (adiabatic case), where the signal acts effectively as a static modulation of the inhibitor  $y$  nullcline. A negative signal ( $s(t) < 0$ ) shifts the  $y$  nullcline (perpendicular straight line top left in Fig. 1.2) to the right-hand side in the phase space so that the fixed point is in the middle unstable branch of  $f(x)$  (the middle part of the cubic  $x$  nullcline). In this case, the system responds with an oscillatory behavior (limit cycle). Hence, it fires sustainedly even in the absence of noise. During the opposite half period of

the signal, the signal will be positive and the  $y$  nullcline is shifted in the opposite direction. Consequently, the system will be even less excitable (i.e. includes a higher threshold) than in the absence of a signal. As a result no spikes appear in the output. The whole response contains spike trains modulated with the signal frequency  $\omega$ .

The presence of noise leads to a random location of the spikes, but the probability of a firing depends on the signal. In contrast, small-amplitude signals (below the threshold of excitation) cannot stimulate spikes by themselves, but only small oscillations around the resting state so that they change the threshold of excitation. With the help of noise, spikes may nevertheless be generated and will be correlated to the weak signal. The signal effectively modulates the threshold. At a *finite* noise intensity the noise is sufficiently strong to evoke regular spikes during the negative signal (reduced threshold compared to the absence of a signal), as in the optimal CR case, and weak enough not to stimulate reliable spikes in the opposite positive signal phase (enhanced threshold), as in the sub-optimal CR case with a lack of noise. Both an increase and a decrease of the noise intensity from the optimal noise amplitude lead to a reduced synchronization of the system output with the input. This is the basics of SR in excitable systems as it is well known from the literature [38, 39]. An example of the SR in the FHN model can be seen in Fig. 3.1 in chapter 3.2.

The SR behavior becomes evident in the power spectrum of the output, which consists of a noisy background spectrum and an additional peak at the driving frequency and its higher harmonics. Possible quantifications of SR are the weight of the peak itself as well as the signal-to-noise ratio to the background spectrum. Both measurements pass through a maximum as a function of noise intensity by appearing of SR. The amplitude of the signal frequency in the output can be measured also in a noise-free situation, which allows a comparison with the deterministic case and is the preferential measure of SR in this thesis. This measure is defined in the following as the linear-response parameter  $Q$  (see Refs. [39, 40] and Eqs. (2.3)-(2.5)).

Scientific interest in SR is evoked by its wide occurrence in many research fields. SR has been found among other phenomena in monostable [41], excitable [19, 38], non-dynamic [42] and non-potential [43] systems. There exist many examples of SR in realistic models and different experimental set-ups. In particular, one should mention SR in an ice-age model [44], where the notation SR was introduced. SR has also been found in ring lasers [45], in systems with electronic paramagnetic resonance [46], in tunnel diodes [47], in experiments with Brownian particles [48], in chemical systems [49, 50], in visual perception [51, 52], in the food detection system of paddlefish [6] and in human cognition [53].

Next I review noise-induced transitions, which lead to a qualitative changing of system-immanent properties.

### 1.2.3 Noise-induced transitions

In such noise-induced effects as CR (chapter 1.2.1) or SR (chapter 1.2.2) noise does not change the system qualitatively. In contrast, *Noise-induced Transition* (NIT) describes the modification of the system's immanent features due to noise, i.e. changing the noise intensity leads to a new state, which is qualitatively different to the previous one. This transition can be described by an appropriate order parameter. One can regard NIT in non-equilibrium systems as a generalization of phase transitions in equilibrium systems. Following the analogy between the equilibrium phase transition and the non-equilibrium NIT, the noise plays the role of the temperature and the order parameter describes the phase of the system [54]. NIT in spatially extended systems can be considered as noise-induced phase transitions in analogy to equilibrium phase transitions in the thermodynamics. Some possible classification of NITs can be given as follows:

1. NITs in zero-dimensional systems
  - (a) NITs which lead to the appearance of additional extrema (maxima or minima) in the system's probability distribution
  - (b) NITs which lead to the parametric excitation of oscillations
2. NITs in spatially extended systems, or *bona-fide phase transitions*
  - (a) NITs in spatially extended systems which lead to the appearance or the disappearance of new stable states
  - (b) NITs in spatially extended systems which lead to the appearance or the disappearance of new behavior regimes.

This classification of NITs does not claim to be final, because NITs are an ongoing topic and I expect further discoveries of new transitions. Nevertheless, the suggested classification, as an enlargement of the one in Ref. [55], should help the interested reader to recognize the differences and common features in the wide field of NITs.

The first class of NITs (1a) occurs in zero-dimensional systems with multiplicative noise and describes the appearance of additional extrema (maxima) in the system probability distribution (see the book [2]) or the disappearance of old ones [56]. This NIT is based on the effect, that multiplicative noise changes the "stochastic" potential, which effectively determines the behavior of the system. In this case, the location of the extrema in the system probability distribution can be used as the order parameter. Such a transition type has been observed, for instance, in biological models describing the dynamics of population growth, in the genetic model used for theoretical and experimental study of genotype dynamics in a fluctuational environment [2, 57], in chemical reactions [2], and in an electrical parametric oscillator [58].

The second kind of NIT (1b, excitation of oscillations, for review see Ref. [59]) can be found in oscillatory systems. In this situation, the average of the instantaneous amplitude of oscillations or the average of its square is a proper order parameter. There exists a critical noise value. Above it, oscillations are excited, whereas below it, no oscillations appear. The parametric excitation of oscillations due to multiplicative noise is the reason of these NITs and the multiplicative noise changes the frequency randomly. This type of NIT can be found e.g. in a pendulum with randomly vibrated axis [60] and in nonlinear models to describe the dynamics of childhood epidemics [61].

All *bona-fide phase transitions* (class 2a and 2b) are based on an averaged influence of multiplicative noise and the stabilizing effect of coupling. A simple explanation could be to “heat” a previously stable deterministic state, whereas other regions in the state space are “cooled”. The noise strength has to be large enough to exceed the deterministic restoring force and to enhance nonlinear behavior. In zero-dimensional systems, the noise-induced transition cannot be observed clearly, because the new state is a compromise between the deterministic restoring force and the selective heating / cooling due to the multiplicative noise being overwhelmed by the randomness of noisy motion. The necessary coupling provides for a suppression of large fluctuations.

The third kind of NIT (2a) describes transitions in spatially extended systems which lead to qualitative changes in the stable states (for review see Ref. [62]). In particular, NIT leads to bistability in the mean field in a deterministic monostable system and evokes a doubling and shifting of the stable state. Afterwards, due to the coupling, the elements in the spatially extended systems tend either to the left or to the right well of the bistable mean field potential, and then the symmetry and ergodicity are broken compared to the deterministic monostable system. In this case the order parameter, which determines the phase of a system, is the mean field. Such NITs have been found in biological systems with diffusion [63], in generic models [64–67], or in particular Ginzburg-Landau equations. The additional memory of colored noise is critical for these transitions [68–70] and leads to a growing disorder in the system by increased correlation.

The last class of NIT which leads to qualitative changes in the behavior regime (2b) results on the one hand in a qualitative jump in the oscillation amplitude from a nonzero value to zero (in practice close to zero due to random fluctuations) or vice versa. On the other hand this NIT induces a qualitative change in the recurrence mechanism to a stable state. In this case the response of the system can be given in terms of an averaged trend, expressed by the small-noise-expansion [1, 62]. Such kind of phase transition has been found in models of neural networks for a transition from an excitable to an oscillatory behavior [71, 72], from a bistable to an excitable dynamics [73, 74] and conversely from an excitable to bistable dynamics [19]. The phase transition from an oscillatory state to an excitable regime (see chapter 4.1 and [75]) discussed in this work, belongs also to this class

of NIT. The choice of a proper order parameter depends on the NIT considered. For instance, the NIT from an excitable to a bistable regime can be described by the size and the statistics of coherent space-time clusters [19] which represent the excited or quiescent cells in a three-dimensional space formed by the two spatial dimensions and the temporal axis. The relative resting time has turned out to be a proper order parameter for the NIT from the self-sustained oscillatory regime to the noise-induced excitable dynamics [75] and measures the time which oscillators spend in the vicinity of the noise-induced stable fixed point related to the whole measuring time.

The introduction proceeds with a sketch of the theoretical treatment of systems with multiplicative noise.

### 1.2.4 Theoretical treatment of systems with multiplicative noise

In this chapter I review the small-noise-expansion which I use in chapter 4.1 to evaluate the systematic contribution of the multiplicative noise, i.e. we separate the systematic contribution from the stochastic one. For a deeper review see e.g. books [1, 62]. The explanation and notations follow the one in book [62] and have a general character.

We consider the following one-dimensional reaction-diffusion equation for field  $\phi(x, t)$ :

$$\frac{\partial \phi}{\partial t} = \frac{\partial^2 \phi}{\partial x^2} + f(\phi) + \varepsilon^{1/2} g(\phi) \eta(x, t), \quad (1.4)$$

where parameter  $\varepsilon$  measures the strengths of the noise explicitly. We assume that  $\eta(x, t)$  is a Gaussian white noise with zero mean and correlation given by

$$\langle \eta(x, t) \eta(x', t') \rangle = 2C \left( \frac{|x - x'|}{\lambda} \right) \delta(t - t'). \quad (1.5)$$

The parameter  $\lambda$  is the characteristic length of the spatial correlation of the noise. It is well known that in zero-dimensional systems (i.e., systems with no spatial dependence), multiplicative noise induces new phenomena, which cannot be observed in the presence of additive noise [2]. The difference results from the systematic contribution coming from the multiplicative noise coupling. The key point of this approach is the fact that the noisy term in Eq. (1.4) has a non-vanishing mean when the coupling function  $g(\phi)$  is not a constant. The mean value of the noisy term can be evaluated with help of the spatially extended version of Novikov's theorem [62]:

$$\langle g(\phi) \eta(x, t) \rangle = \int_0^t dt' \int dx \langle \eta(x, t) \eta(x', t') \rangle \left\langle \frac{\delta g(\phi(x, t))}{\delta \eta(x', t')} \right\rangle. \quad (1.6)$$

By inserting the correlation function Eq. (1.5) in Eq. (1.6) and conducting the time integration one achieves:

$$\langle g(\phi)\eta(x,t) \rangle = \int dx C(x,x') \left\langle g'(\phi(x,t)) \frac{\delta\phi(x,t)}{\delta\eta(x',t')} \Big|_{t'=t} \right\rangle. \quad (1.7)$$

Formal time integration of  $\phi(x,t)$  in Eq. (1.4) and afterwards derivation with respect to  $\eta(x',t')$  allows the evaluation of the response function,

$$\frac{\delta\phi(x,t)}{\delta\eta(x',t')} \Big|_{t'=t} = \varepsilon^{1/2} C(0) g(\phi(x,t)) \delta(x-x'). \quad (1.8)$$

By inserting Eq. (1.8) in Eq. (1.7) and integration one obtains

$$\langle g(\phi)\eta(x,t) \rangle = \varepsilon^{1/2} C(0) \langle g(\phi)g'(\phi) \rangle. \quad (1.9)$$

According to this result, Eq. (1.4) can be rewritten then with a noise-free systematic part and a mean-free stochastic contribution,

$$\frac{\partial\phi}{\partial t} = \frac{\partial^2\phi}{\partial x^2} + h(\phi) + \varepsilon^{1/2}\xi(\phi,x,t), \quad (1.10)$$

with a new systematic reaction term

$$h(\phi) = f(\phi) + \varepsilon C(0)g'(\phi)g(\phi), \quad (1.11)$$

and a new noise term  $\xi(\phi,x,t)$  of zero mean

$$\xi(\phi,x,t) = g(\phi)\eta(x,t) - \varepsilon^{1/2}C(0)g'(\phi)g(\phi). \quad (1.12)$$

Now I go back to my special situation of Gaussian white noise with zero mean and  $\delta$ -correlation in space and time,

$$\langle \eta(x,t)\eta(x',t') \rangle = \sigma_m^2 \delta(t-t') \delta(x-x'). \quad (1.13)$$

Then Eq. (1.11) reads,

$$h(\phi) = f(\phi) + \frac{1}{2}\sigma_m^2 g'(\phi)g(\phi), \quad (1.14)$$

where  $\sigma_m^2$  represents the multiplicative noise intensity.

Next I complete the introduction with the motivation, the aims and the sketched structure of my thesis.

### 1.3 Aims, motivation and structure of the thesis

The past several decades have been marked by intensive investigations of noise-induced phenomena in excitable neural models. These studies have included both experiments in vivo [6] as well as extensive numerical simulations and theoretical approximations [19]. However, despite these investigations main questions have remained unclear; I will discuss in this dissertation a few of them.

The response of an excitable system to a bichromatic periodic signal with two very different frequencies and the influence of additive noise upon this system set up has not been investigated. Such bichromatic signals are pervasive in different fields, e.g. in brain dynamics [76], where for instance bursting neurons may exhibit two widely different time-scales, in telecommunications [77], where information carriers are usually high-frequency waves modulated by a low-frequency signal that encodes the data, in laser physics [78], and in neuroscience [79]. The beneficial role of high-frequency (ultrasonic) driving has already been reported as increased drug uptake by brain cells [80], acceleration of bone and muscle repair [81], and resonantly enhanced biodegradation of micro-organisms [82]. Additionally, ultrasonic irradiation of two widely different frequencies has been seen to enhance cavitation yield [83]. The response of a bistable potential system to a bichromatic periodic signal has been investigated in Ref. [40] and denoted the enhancement of the signal processing at a low frequency by an additional high-frequency signal as vibrational resonance. Nevertheless, it was unclear whether such an enhancement can be observed also in excitable systems. The influence of noise and the interplay of noise and high-frequency signal upon the signal processing at the desired low frequency were interesting open problems. In this field, the question arose whether noise can replace the high frequency and vice versa. This topic becomes more complicated when the excitable system offers a second subthreshold eigenfrequency.

Typically, studies of SR do not demonstrate a sensitive dependence on the frequency of the forcing. The role of the signal frequency for excitable systems has been studied in [84–89] for isolated FHN, when the characteristic time of the system, defined by an external period providing the maximal level of synchronization, practically coincides with the excursion time of an excitable element, and this time is the single natural reference point for time scale. Such a form of frequency selectivity can also be important for biological membranes in enzymatic systems [90]. In other studies the frequency sensitivity in weak signal processing results from a resonance between small oscillations around a steady state and a signal [91–94]. Hence, despite different excitation mechanisms, the oscillation frequency is defined by the parameters of isolated elements. On the other hand, it has been shown that the dominance of inhibitory coupling between identical oscillators results in the generation of many stable limit cycles with different periods and phase relations [95, 96]. This form of coupling between oscillators may provide a broad spectrum of additional frequencies in the system’s behavior. Os-

cillatory media with inhibitory coupling have very rich dynamics and have been reported to be important in numerous physical [97], electronic [98], and chemical systems [99, 100]. The influence of this new resonance frequency evoked by different phase relations between the inhibitor-coupled oscillators on the Stochastic Resonance and the frequency-selective information transmission has not yet been considered.

It was not clear whether noise can suppress oscillations and induce excitable properties, i.e. whether a noise-induced phase transition from a self-sustained oscillatory state to an excitable regime exists. In contrast to standard phase transitions and other studies on excitable systems [71–74, 101], in this noise-induced phase transition the increase of noise enhances the stability in the system and restores excitable properties instead of further randomizing the dynamics or oscillation excitation. The interplay between excitable and oscillatory dynamics in noisy systems is an important current issue [102]. In particular, such a noise-induced phase transition could be a possible mechanism to suppress undesirable global oscillations in neural networks, which are usually characteristic of abnormal medical conditions such as Parkinson’s disease or epilepsy. Then the action of noise is used to restore excitability, which is the normal state of neural ensembles.

The need to study these unresolved problems and to shed light on the constructive role of stochasticity in information exchange between neural clusters has motivated the present research and contributed to the aim of this work. It is to investigate new nonlinear phenomena in complex noisy neural systems which may result in changing dynamical regimes or in the appearance of excitability itself. Following this aim, I study the following problems:

1. I investigate new resonance phenomena in excitable systems. I consider the influence of a bichromatic signal consisting of a low-frequency component (that contains the information) and a high-frequency component and compare it with the Stochastic Resonance effect. I demonstrate the vibrational resonance effect in excitable systems. I extend the vibrational resonance to spatially distributed systems as the vibrational propagation. Further on, I investigate the interplay between a high-frequency driving force, a subthreshold eigenfrequency and the system response at a different signal frequency.
2. I study the Stochastic Resonance effect in inhibitor-coupled FitzHugh-Nagumo models consisting of two or three coupled excitable oscillators. Especially, I consider the frequency selectivity due to the different phase relation between the elements. I investigate whether the information can be transmitted through the region with hidden or suppressed oscillations.
3. Finally, I suggest a new noise-induced phase transition from a self-sustained oscillatory state to an excitable regime. I explain the noise-induced ex-

citability analytically with the help of the small-noise-expansion and investigate numerically the conditions of this transition. I demonstrate the Stochastic Resonance effect in the new noise-induced excitable system as a doubly stochastic effect. In this effect both multiplicative and additive noise have to be optimized independently to maximize the system response at a signal frequency. The noise-induced excitability can be used for reliable information transmission. To demonstrate this I study a wave front propagation and a spiral formation in a two-dimensional lattice of noise-induced locally-coupled excitable systems.

The work is structured as follows: In chapter 2 I present new resonance phenomena in excitable systems. Then I discuss in chapter 3 the frequency selective Stochastic Resonance effect in chains of inhibitor-coupled excitable FitzHugh-Nagumo models. After that, I investigate in chapter 4 a new noise-induced phase transition from a self-sustained oscillatory state to an excitable regime and demonstrate the doubly Stochastic Resonance (chapter 4.2) and a reliable information transmission (chapter 4.3). Finally in chapter 5 I summarize the results and discuss the outlook of the present research. The thesis ends with acknowledgements, bibliography and an appendix.

## Chapter 2

# New resonance phenomena in excitable systems

Signal detection by nonlinear systems can be considerably affected by external influences. The most relevant example of this fact is Stochastic Resonance (SR), where the response of a nonlinear system to a weak deterministic signal is enhanced by external random fluctuations [39] (see also chapter 1.2.2 and Fig. 1.4). Initially reported in bistable systems [44], SR has been found in many models and even natural systems [45, 103], including excitable media [38].

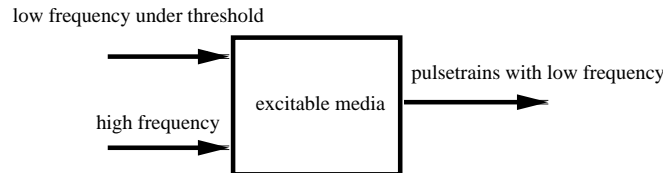


Figure 2.1: Vibrational resonance principle: high-frequency vibrations optimize the signal transmission at a low-frequency signal.

In bistable systems, it has been shown that the role of noise in improving the quality of signal detection can be played by other types of driving, such as a chaotic signal [104] or a high-frequency periodic force [40]. In the latter case, known as *vibrational resonance* (VR), the system is under the action of a two-frequency signal [Fig. 2.1]. Such bichromatic signals are pervasive in different fields, including brain dynamics [76], where for instance bursting neurons may exhibit two widely different time scales, and telecommunications [77], where information carriers are usually high-frequency waves modulated by a low-frequency signal that encodes the data. Two-frequency signals are also of interest in several other fields, such as laser physics [78], acoustics [105], neuroscience [79], and physics of the ionosphere [106]. The beneficial role of high-frequency (ultrasonic) driving has already been reported as increased drug uptake by brain cells [80], acceleration of bone and muscle repair [81], and resonantly enhanced biodegra-

dition of micro-organisms [82]. Additionally, ultrasonic irradiation of two widely different frequencies has been seen to enhance cavitation yield [83].

I start the investigations with the vibrational resonance effect in an excitable neural FitzHugh-Nagumo model.

## 2.1 Vibrational resonance and vibrational propagation

In contrast to the investigations in bistable systems, in this work I analyze the effect of high-frequency forcing in signal detection by *excitable* systems, and demonstrate the occurrence of VR in excitable media. As explained in chapter 1.1, excitable systems have only one stable fixed point, but perturbations above a certain threshold induce large excursions in phase space, which take the form of spikes of fixed shape. The duration of these excursions introduces an intrinsic time-scale in the system. Excitable systems are naturally sensitive to external perturbations. By way of example, they exhibit a resonant response to external harmonic driving [92, 107]. Here I establish that this response can also be enhanced by a second, higher-frequency periodic driving. In essence, I show that for an optimal amplitude of the high-frequency forcing, signal processing at the low-frequency driving is enhanced. This result indicates that the role of noise in standard Stochastic Resonance in excitable systems can also be played by a monochromatic driving.

First, I show that VR occurs in a simple electronic circuit with excitable properties, and confirm this effect by numerical simulation of the paradigmatic FitzHugh-Nagumo (FHN) model in an excitable regime. Next I study the effect of noise on this phenomenon, concluding that SR in excitable systems can be controlled by high-frequency driving. Finally, I show that this effect can also be observed in spatially extended systems of coupled excitable oscillators, in the form of resonant vibrational propagation of a low-frequency signal through the system for an optimal high-frequency driving applied to all elements in the system. Again, this result parallels the constructive role of noise in signal propagation through nonlinear media, which has been substantially studied in recent years in excitable [108], bistable [109], and even monostable [110] systems. The present results show that similar enhanced propagation can be obtained by replacing the broadband noisy driving with a single-frequency signal.

### 2.1.1 Vibrational resonance in an excitable electronic circuit

In order to demonstrate the occurrence of VR in an excitable system, I start with an experimental system and we have constructed an electronic circuit based on Chua's diode, which has been implemented with an operational amplifier (OA) taken from the integrated circuit TL082 [Fig. 2.2]. When the voltage that controls this OA is asymmetric the circuit becomes excitable [74]. The experiment and the measurements were performed by my collaborators in Spain.

The signals from two function generators operating at widely different frequencies (1 kHz/50 kHz) are added and introduced into the system through the

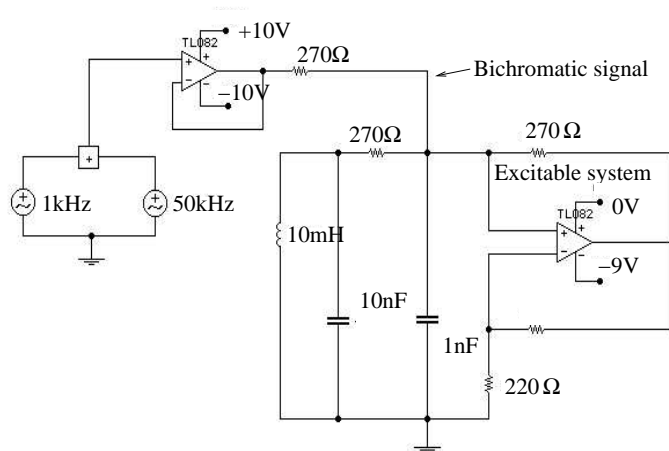


Figure 2.2: Excitable electronic circuit exhibiting vibrational resonance.

1 nF condenser, as shown in Fig. 2.2. We have analyzed the behavior of the circuit for increasing amplitudes of the high-frequency (HF) harmonic driving, while keeping the amplitude of the low-frequency (LF) signal component fixed. The results are plotted in Fig. 2.3 (left) in terms of the voltage drop at the 1 nF condenser. For a small enough amplitude of the HF component the total signal is below threshold, and hence there are no spikes in the system output, as shown in regime A of Fig. 2.3 (left). If we increase slightly the amplitude of the HF component, spikes start to appear at the low-frequency (regime B). In this regime processing of the information (which is encoded in the LF signal) begins to occur, but can be considerably improved by further increasing the number of spikes per half period of the LF signal, since in this way the energy contained at this frequency is also increased. This happens in regimes C and D, which show the optimal detection of the LF signal. With further increase of the HF amplitude (regime E), the system fires immediately after reaching the stable point, so that the output mainly contains only the frequency of the excitable system itself (eigenfrequency). Hence the LF component basically disappears from the system output, and signal processing is degraded again. This is a manifestation of vibrational resonance in an excitable medium, where an intermediate amplitude of a high-frequency driving leads to a resonant response at the low-frequency signal. A qualitative analysis of VR in this electronic circuit can be found in Fig. 2.5 by the calculation of the linear response  $Q$  of the system at the low-frequency signal in the output according to Eqs. (2.3)–(2.5) but with respect to voltage time series in Fig. 2.3 (left) instead of  $y(t)$ .

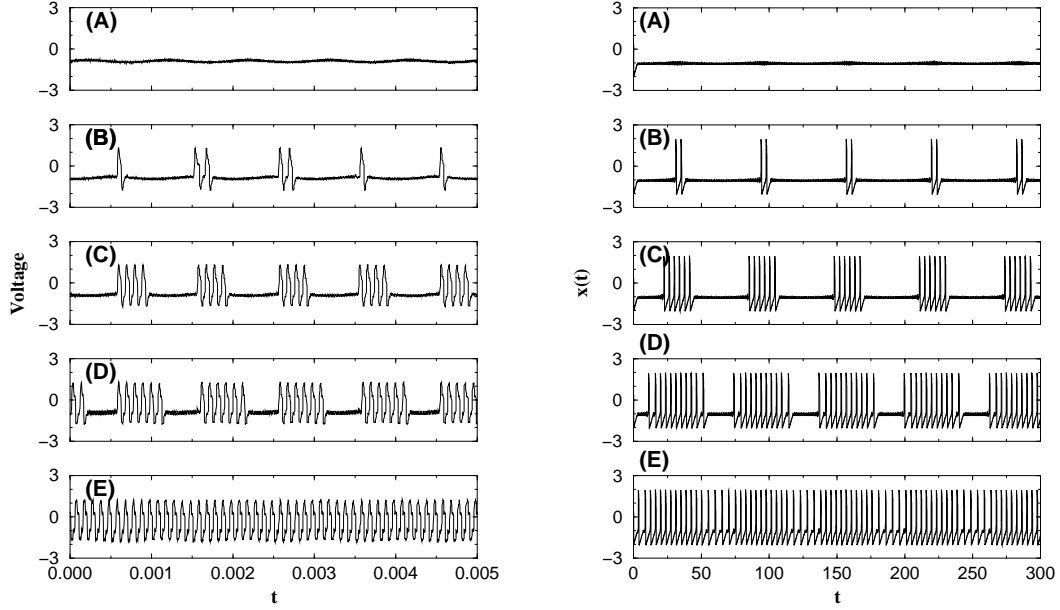


Figure 2.3: Left: Experimental results exhibiting vibrational resonance in the excitable electronic circuit of Fig. 2.2 under the action of a bichromatic signal. The voltage drop at the 1 nF condenser is plotted for different amplitudes of the high-frequency harmonic forcing: (A) 0.435 V, (B) 0.465 V, (C) 0.66 V, (D) 0.985 V, and (E) 1.385 V. The amplitude of the low-frequency component is fixed to 1.3 V. Right: Corresponding regimes obtained by numerical simulations of the FitzHugh-Nagumo model (Eqs. (2.1) and (2.2)) for different HF amplitudes: (A)  $B=0.05$ , (B)  $B=0.0505$ , (C)  $B=0.055$ , (D)  $B=0.065$ , and (E)  $B=0.07$ . The other parameters for the numerical simulation are:  $\varepsilon = 0.01$ ,  $a = 1.05$ ,  $A = 0.01$ ,  $\omega = 0.1$ ,  $\Omega = 5.0$ , and  $\sigma_a^2 = 0.0$ .

### 2.1.2 Vibrational resonance in the FitzHugh-Nagumo model

**The model.** Next I show that the behavior reported in the previous section is not particular to the special experimental system considered, but is a typical property of excitable systems. To that end I study numerically the FitzHugh-Nagumo (FHN) model, which is a paradigmatic model describing the behavior of firing spikes in neural activity [18], and in general the activator-inhibitor dynamics of excitable media [10] instead of the differential equations describing the Chua's diode. In the presence of two harmonic signals, this model is defined by the following set of coupled equations:

$$\varepsilon \frac{dx}{dt} = x - \frac{x^3}{3} - y, \quad (2.1)$$

$$\frac{dy}{dt} = x + a + A \cos(\omega t) + B \cos(\Omega t) + \xi(t), \quad (2.2)$$

where  $x(t)$  is the activator variable (representing the membrane potential in the neural case) and  $y(t)$  is the inhibitor (related to the conductivity of the potassium channels existing in the neuron membrane [18]). The value of the time scale ratio  $\varepsilon = 0.01$  is chosen so that the activator evolves much faster than the inhibitor. Under these conditions the system is excitable for  $a > 1$  [32]; I choose  $a = 1.05$ .  $\xi(t)$  is a Gaussian white noise with zero mean and correlation  $\langle \xi(t)\xi(t') \rangle = \sigma_a^2 \delta(t - t')$ . The terms  $A \cos(\omega t)$  and  $B \cos(\Omega t)$  stand for the low- and high-frequency components of the external signal, respectively. In what follows I will choose  $A = 0.01$ , so that the system is below the excitation threshold (which is  $A_{\text{thr}} \approx 0.075$  for  $B = 0$ ), and  $\Omega \gg \omega$ , in particular  $\Omega = 5$  and  $\omega = 0.1$ . In Eq. (2.2) I have considered no phase shift between the two driving signals, but as demonstrated below, the existence of an arbitrary phase shift does not alter the results that follow. To integrate the model (2.1)-(2.2) I have used Heun's algorithm [62].

**The manifestation of VR in the time series.** First I consider the noise-free case  $\sigma_a^2 = 0$  and, mimicking the electronic implementation described in the previous section, I fix the amplitude of the LF signal component and increase the HF amplitude. The different regimes exhibited by the FHN model under these conditions are shown in Fig. 2.3 (right). These regimes closely resemble the preceding observations made in the electronic circuit (compare left and right plots in the figure). As in that case, an increase of the HF amplitude  $B$  initially improves (regimes A-D) and finally degrades (regime E) signal processing at the low frequency, in what constitutes another case of vibrational resonance. Several additional aspects of the system behavior can be found in this model with respect to the electronic implementation. For instance, in regime E [Fig. 2.3

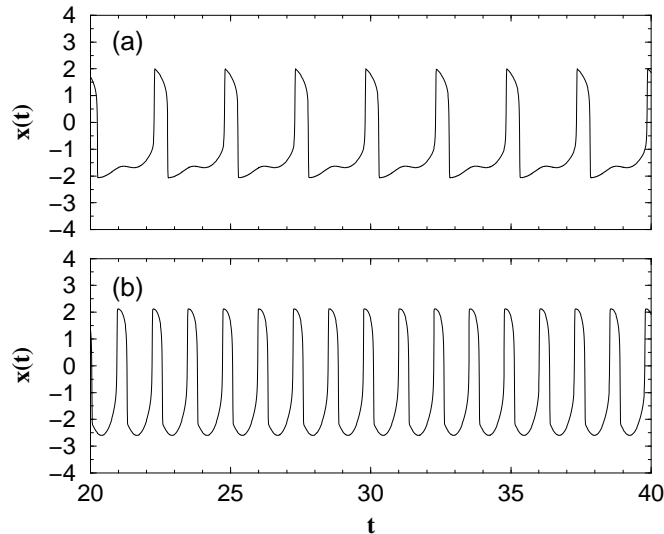


Figure 2.4: (a) Oscillations exhibited by the bichromatically forced FHN model Eqs. (2.1)-(2.2) at a frequency close to the system’s own frequency, and (b) at the driving high-frequency. The amplitude of the HF forcing is  $B = 0.1$  and  $10$ , respectively. The other parameters are the same as in Fig. 2.3 (right).

(right)] it is clearly seen that the intervals between spikes are not constant. This happens when the amplitude of the HF force is such that the system starts to fire asynchronously with respect to the signal. In this case, during one half of the signal period the system has to wait some time before spiking, whereas in the other half period the system can fire sooner once it reaches the stable point. This happens because in the latter case the time during which the signal is above threshold is larger, while the waiting time is close to the half period of the high-frequency force. Increasing the amplitude  $B$  further leads to a very regular spiking, as in the regime E of the electronic circuit [see also Fig. 2.4(a)]. Finally, for large enough values of  $B$  I obtain a new regime that has not been observed in the circuit. In this regime, the oscillations happen with a frequency different from the system’s own frequency (i.e. the one related to the intrinsic time scale of the spiking behavior), but correspond in fact to the high-frequency component ( $\Omega = 5$  in this case). This regime is depicted in Fig. 2.4(b), where it is compared with the above-mentioned case where each spike follows the previous one almost periodically with the system-internal frequency [Fig. 2.4(a)].

**The linear response  $Q$  as a measure of VR.** The VR effect illustrated in Fig. 2.3 can be quantified by computing the linear response  $Q$  of the system (i.e. the component from the Fourier spectrum) at the signal frequency  $\omega$ , which is given by [39, 40]:

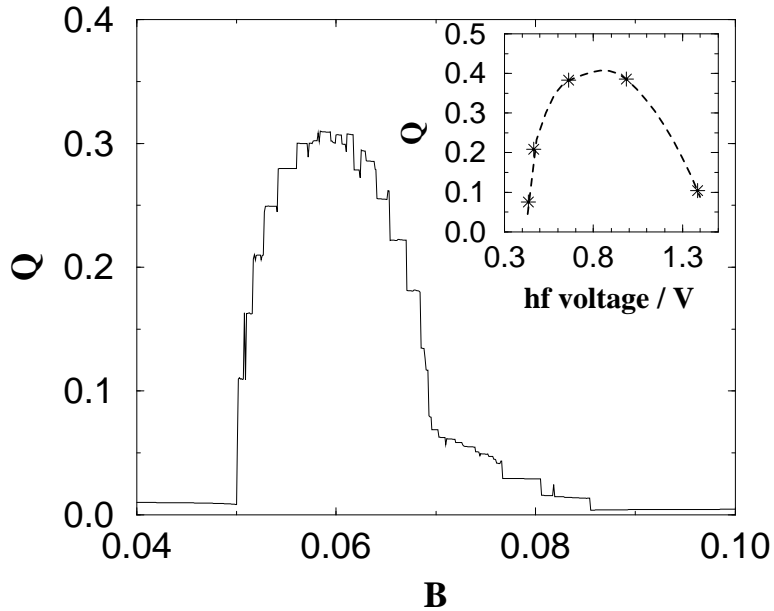


Figure 2.5: Linear response  $Q$  of the FHN model (Eqs. (2.1)-(2.2)) at the low-frequency  $\omega$  versus the amplitude  $B$  of the high-frequency input signal. The parameters for the numerical calculations are:  $\varepsilon = 0.01$ ,  $a = 1.05$ ,  $A = 0.01$ ,  $\omega = 0.1$ , and  $\Omega = 5.0$ . The inset shows the corresponding figure for the electronic circuit results presented in Fig. 2.3 (left).

$$Q_{sin} = \frac{\omega}{2n\pi} \int_0^{\frac{2\pi n}{\omega}} 2y(t) \sin(\omega t) dt, \quad (2.3)$$

$$Q_{cos} = \frac{\omega}{2n\pi} \int_0^{\frac{2\pi n}{\omega}} 2y(t) \cos(\omega t) dt, \quad (2.4)$$

$$Q = \sqrt{Q_{sin}^2 + Q_{cos}^2}, \quad (2.5)$$

when  $n$  is the number of periods  $T_s = \frac{2\pi}{\omega}$ , covered by the integration time. The linear response  $Q$  depicts the amplitude of the LF signal in the output.

The dependence of this linear response on the amplitude of the high-frequency driving [Fig. 2.5] displays a resonant form with a clearly expressed maximum at  $B \sim 0.06$ , similar to what happens in SR. The staircase form of this dependence is caused by the abrupt discrete appearance of new spikes or the discrete shifting of a spike about a high-frequency period in the spike train as the forcing amplitude increases. For a detailed description of the VR effect in the excitable FHN model,

first, I explain the origin of the staircase pattern of the linear response  $Q$  in Fig. 2.5, then I consider the influence of a phase shift and different frequency ratios of the bichromatic signal and finally I investigate the influence of additive noise.

**Origin of the staircase pattern in the linear response  $Q$ .** Fig. 2.6 describes in exemplary form the dip in the linear response  $Q$  at  $B \approx 0.062$  in Fig. 2.5. Increasing of  $B$  from 0.0613 (a) to 0.0617 (b) leaves the time series unchanged and so the linear response  $Q$  persists. The increase of  $B$  up to 0.0618 (c) results in a shifting of the first spike about one HF period in advance and in the appearance of an additional spike at the end of the spike train, but the

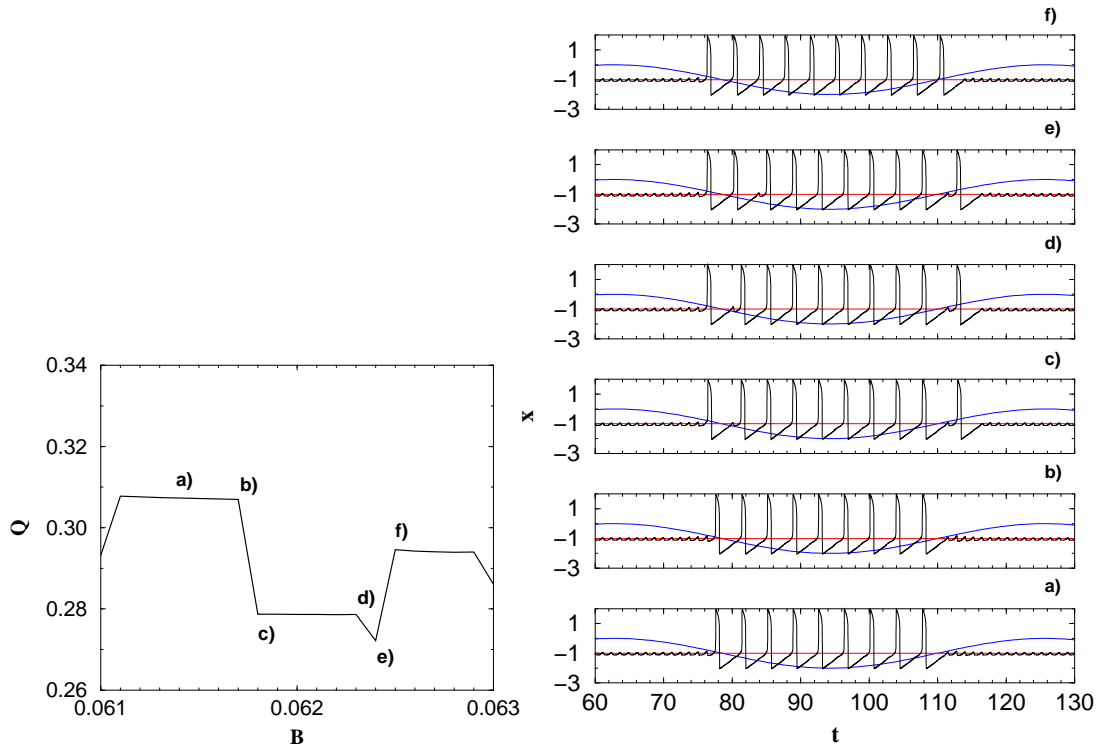


Figure 2.6: Left: the zoomed linear response of the system at the low-frequency  $\omega$  versus the amplitude  $B$  at  $B \approx 0.062$  [see Fig. 2.5]. The letters a-f refer to the underlying time series on the r.h.s. Right: time series of the activator variable  $x$  corresponding to the edges of the linear response  $Q$  at  $B \approx 0.062$  l.h.s. The parameters are:  $\varepsilon = 0.01$ ,  $a = 1.05$ ,  $A = 0.01$ ,  $\omega = 0.1$ ,  $\Omega = 5.0$  and (a)  $B = 0.0613$ , (b)  $B = 0.0617$ , (c)  $B = 0.0618$ , (d)  $B = 0.0623$ , (e)  $B = 0.0624$ , (f)  $B = 0.0625$ . The dashed line illustrates one period of the input signal with the frequency  $\omega = 0.1$ . The input signal is shifted vertically and rescaled for a better matching with the output.

other eight spikes remain in the previous position. According to Eqs. (2.3)-(2.5) the first and last spike decrease the linear response  $Q$ , because they are located in the opposite period of the signal compared to the rest of the spikes. The rise up to  $B = 0.0623$  (d) does not alter the spike contribution in the time series and hence the linear response  $Q$  persists again. Increased amplitude  $B = 0.0624$  (e) shifts only the second spike about one HF period in advance closer to the border of the half LF period and hence  $Q$  is decreased again. Further increasing of  $B$  up to 0.0625 (f) shifts all spikes from number three up to one or two (only the last one) HF periods forward in time. As result, one more spike is concentrated in the half LF period of the signal, and consequently the linear response  $Q$  is increased.

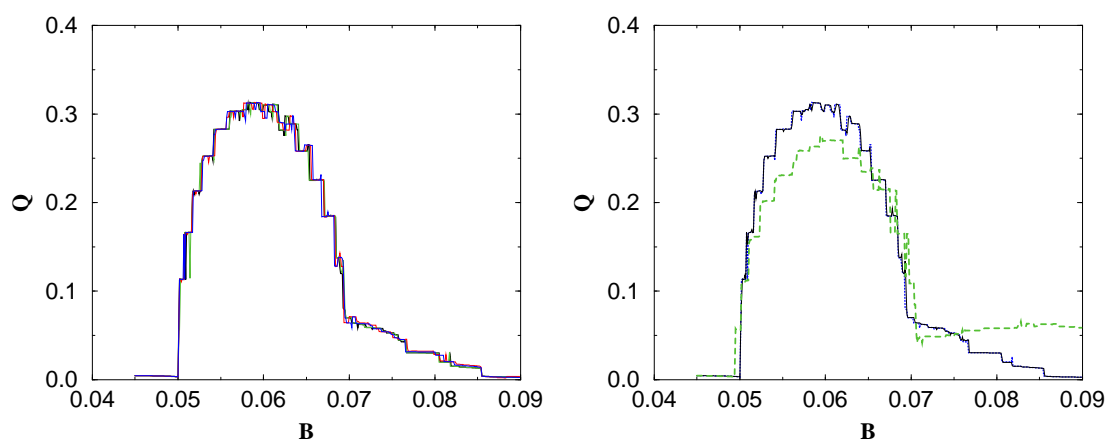


Figure 2.7: Left: the linear response of the system  $Q$  at the low-frequency  $\omega$  versus the amplitude  $B$  for different phase shifts between high and low-frequency signal. The bold line includes no phase shift ( $\varphi = 0.0$ ) as in Fig. 2.5 and the other lines illustrates exemplary the phase shifts  $\varphi = 0.628, 2.512, \text{ and } 3.758$ . Right: the linear response of the system  $Q$  at the low-frequency  $\omega$  versus the amplitude  $B$  for different frequencies  $\Omega$  without phase shift. The frequency  $\Omega$  is: 5.0 (dotted bold line),  $1.84 \times e$  (solid line), and 5.3 (dashed line). The bold dotted line and the solid lines partially coincide. All the other parameters, except for the noted ones, are the same as in Fig. 2.5.

**Influence of phase shift and frequency.** The staircase pattern persists (although its shape may change) when a phase shift between high and low frequency is added or when the frequency ratio between the two periodic signals changes, even when this ratio is incommensurate. Fig. 2.7 (left) illustrates the persistence of the stepped form of the linear response  $Q$  by introducing a phase shift  $\varphi$  in the high-frequency signal  $B \cos(\Omega t + \varphi)$ . The different phase relations result only in a small variation of the linear response  $Q$ . Fig. 2.7 (right) shows the qualitative persistence of the stepped form by changing the frequency ratio in a small

range. I have checked that the resonance displayed in Fig. 2.5 persists for a wide range of values of the high frequency around  $\Omega = 5.0$  (the values tested cover the range 2.4–17.0 [Fig. 2.8]). However, due to the additional interplay between the HF signal and sub-threshold oscillations, the position and amplitude of the resonance peak vary with the value of the high frequency. This interplay, related to the so called Canard trajectories, will be discussed in detail in chapter 2.2. This dependence of the VR effect from the high frequency constitutes a difference with respect to the standard SR effect, and could be useful for determining the system's natural selectivity of special frequency components from the white noise when SR occurs.

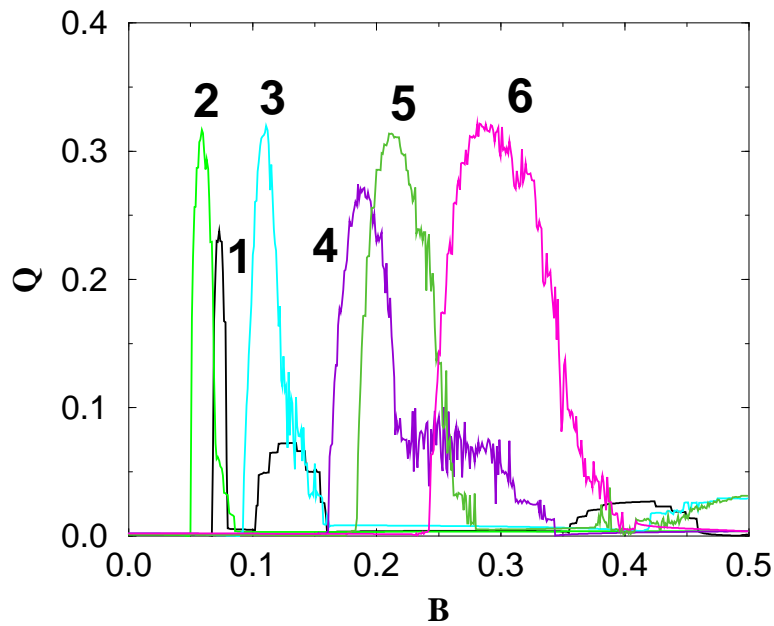


Figure 2.8: The linear response of the system  $Q$  at the low-frequency  $\omega$  versus the amplitude  $B$  for different high frequencies  $\Omega$ . 1:  $\Omega = 2.4$ , 2:  $\Omega = 5.0$ , 3:  $\Omega = 10.0$ , 4:  $\Omega = 14.0$ , 5:  $\Omega = 15.0$ , and 6:  $\Omega = 17.0$ . All the other parameters are the same as in Fig. 2.5.

**Influence of additive noise.** So far we have not considered the influence of noise in the behavior of the FHN model. In order to study the interplay of VR and SR in this system, I now increase the intensity  $\sigma_a^2$  of additive noise in the system. Fig. 2.9 (left) shows that by adding noise to the system the linear response dependence is shifted to the left and decreased. Hence, with increasing noise the maximum of the linear response is achieved for a smaller value of  $B$  [compare curves 1 and 2 in Fig. 2.9 (left)]. This fact could be relevant for efficient information processing, because natural fluctuations or noise (unavoidably present in

experimental systems) are able to replace a fraction of the high-frequency driving and help to reduce the necessary input energy. If the noise intensity is too large, VR disappears [curve 4 in Fig. 2.9 (left)].

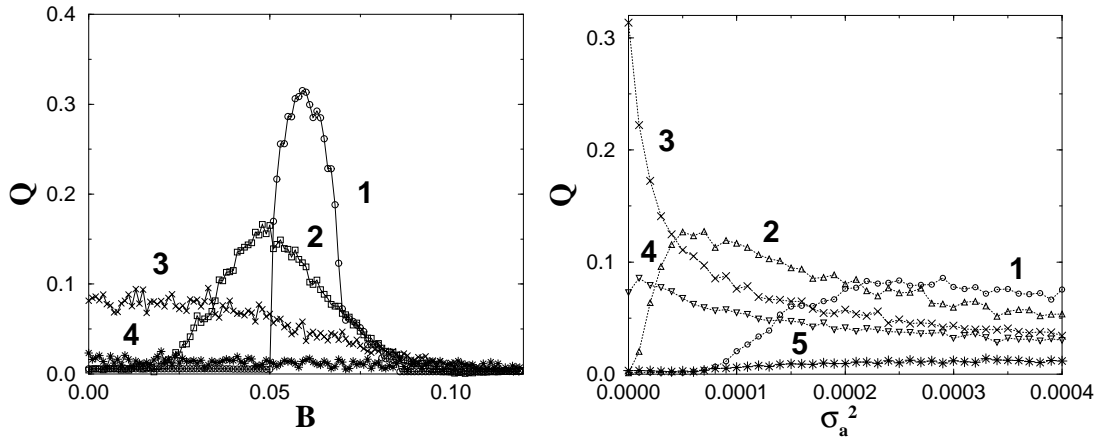


Figure 2.9: Linear response of the system at the low-frequency  $\omega$  in the presence of additive noise: left versus the HF amplitude  $B$  for different intensities of additive noise (curve 1 –  $\sigma_a^2 = 0$ , curve 2 –  $\sigma_a^2 = 0.05 \times 10^{-3}$ , curve 3 –  $\sigma_a^2 = 0.25 \times 10^{-3}$ , curve 4 –  $\sigma_a^2 = 3 \times 10^{-3}$ ); and right versus the noise intensity  $\sigma_a^2$  for different HF amplitudes (curve 1 –  $B = 0$ , curve 2 –  $B = 0.04$ , curve 3 –  $B = 0.06$ , curve 4 –  $B = 0.07$ , curve 5 –  $B = 0.1$ ).

Next I analyze the linear response of the system as a function of noise intensity for varying amplitude  $B$  of the HF forcing [Fig. 2.9 (right)]. For no HF amplitude (curve 1 in the figure) standard SR is found. Adding then a high-frequency driving to the signal improves SR, because the resonance curve is shifted to lower values of  $\sigma_a^2$  and is increased [curve 2 in Fig. 2.9 (right)]. Hence the amount of noise needed for optimal signal processing is smaller. One can thus interpret that a high-frequency driving allows us to control Stochastic Resonance, i.e. a HF signal can replace a fraction of additive noise in the SR effect and improves the signal processing in the SR effect. Further increase of  $B$  to the value which corresponds to the optimal amplitude  $B = 0.06$  in the noise-free case leads only to a monotonous decrease of the quality of signal processing with increasing noise intensity  $\sigma_a^2$ , shown as curve 3 in Fig. 2.9 (right). But its value at zero noise is the largest one among all curves, as expected from the optimal driving amplitude – compare the values at  $\sigma_a^2 = 0$  of all the curves in Fig. 2.9 (right) with curve 1 in Fig. 2.9 (left). For even larger values of  $B$ , signal processing has very bad quality for all intensities of additive noise (curves 4 and 5).

### 2.1.3 Resonant vibrational propagation

When excitable systems are coupled spatially in an extended medium, excitation pulses are able to propagate through the system in a very efficient way. Consequently, it is interesting to analyze whether the phenomenon of vibrational resonance can be generalized to the case of spatially extended systems. To that end I consider a chain of coupled excitable oscillators, whose behavior I represent now by the Barkley model [111] to illustrate the general aspect of VR:

$$\begin{aligned}\frac{du_i}{dt} &= \frac{1}{\varepsilon} u_i(1 - u_i) \left( u_i - \frac{v_i + b}{a} \right) + \frac{D}{\Delta x} \sum_{j \in N(i)} c_{ij} u_j + A_i \cos(\omega t) + B \cos(\Omega t), \\ \frac{dv_i}{dt} &= cu_i - v_i,\end{aligned}\tag{2.6}$$

where  $i$  is the cell index along the chain, and I take  $A_i = 0$  for  $i > i_{ex}$ . In what follows I used the following values for the model parameters:  $\varepsilon = 0.01$ ,  $a = 0.85$ ,  $b = 0.18$ , and  $c = 0.7$  (for which the system operates locally in an excitable regime) and the coupling strength is taken  $D = 0.05$ . The weight coefficients  $c_{ij}$  correspond to the first-order discretization of the Laplacian operator [112] with  $\Delta x = 0.25$ . Every oscillator in the chain is driven by a high-frequency signal  $B \cos(\Omega t)$ , with  $\Omega = 5.0$ , and the oscillators with  $i < i_{ex}$  are additionally under the action of the low-frequency information-carrying signal  $A \cos(\omega t)$ , with  $\omega = 0.1$  and  $A = 3.0$ .

The behavior of this spatially extended system is illustrated in Fig. 2.10. When no high-frequency vibration ( $B = 0$ ) is applied to the oscillators the signal is unable to propagate for the coupling strength chosen [Fig. 2.10 (left)]. However, if I now apply a HF vibration ( $B = 1.6$ ) to all oscillators in the chain, the LF information-carrying signal propagates through the whole chain of oscillators as a train of pulses [Fig. 2.10 (right)]. The mechanism of this effect is based on the occurrence of VR in single oscillators, but now the input of each oscillator (for  $i > i_{ex}$ ) comes from the output of the previous element in the chain. For oscillators out of the signal-input area ( $i > i_{ex}$ ), the LF signal input originates from the response of the left neighbor due to the local coupling. The stimulations from the spiking behavior of this neighbor are too weak to force the oscillator beyond the threshold of excitation and therefore to evoke a spike without any additional forcing because the coupling is too small. Only in the presence of HF forcing in every element, these oscillators ( $i > i_{ex}$ ) are able to reach the threshold of excitation and produce spikes. At a suitable and finite HF amplitude, only spikes synchronized with the LF signal are evoked and an optimal signal transmission controlled by the HF forcing appears [Fig. 2.10 (right)]. A further increase of the HF amplitude beyond this optimal value leads to a permanent spiking behavior of all oscillators and the synchronization with the LF signal vanishes, i.e. the signal transmission decreases again. Hence, the effect of VR in excitable oscillators can

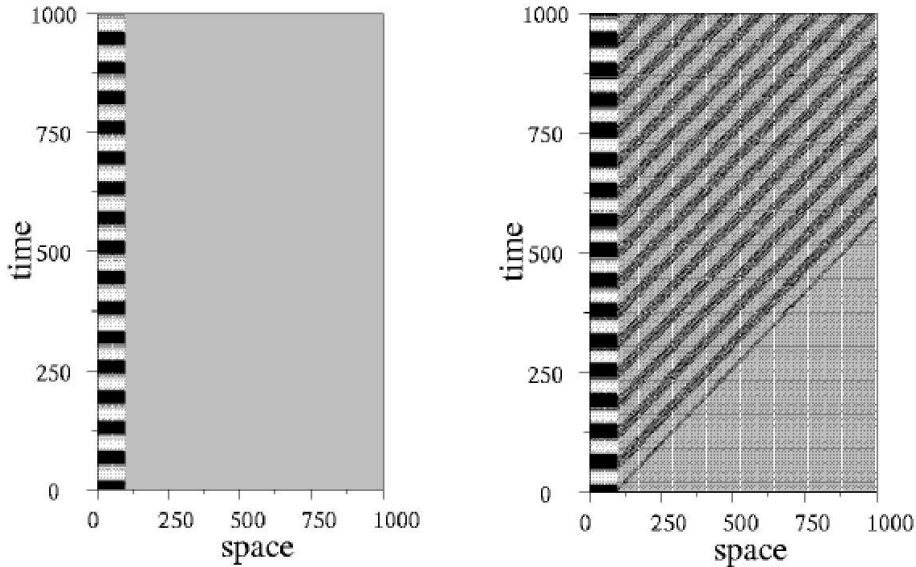


Figure 2.10: Resonant vibrational propagation in a excitable medium. A chain of coupled oscillators (Eqs. 2.6) is represented along the horizontal axis  $z$ . Time evolution goes from bottom to top. Left: without HF vibration ( $B = 0$ ); right: with HF vibration ( $B = 1.6$ ). The first 100 oscillators ( $i < i_{ex}$ ) are always driven by the low-frequency signal. An increase of high-frequency vibration leads to propagation of the information LF signal.

be observed in spatially extended systems as a resonant *vibrational propagation* (VP).

*In conclusion*, I have studied several aspects of the dynamic response of excitable systems to bichromatic signals with two very different frequencies. I have demonstrated the existence of two phenomena: vibrational resonance in zero-dimensional systems and resonant vibrational propagation in spatially extended media. Experimental results obtained in an excitable electronic circuit have been confirmed by a numerical analysis of the FitzHugh-Nagumo model. In particular, it has been shown that an optimal amplitude of the high-frequency component of the signal can optimize signal processing of the low-frequency component, which encodes the information. I have also shown that, in the presence of noise, high-frequency driving can substitute a fraction of the noise and hence control the effect of Stochastic Resonance. The reverse is also true: additive noise can replace a fraction of the high-frequency vibrations in the vibrational resonance effect. The latter case could be interesting to reduce the needed input energy in the VR effect, because noise is everywhere present in natural systems. In spatially extended excitable media, vibrational resonance enhances propagation of the low-frequency signal through the system by means of the action of the high-

frequency driving. I have reported vibrational resonance and resonant vibrational propagation in simple systems and paradigmatic models, and have studied these effects in a general framework, hence I expect that these findings will be relevant for different fields, including communication technologies, optics, chemistry, neuroscience, and medicine. Given the ubiquity of two-frequency signals in neural systems, mentioned already in the introduction, this result could be of special interest in the study of the activity of neural ensembles, and in general in wave propagation in excitable activatory-inhibitory systems.

Next I extend the study of new resonance phenomena in excitable systems to systems with additional Canard dynamics.

## 2.2 Canard-enhanced Stochastic Resonance

In this part of the work I study the SR effect in another class of systems, that differs from those already explored by the fact that this class possesses properties of both oscillatory and excitable behavior. As a paradigmatic model for such systems I consider again the FitzHugh Nagumo (FHN) oscillator.

Generally, the FHN model is tuned to exhibit either an oscillatory behavior with strongly nonlinear oscillations in the system or an excitable behavior with a stable fixed point and the feature that relatively small perturbations can lead to a large excursion (excursion loop or spike) [32, 38, 113]. In contrast to this we are interested in a FHN model that is tuned to have both oscillatory and excitatory properties. Such dynamics take place in FHN-like models [114] or in biophysical models [115, 116], if their parameters are chosen in the region of the so-called “Canard” bifurcation [117, 118]. In these works a Canard solution is a solution of a singular perturbed system which passes close to a bifurcation point and follows a repelling slow manifold for a considerable amount of time.

For the FHN model the Canard phenomenon means that there are quasi-harmonic oscillations with small amplitude and small periods [Fig. 2.11]. The parameter region between pure excitable and oscillatory cases is typically very narrow if the stiffness of the oscillator is large ( $\varepsilon \ll 1$ ). But the value of stiffness is not obligatorily large and is defined by the kinetic parameters of the specific models. A crucial feature of Canard-like behavior is that a very small change in the control parameter may lead to a large difference in the trajectories and hence produce oscillations with different frequencies. This change can be also induced by the action of noise, if the system possesses Canard-like oscillations.

The idea of using a system with several intrinsic frequencies as a signal receiver in the presence of noise has been already reported in the literature. For example, in a bistable underdamped system, Stochastic Resonance may happen due to intrawell as well as to interwell motion [119]. Further on, it was described that non-adiabatic resonance under the action of a high frequency can exist in a noisy excitable system [85]. In all these works, the improvement of signal processing occurs due to the resonance interplay between an incoming periodic signal and one of the internal frequencies of the oscillating system. In contrast to this case, I consider here the situation in which an additional high-frequency signal improves the detection of a low-frequency signal, i.e. it is crucial that the system is under the action of multi-frequency signal. A similar problem formulation was studied in [120], where it was shown that adding a high-frequency signal may help the detection of a low-frequency signal and leads to a heterodyning effect in a two-dimensional oscillator with one internal frequency near a saddle-node bifurcation. However, this effect occurs due to the action of a resonant high-frequency signal on a detection threshold near a saddle-node bifurcation (see also a case of coupled oscillators [121]), whereas in our case we investigate a noisy system with two different internal frequencies under the action of a two-frequency signal, and the

resonance effect at one higher internal frequency leads to the amplification of Stochastic Resonance at another low frequency.

I consider FHN systems under the action of a subthreshold bichromatic signal, which consists of two parts: the first one has the frequency of an investigated signal, and the second one has a higher frequency. I demonstrate the effect of SR amplification when the higher frequency is in resonance with the frequency of the Canard oscillations of this system. Let me point out again, two-frequency signals are widely used in communications [77], neuroscience [79], laser-physics [78], and acoustics [105]. Additionally, a beneficial role of high-frequency (HF) driving has already been found in several biological phenomena, such as increased drug uptake by brain cells [80], improvement of bone and muscle healing [81], or enhanced biodegradation of micro-organisms [82]. The effect, discussed in this part, is also closely connected to the vibrational resonance (VR) in excitable systems previously presented (see chapter 2.1 and [122]), where the high-frequency driving acts as noise and improves the signal processing. VR demonstrates a resonance-like behavior with respect to the amplitude of the HF signal. In contrast to VR, in Canard-enhanced SR it is crucial that not the amplitude but *the frequency* of the HF signal should be in resonance with the oscillatory behavior of a system.

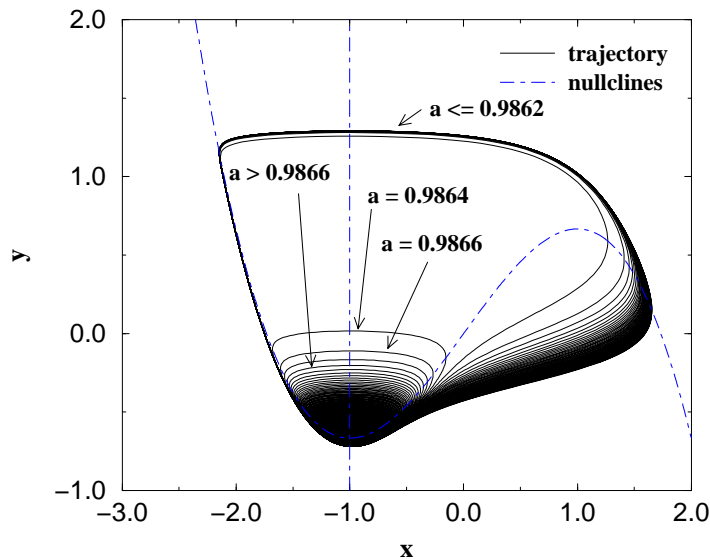


Figure 2.11: The dependence of the trajectories and the appearance of Canard trajectories on the parameter  $a$  in the FHN model without noise and without driving forces.

### 2.2.1 The model with Canard dynamics

I study the following known FHN model (see Eqs. (2.1) and (2.2)):

$$\varepsilon \frac{dx}{dt} = x - \frac{x^3}{3} - y, \quad (2.7)$$

$$\frac{dy}{dt} = x + a + \xi(t) + s(t), \quad (2.8)$$

where  $\xi(t)$  is Gaussian white noise of the intensity  $\langle \xi(t)\xi(t') \rangle = \sigma_a^2 \delta(t - t')$  and the parameter  $a$  determines the behavior of the system. For  $a > 1.0$  the unforced FHN model ( $s(t) = 0$ ,  $\sigma_a^2 = 0$ ) is excitable and for  $a < 1.0$  it shows an oscillatory behavior. At this bifurcation point  $a = 1.0$  the stability of the only fixed point  $x_0 = -a$ ,  $y_0 = \frac{a^3}{3} - a$  will be changed. Between these two cases an intermediate behavior can appear. For values of the parameter  $a$  slightly beyond the bifurcation point, small oscillations near the unstable fixed point exist instead of large spikes. To illustrate this, in Fig. 2.11 trajectories in the phase space of the FHN system without driving force and noise are plotted in dependence on the parameter  $a$ . For  $a \leq 0.9862$  and  $\varepsilon = 0.1$  (much larger than in chapter 2.1.2) the FHN model oscillates on the well-known big excursion loop. In the intermediate parameter region  $0.9864 \leq a < 1$  and  $\varepsilon = 0.1$  there is also an oscillatory behavior but the loops (Canard trajectories) in the phase space are much smaller than the excursion loops. Between both possible traces there is a clear gap so that these both kinds of oscillations can be easily distinguished.

The Canard trajectories exist also for smaller  $\varepsilon$  like 0.01 (which I use in the chapters 2.1.2 and 4), but the intermediate parameter region of  $a$  (where Canard oscillations exist) tends to zero for decreasing  $\varepsilon$  and the period of subthreshold oscillations near the bifurcation point is  $T_{sth} \approx 2\pi\sqrt{\varepsilon}$  [114]. Hence, for  $\varepsilon = 0.01$  the subthreshold oscillations are very fast and so the trajectory loops are very small. In the following I fix the parameter  $\varepsilon = 0.1$  to have a system with a significant intermediate region where Canard oscillations exist. Similar values of  $\varepsilon$  (parameter to separate a slow- and fast-moving variable) were used also in different papers for the modeling of biological and chemical processes [123–125] and so the choice has natural links. In spite of the fact that frequently-used harmonic and singular approximations of FHN studies are very suitable for the mathematical treatment of model behavior, in the real processes the stiffness is in between these two limit cases.

An important fact of the treatment of the Canard oscillations is that a very small change in the parameter  $a$  leads to a large difference in the trajectories. This change in the parameter  $a$  can be caused by some instantaneous influence of noise. Beside the expected case for the parameter  $a$  typical for the Canard phenomenon, Canard-like trajectories can be observed also in the excitable regime  $a > 1$  close to the bifurcation point if the FHN system is forced by additive noise

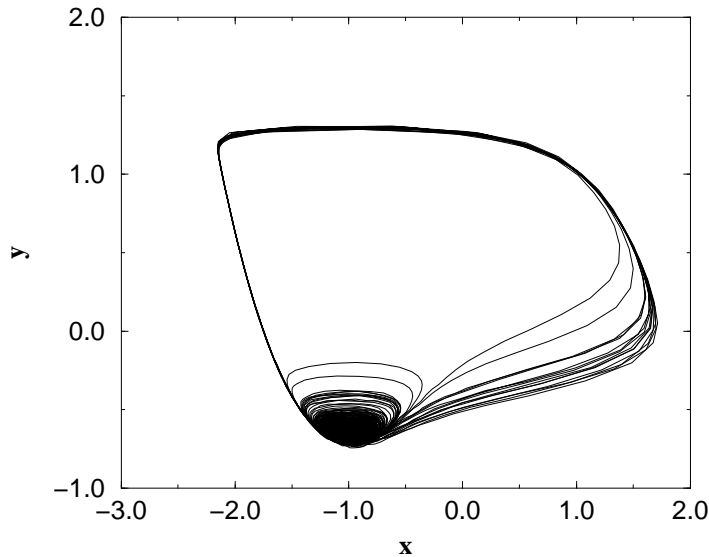


Figure 2.12: Occurrence of spike and Canard trajectories in a noise-driven FHN model (Eqs. (2.7) and (2.8)) in the excitable regime. The parameters are  $\varepsilon = 0.1$ ,  $a = 1.01$  and  $\sigma_a^2 = 0.0004$ .

$\xi(t)$ . This can be easily seen in Fig. 2.12, where trajectories in the phase space were plotted for the parameters  $\varepsilon = 0.1$ ,  $a = 1.01$ ,  $\sigma_a^2 = 0.0004$  (in the excitable regime) and there are no periodic driving forces. Only the noise drives the FHN system and leads to the Canard-like trajectories and the spikes and therefore, again the FHN system behaves with two different frequencies of the two cycles which can certainly be used in signal processing.

These different trajectories manifest themselves in a polymodal interspike interval histogram (ISIH) not only when the parameter  $a$  is chosen from the interval corresponding to the Canard orbits (as in Ref. [114]) but for  $a$  which provides an excitable regime [Fig. 2.13]. I have chosen the most pronounced examples of ISIH polymodality but this type of distribution is preserved in some intervals of the essential parameters:  $a \in [1.0, 1.05]$ ,  $\varepsilon \in [0.02, 0.2]$  under the appropriate noise amplitudes. The first peak in the ISIH [Fig. 2.13] corresponds to the excursion time  $t_e$  of the large spikes and the Canard trajectories lead to the polymodality. The period duration of the Canard loops coincides with the distance between two consecutive peaks in the ISIH.

Next I add a driving force  $s(t) = A\cos(\omega t)$  and investigate the linear response  $Q$  of the periodic driven system at the input frequency  $\omega$ . To evaluate the amplitude of the input frequency in the output signal, I calculate the Fourier coefficient  $Q$  for the input frequency  $\omega$ . I use the linear response  $Q$  instead of the power spectrum because I am interested in the transmission of the information encoded in the frequency  $\omega$ . For this task the linear response  $Q$  is a much more compact

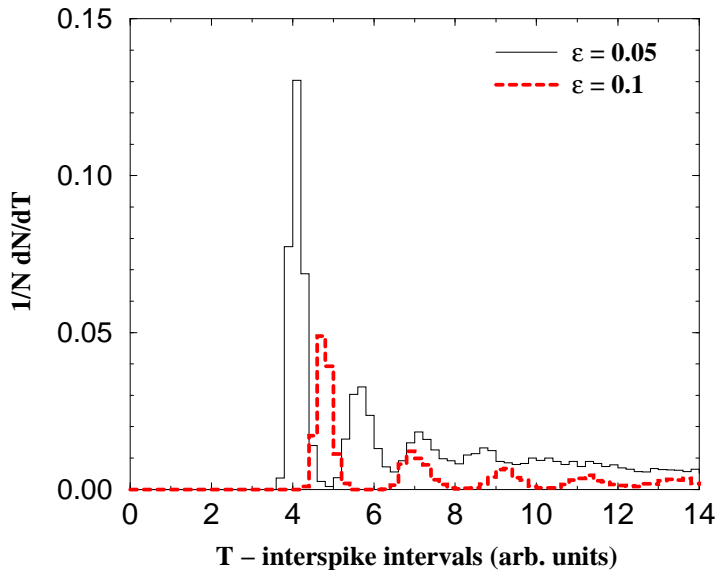


Figure 2.13: ISIH in a noise-driven excitable FHN model (Eqs. (2.7) and (2.8)). The parameters are  $a = 1.01$  and  $\sigma_a^2 = 0.0004$ . There is no signal ( $s(t) = 0.0$ ) and the parameter  $\varepsilon$  is variable.

tool than the power spectrum [39, 110]. In contrast to Eqs. (2.3)-(2.5), now the linear response  $Q$  is based on the activatory variable  $x$ .

First I look for the resonance frequencies of the system to find both internal frequencies (Canard frequency and frequency of the spiking behavior). Therefore I calculate the linear response  $Q$  versus the circle frequency of the driving force. I consider three cases: a)  $a = 1.01$ , FHN in a mono-stable excitable regime; b)  $a = 1.0$ , FHN at the bifurcation point; and c)  $a = 0.998$ , FHN in an oscillatory regime with small Canard oscillations around the unstable fixed point and small amplitudes compared with the amplitude of a spike. The amplitude of the periodic driving force is chosen small enough so that the system needs noise to reach the threshold and to produce a spike. The following Figs. 2.14 - 2.16 show the dependence of the linear response  $Q$  on the input frequency for these three cases and various noise intensities  $\sigma_a^2$ . The linear response  $Q$  refers to the variable input frequency and measures the amplitude of the input frequency in the output signal.

The first peak in all Figs. 2.14 - 2.16 at  $\omega = 1.3$  corresponds to a period length of  $T = 4.83$  and is caused by the firing of a spike. The second peak at about  $\omega = 2.6$  to  $2.9$  is caused by the Canard oscillations near the fixed point  $x_0, y_0$  with a small amplitude compared with the big spike. In opposition to the resonance frequency of the spike, the position of the Canard-resonance frequency ( $\Omega_C$ ) depends on the parameter  $a$  and the noise intensity  $\sigma_a^2$ . This can also be easily seen in the phase space in Figs. 2.11 - 2.12. The trace of the spikes is

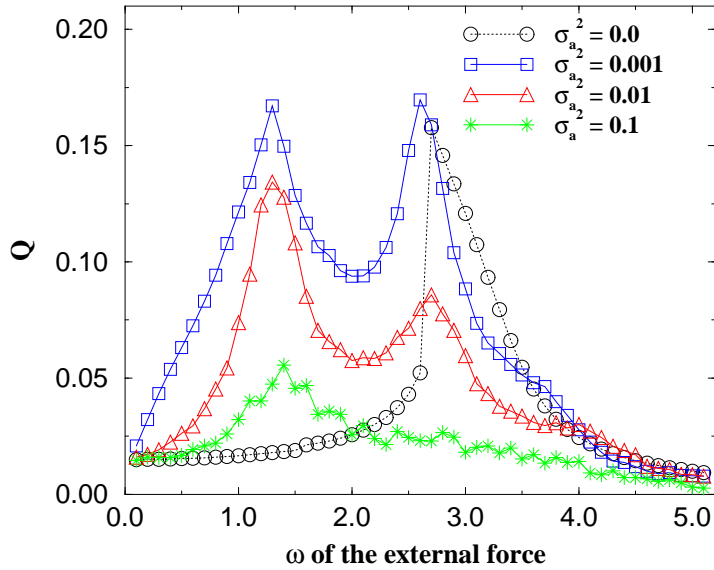


Figure 2.14: Resonances for the periodically driven ( $A = 0.03$ ) FHN system in the excitable regime ( $a = 1.01$ ) under the influence of different noise intensities.

very stable and narrow and so the time for one round trip during a spike is independent of the parameter  $a$  and the noise while the traces for the Canard oscillations fill a much wider area in the phase space and we can observe a shifting of the Canard-resonance frequency by changing  $a$  and  $\sigma_a^2$ . It is important to note that a peak at the Canard frequency exists even for smaller noise intensities, when the peak at the spiking frequency is not yet pronounced. This explains the fact that adding the driving force at this Canard frequency can be successfully used in the improvement of signal-receiving, even if the information is carried by another low frequency.

It is noteworthy that similar high-frequency resonance has been described recently in the Hodgkin-Huxley model [126] and it was proposed in the “resonate-and-fire” neural model [91] but its background is the oscillatory convergence to the rest state instead of the Canard phenomenon. For a more stiff FHN oscillator only the low-frequency peak in ISIH is observed and its coherence is maximal if the period is equal to the time of cycle excursion, as has been shown in Ref. [85].

## 2.2.2 Enhancement of Stochastic Resonance

With the knowledge of the Canard-resonance frequency I demonstrate that the response of the system to a given input frequency is improved. We now force the FHN system with two different but fixed frequencies

$$s(t) = A\cos(\omega t) + B\cos(\Omega t).$$

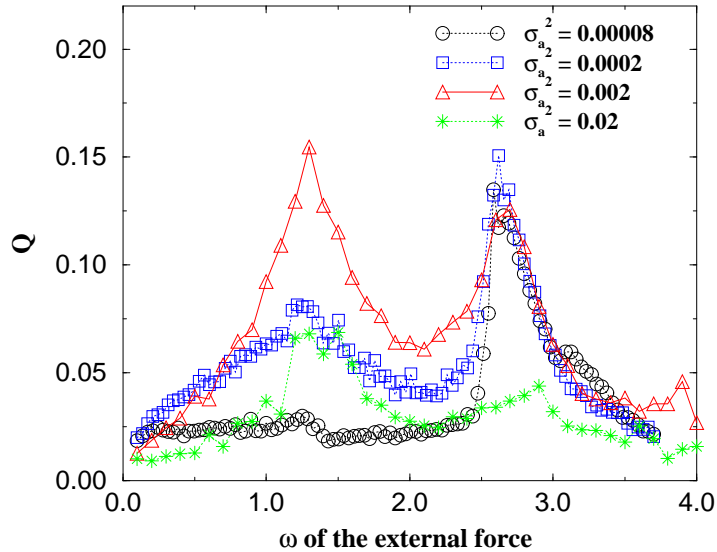


Figure 2.15: Resonances for the periodically driven ( $A = 0.02$ ) FHN system at the bifurcation-point ( $a = 1.0$ ) under the influence of different noise intensities.

The basic idea is that the information is stored in a low-frequency input signal with a circle frequency  $\omega$  and an amplitude  $A$ . The additional high-frequency input signal  $B\cos(\Omega t)$  and the noise afford the threshold to be reached and so both are necessary to produce a spike. The amplitude of both periodic input signals are chosen small enough that they cannot produce a spike without noise. A similar situation was in the study of the vibrational resonance in the previous section 2.1 [122]. But the setup of the parameters there did not support the use of the Canard resonance in the signal-processing very well.

In Fig. 2.17 two typical time series of the  $x$  variable are plotted for the Canard-resonant case [Fig. 2.17(a)] and the non-resonant case [Fig. 2.17(b)]. The difference between these two figures is the frequency  $\Omega$  of the high-frequency input signal: the first shows the case of resonant forcing with the Canard frequency ( $\Omega = \Omega_C$ ) and the second corresponds to the forcing out of the Canard frequency ( $\Omega \neq \Omega_C$ ). As an important result the amplitudes of the small oscillations around the fixed point in the original time series  $x(t)$  are different. Because of the resonance between the external high-frequency force and the noise-induced small-amplitude oscillations in the Canard-resonant case, the amplitude of these small oscillations are enhanced and the FHN in this regime can more easily reach the firing threshold with the help of noise. As a result, we can observe a behavior that is more synchronized with the low-frequency input signal.

In natural systems with such a spiking behavior like neurons only the spikes themselves are important for the information transmission. As shown above, small Canard oscillations near the fixed point are very important for the behavior of the FHN itself, but not for the information transmission. To evaluate the

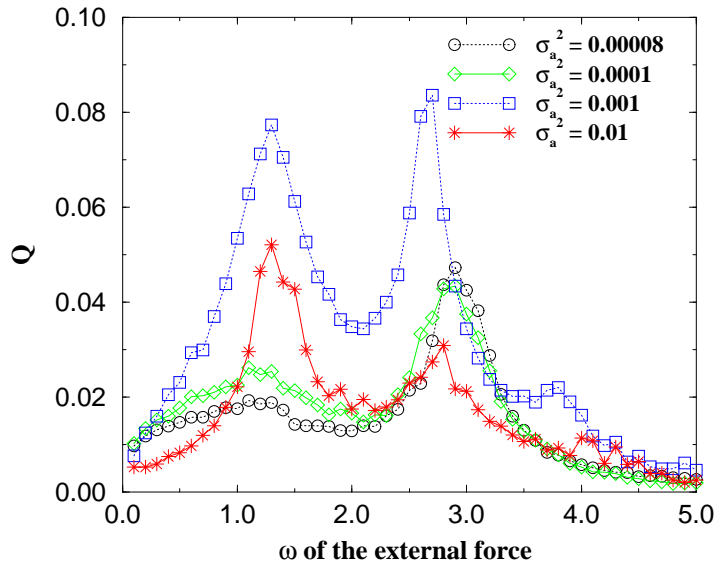


Figure 2.16: Resonances for the periodically driven ( $A = 0.01$ ) FHN system in the oscillatory regime ( $a = 0.998$ ) under the influence of different noise intensities.

information transmission, I calculate again the response of the system  $Q_{th}$  but replace the original time series  $x(t)$  by a reduced time series without oscillations around the fixed point but with the spikes which are responsible for the information exchange. To distinguish between a spike and the subthreshold oscillations I set the threshold of detection  $x_{th} = 0.0$ . If  $x(t)$  is smaller than  $x_{th}$ , I replace  $x(t)$  by the value of the fixed point  $x_0$ . For  $x(t) \geq x_{th}$  I use the original value of  $x(t)$ . This replacement is used only for the calculation of the  $Q_{th}$  parameter and not for the simulation of the original time series with the Heun method. The filtered time series are also plotted in Fig. 2.17 by the dashed line. In Figs. 2.18 - 2.20 (excitable regime, at the bifurcation point, and oscillatory regime, respectively) the dependencies of the quality of the information transmission (represented by the  $Q_{th}$  parameter at the low-frequency  $\omega$ ) on the noise intensity  $\sigma_a^2$  are depicted for different frequencies  $\Omega$  of the high-frequency driving force. In this way we consider only the spikes for the information transmission.

All three cases have in common that without noise ( $\sigma_a^2 = 0$ ) we observe no information transmission, because  $Q_{th}$  is zero. That means the FHN system does not show a spiking behavior. These figures demonstrate the bell-shaped form of  $Q_{th}$ , a well known SR effect [39], for all different high-frequencies. In the range of lower noise it can be clearly seen that for the HF part of the signal being in resonance with Canard frequency, the SR effect at the low-frequency  $\omega$  is significantly enhanced. In this region there is a significant difference in the  $Q_{th}$  parameter between the forcing at the Canard-resonance frequency ( $\Omega = \Omega_C$ ) and the forcing out of the Canard resonance ( $\Omega \neq \Omega_C$ ). The difference in the  $Q_{th}$

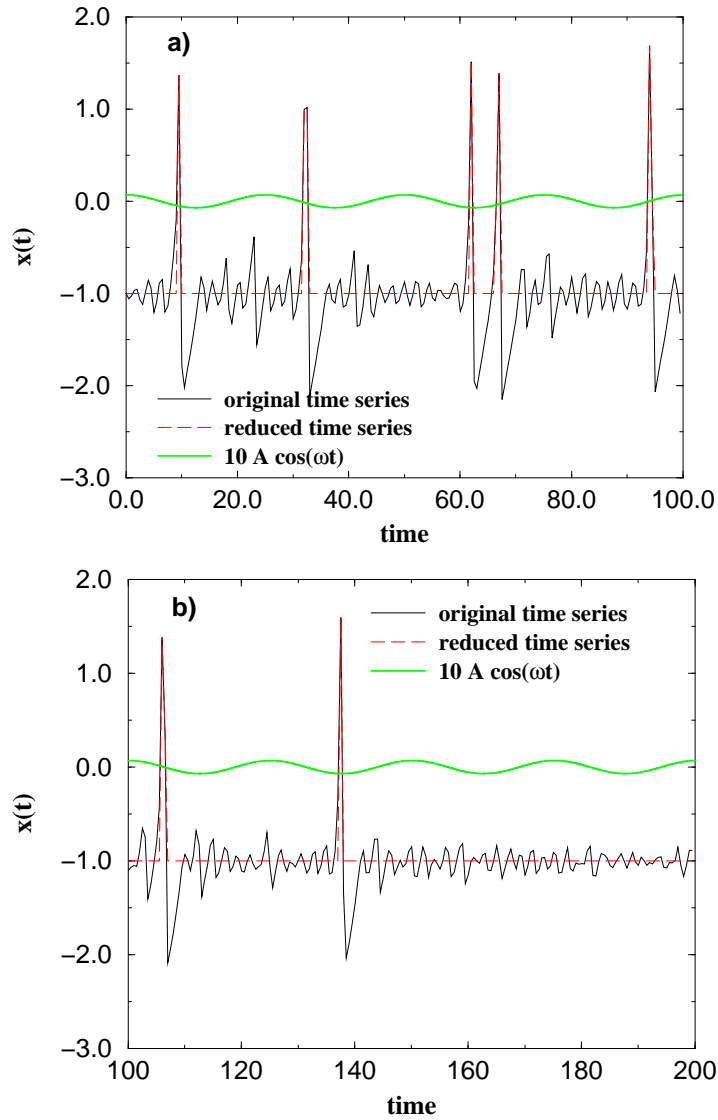


Figure 2.17: Time series of the activatory variable  $x(t)$  for the excitable FHN system driven by additive noise and two periodic forces. The high-frequency input signal is in resonance with the Canard frequency  $\Omega = \Omega_C = 2.73$  (a) and out of resonance with the Canard frequency  $\Omega = 2.0 \neq \Omega_C$  (b). For a better recognition of the signal processing with the low-frequency input signal this periodic input signal is also plotted (with a 10 times higher amplitude than in the model). The other common parameters are  $\varepsilon = 0.1$ ,  $a = 1.01$ ,  $\sigma_a^2 = 0.000375$ ,  $A = 0.007$ ,  $\omega = 0.251$  and  $B = 0.025$

parameter is caused only by a change of the frequency  $\Omega$  of the HF signal because the amplitudes are the same within one figure. This effect can be understood as the coexistence of two resonances. The first resonance happens between the

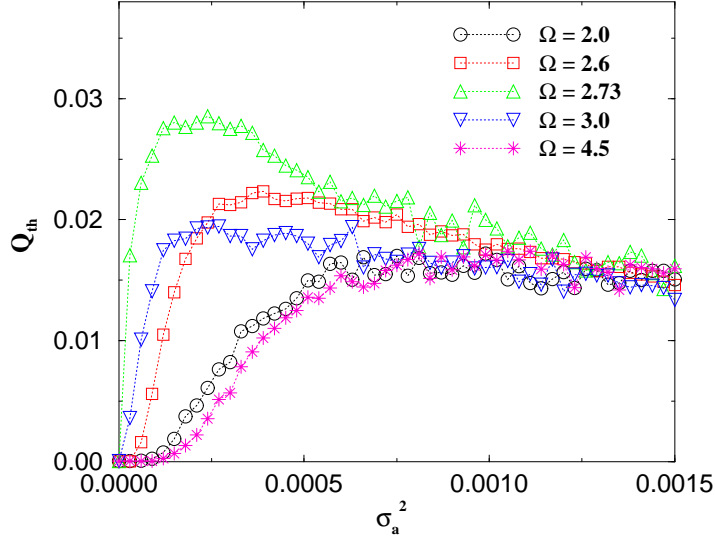


Figure 2.18: Signal processing at the low-frequency  $\omega$  input-signal versus the noise intensity for various frequencies of the high-frequency input-signals  $\Omega$  for the FHN system in the excitable regime. Parameters:  $a = 1.01$ ,  $A = 0.007$ ,  $B = 0.025$ ,  $\omega = 0.251$ . The Canard-resonance frequency is  $\Omega_C = 2.73$  [Fig. 2.14].

high-frequency of a signal and the frequency of Canard oscillations. If these two frequencies are similar, this resonance amplifies the conventional SR for a signal with low frequency.

The signal enhancement may be presented also in the form of interspike interval histograms. In Fig. 2.21 the ISIH is depicted for the same parameters which are used for both time series in Figs. 2.17(a) and (b). Both ISIHs were calculated with the same length of 100000 time units for the underlying time series in Canard resonance ( $\Omega = 2.73 = \Omega_C$ ) and out of resonance ( $\Omega = 2.0 \neq \Omega_C$ ). In the resonant case many more spikes occur and, hence, the peaks of ISIH have higher values. The first maximum in the ISIH for both time series is between  $T = 4.8$  and  $4.9$  and corresponds exactly to the resonance frequency of the spikes. The time of the first maximum is the minimal time between two adjacent spikes when one spike follows the other one without any waiting time, i.e. without any small Canard oscillation.

For the Canard-resonant case we observe the expected multimodal structure with peaks located at multiples of the period length of the Canard oscillations or high-frequency force at  $T_{hf} = 2.3$  (respectively  $\Omega = 2.73$  with  $T_{hf} = \frac{2\pi}{\Omega}$ ). This modulation is very regular. By forcing out the Canard resonance with  $\Omega = 2.0$  (i.e.  $T_{hf} = 3.14$ ) the first three peaks are approximately at the same position as in the resonant case. Although I force out the Canard frequency, one or two Canard periods can occur between two adjacent spikes. Except for these three peaks in the ISIH the multimodal structure with the period of the Canard period

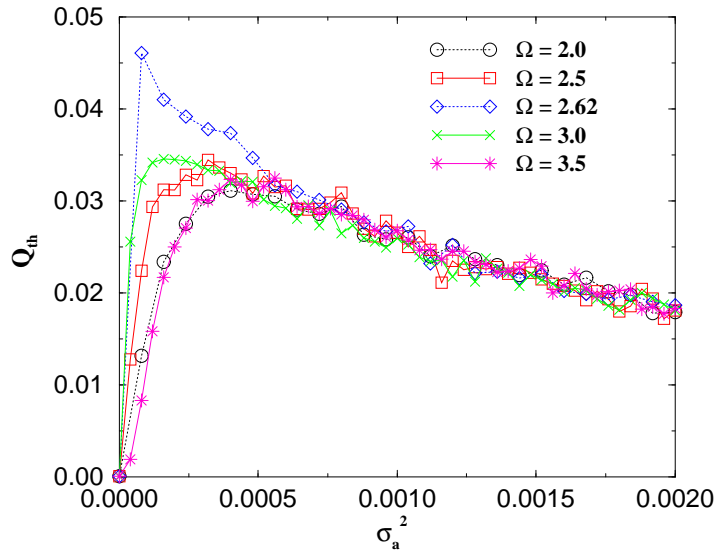


Figure 2.19: Signal processing at the low-frequency  $\omega$  input signal versus the noise intensity for various frequencies of the high-frequency input signals  $\Omega$  for the FHN system at the bifurcation point. Parameters:  $a = 1.0$ ,  $A = 0.01$ ,  $B = 0.02$ ,  $\omega = 0.251$ . The Canard-resonance frequency is  $\Omega_C = 2.62$  [Fig. 2.15].

is suppressed. For higher interspike intervals a modulation with the period of  $T \approx 3$  can be observed, that corresponds to the high-frequency input signal. In this case the Canard oscillation can succeed only for two periods and loses the competition with the high-frequency forcing after this time and the waiting time will be dominated now by integer numbers of the high-frequency period.

*In conclusion*, I have considered signal processing in the noisy system which possesses both oscillatory and excitable properties under the action of an additional HF signal. This system was represented by the FHN model with a stiffness between pure excitable and oscillatory regime. I have demonstrated the possibility of amplifying the SR effect in such systems using the Canard oscillations. In this effect the HF signal that is in resonance with the frequency of Canard oscillations strongly improves signal processing of the low-frequency signal. The effect shows a frequency selectivity and disappears in the region out of resonance with the Canard frequency.

For supercritical Hopf bifurcation in FHN-like models this phenomenon is relevant for biology if the stiffness of the system (a degree of excitability) is limited by the interval  $\varepsilon \in [0.01, 0.2]$  in order to get the observable periods of noise-induced Canard-like orbits. In this interval very small noise is necessary for a significant improvement of signal processing. It means, e.g for neurons, the possibility of a new regulation of signal processing which, in addition to the choice of the value of the bifurcation parameter, can control the signal transmission in a small noisy environment.

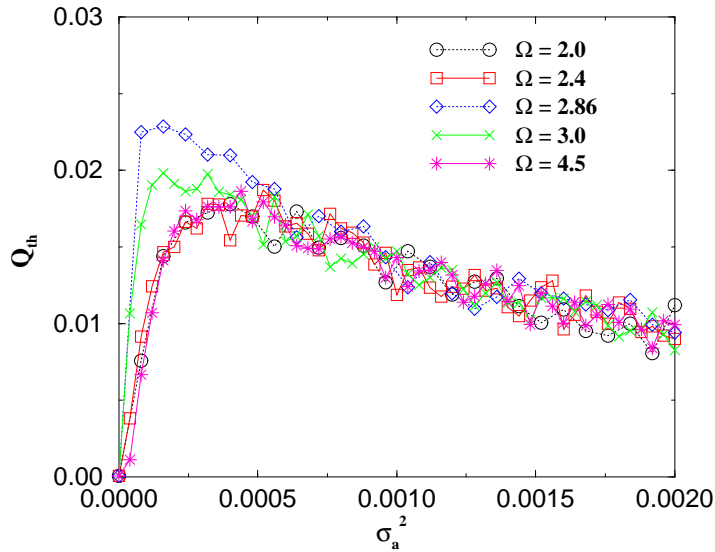


Figure 2.20: Signal processing at the low-frequency  $\omega$  input signal versus the noise intensity for various frequencies of the high-frequency input signals  $\Omega$  for the FHN system in the oscillatory regime. Parameters:  $a = 0.998$ ,  $A = 0.005$ ,  $B = 0.01$ ,  $\omega = 0.251$ . The Canard-resonance frequency is  $\Omega_C = 2.86$  [Fig. 2.16].

I hope that these theoretical findings will stimulate experimental work to find new possibilities of signal reception and propagation in systems which demonstrate Canard-like oscillations, especially in nonlinear chemical systems [127] or in biophysical models [115, 116]. Moreover, dynamic systems which have some specific regime between excitable and oscillatory states are not limited by the FHN with Canard phenomenon. Recently it has been shown that the modified Oregonator equations have three steady states and excitation occurs via resonance between damped HF oscillations around the stable fixed point and periodic perturbations with an appropriate tuning frequency [92]. A similar SR enhancement by HF signal may be also expected in this chemical system with low excitability.

In the next chapter, I investigate spatially extended FitzHugh-Nagumo models with an inhibitory coupling and their frequency selectivity.

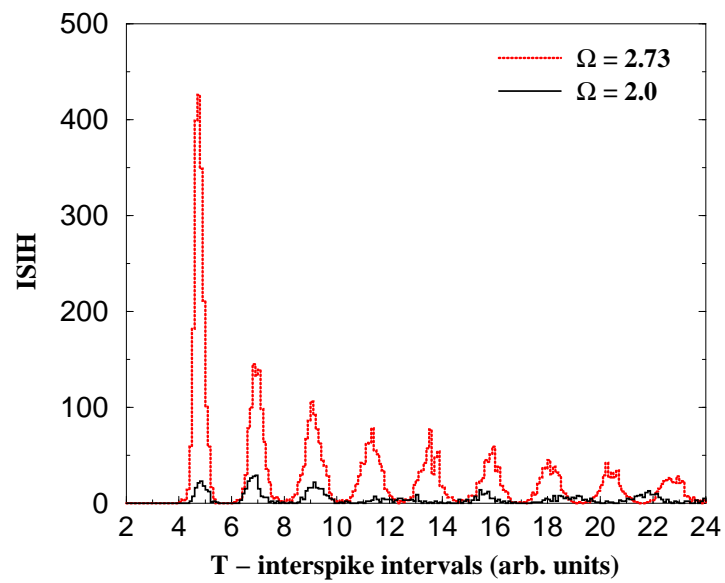


Figure 2.21: ISIH by forcing of the excitable FHN system in ( $\Omega = 2.73 = \Omega_C$ ) and out of the Canard resonance ( $\Omega = 2.0 \neq \Omega_C$ ). The other common parameters are  $\varepsilon = 0.1$ ,  $a = 1.01$ ,  $\sigma_a^2 = 0.000375$ ,  $A = 0.007$ ,  $\omega = 0.251$  and  $B = 0.025$  (as in Fig. 2.17).

## Chapter 3

# Noise-induced signal processing in systems with complex attractors

Typically, studies of SR do not demonstrate a sensitive dependence on the frequency of the forcing. Partially this is caused by using an adiabatic approximation which is applied to get analytic results about SR. There are only some investigations in which the frequency of the signal is the essential parameter. Gang et al. [128] have shown that SR in specifically globally coupled large bistable systems with two series of cells demonstrates the bell-shaped dependence on the signal frequency. Lindner et al. [129] have shown the amplification of the spectral power at particular frequencies in small arrays of underdamped monostable oscillators. The role of the signal frequency for *excitable* systems has been studied for isolated FHN [84–89], when the characteristic time of the system, defined by an external period providing the maximal level of synchronization, practically coincides with the excursion time of an excitable element, and this time is the single natural reference point for time scale. Such a form of frequency selectivity can also be important for biological membranes in enzymatic systems [90]. In other studies the frequency sensitivity in weak signal processing results from a resonance between small oscillations around steady state and a signal [91–94]. Hence, despite different excitation mechanisms, the oscillation frequency is defined by the parameters of isolated elements. On the other hand, our mechanism of frequency-selective SR is based on the appearance of new resonance frequencies due to special phase relations in an inhibitor-coupled array.

Oscillatory media with inhibitor-coupling have very rich dynamics and have been reported to be important in numerous physical [97], electrical [98], and chemical systems [99, 100]. To be specific, the inhibitory form of coupling is used to explain morphogenesis in Hydra regeneration and animal coat-pattern formation [130], or to provide the understanding of pattern formation in an electron-hole plasma and low temperature plasma [97]. In chemistry, the effective increase

of inhibitor-diffusion by reduction of activator-diffusivity via the complexation of iodide (activator) with the macromolecules of starch results in a Turing structure formation [131].

It has been shown that the dominance of such a coupling between identical oscillators results in the generation of many stable limit cycles with different periods and phase relations [95, 96]. This type of diffusion is referred to as the class of “dephasing” interaction because there is a large area of the phase space where the phase points repel each other due to this interaction. Dephasing is a source of multi-rhythmicity, which was observed in different systems [132–135] and leads to a broad spectrum of additional frequencies in the system’s behavior. For excitable noisy elements the dephasing interaction of stochastic limit cycles (instead of deterministic ones) may provide coexistence of spatiotemporal regimes which are selectively sensitive with respect to the period of external signals. In these systems noise plays at least two roles: (i) it stimulates firings of stable elements and, consequently, their interaction during return excursion and (ii) it stimulates transitions between coupling-dependent attractors if they occur and have visible life times.

In this part I investigate the influence of the signal frequency in the SR effects in a system of inhibitor-coupled excitable oscillators. The discussion to this part is structured as follows. After the explanation of the model equations and the method used to estimate signal processing (chapter 3.1), I review the classical SR effect in an isolated excitable oscillator in chapter 3.2 to emphasize the difference with the selective SR in a coupled system. Then I study in chapter 3.3 a chain of two identical inhibitor-coupled excitable oscillators. In this situation the phase relation becomes important for the resonance frequency and the anti-phase motion exhibits another resonance frequency than that of an isolated oscillator. In contrast to an isolated oscillator, the ensemble reacts very sensitively upon the new resonance frequency of the anti-phase attractor. This new frequency selectivity can be used for an enhancement of the signal processing and information transmission in the SR effect at this new resonance frequency. After that, I study in chapter 3.4 a chain of three coupled elements with a richer spectrum of the phase relations and the frequencies. Beside the anti-phase motion (two in-phase oscillators are in anti-phase with the third one), this system demonstrates the so-called “dynamic trap” regime in which the middle element does not produce spikes because of anti-phase motion of neighbors. This additional resonance frequency of the ensemble permits demonstration of frequency-selective modifications of the signal processing.

### 3.1 The model

I study several rather simple small arrays of inhibitory diffusively-coupled stationary but very strongly excitable FitzHugh Nagumo models (FHN) under the action of white additive noise and subthreshold periodic signal which is applied to one of the elements. I show that for some values of the signal period the dependence of SR measures on the noise level has a second maximum and the dependence of SR on the values of the signal period under some fixed noise resembles the conventional resonance.

In order to get the reference frame for further comparisons, I begin with study of the dependence of classical SR on the signal period in the simplest version of the FHN model. The previous investigation [85] was very limited in relation to the value of the periods studied. The model is given by the following Eqs.:

$$\varepsilon \frac{dx}{dt} = y - \frac{x^3}{3} + x, \quad (3.1)$$

$$\frac{dy}{dt} = a - x + \xi(t) + A \sin\left(\frac{2\pi}{T_s} t\right). \quad (3.2)$$

Following a cooperation with a group in Moscow, Russia, here I have adapted some signs in Eqs. (3.1) and (3.2) in comparison with the previously-used differential equations (2.1) and (2.2) for the FHN model to make the results comparable. The small changes lead only to a reflexion of the nullclines in the phase plane at the ordinate and do not influence the qualitative dynamics of the model. Further, I express the circle frequency  $\omega$  in Eq. (3.2) by the period  $T_s$ :  $\omega = \frac{2\pi}{T_s}$ . This should assist a better recognition of the different periods in the multi-rhythmic system. The dynamic of the activator variable  $x$  is much faster than that of the inhibitor  $y$ , as indicated by the small time-scale-ratio parameter  $\varepsilon$ . I fix  $a$  close to the bifurcation in the interval  $a \in [1.01, 1.03]$  (excitable regime) in order not to use high-level noise to excite oscillations and thereby to avoid masking of the fine structure of the interspike intervals histograms. Here  $\varepsilon$  is in the range  $\varepsilon \in [0.0001, 0.001]$ , which is significantly smaller compared to those that are commonly used and which I use in chapters 2 and 4. Such a stiff excitation is needed to provide fast jumping between the attractors. The stochastic forcing is represented by Gaussian white noise  $\xi(t)$  with zero mean and intensity  $\sigma_a^2$ :  $\langle \xi(t)\xi(t') \rangle = \sigma_a^2 \delta(t - t')$ . The harmonic signal is subthreshold,  $A < a - 1.0$ . To evaluate the amplitude of the input frequency in the output signal, I calculated the linear response  $Q$  [39, 40] at the input frequency  $\omega = \frac{2\pi}{T_s}$  according to the Eqs. (2.3) - (2.5) but with respect to the activator variable  $x(t)$ .

### 3.2 Classic Stochastic Resonance in an isolated FitzHugh-Nagumo model

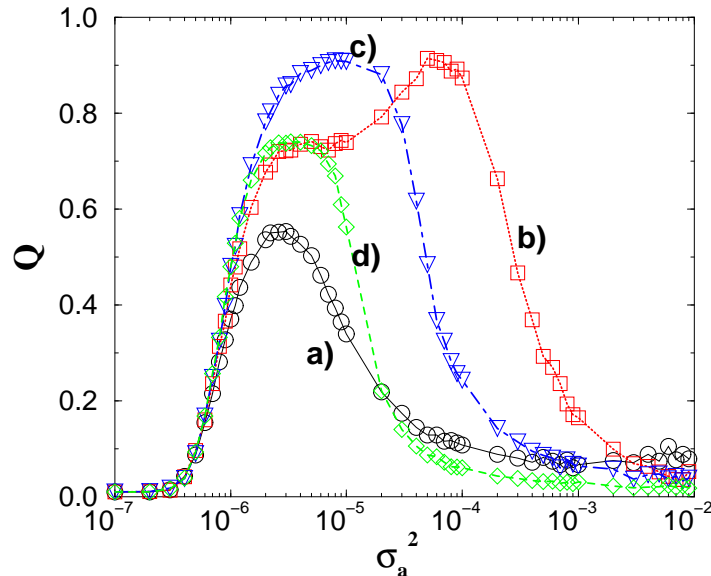


Figure 3.1: The linear response  $Q$  for an isolated FHN (Eqs. (3.1) and (3.2)) as function of the noise intensity  $\sigma_a^2$  for different signal periods  $T_s = 2.8$  (a), 3.2 (b), 3.4 (c) and 4.0 (d). Other parameters are  $a = 1.02$ ,  $\varepsilon = 0.0001$ ,  $A = 0.01$ .

Fig. 3.1 shows the dependence of the linear response  $Q$  on the noise amplitude for different values of the signal period. All curves demonstrate standard SR behavior, but the influence of the period is not weak especially for  $T_s = 3.2$  which corresponds to the duration of excursion time after firing  $t_e$ . For this period the optimal signal amplification takes place in a broad range of noise amplitude. Further on, the resonance frequency depends on the noise intensity  $\sigma_a^2$  and hence the driving period  $T_s$  can be in resonance only at a suitable range of  $\sigma_a^2$  and not overall [Fig. 3.1(b)]. This explains the appearance of the additional maximum in the dependence for  $T_s = 3.2$ . A detailed investigation of the resonant forcing of an isolated FHN can be found in Ref. [85]. Under strong noise, the realizations of stochastic cycles are very similar to corresponding noisy limit cycle (e.g. with  $A=0.99$ ) and the dependence of the linear response  $Q$  on the period under fixed large noise contains the conventional main resonance and secondary resonances at  $T=1.6, 1.08$ , at least [Fig. 3.2].

A conventional resonance occurs when the time moments of the end-of-phase point excursions coincide with “negative” phase of the signal, which significantly facilitates the next firing ( $a$  is shifted closer to 1.0). Fig. 3.2 illustrates that if the signal period is one half or one third of the excursion time  $t_e$  then the secondary resonances occur.

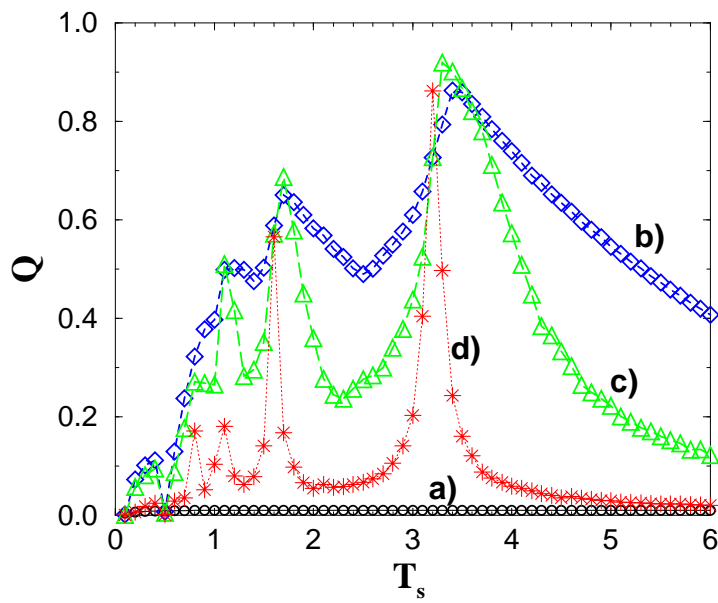


Figure 3.2: The dependence of the linear response  $Q$  for an isolated FHN (Eqs. (3.1) and (3.2)) on the signal period  $T_s$  for several values of the noise level  $\sigma_a^2 = 0.0$  (a),  $3 \times 10^{-6}$  (b),  $1 \times 10^{-5}$  (c),  $1 \times 10^{-4}$  (d).

### 3.3 Frequency-dependent Stochastic Resonance in two coupled oscillators

Now I consider two identical and coupled elements and introduce the diffusion of the inhibitory variables:

$$\varepsilon \frac{dx_{1,2}}{dt} = y_{1,2} - \frac{x_{1,2}^3}{3} + x_{1,2}, \quad (3.3)$$

$$\frac{dy_{1,2}}{dt} = a - x_{1,2} + \xi_{1,2}(t) + A_{1,2} \sin\left(\frac{2\pi}{T_s}t\right) + D(y_{2,1} - y_{1,2}), \quad (3.4)$$

where the signal is applied only to the first element ( $A_1 = 0.01$  and  $A_2 = 0.0$ ), and  $\langle \xi_i(t)\xi_j(t') \rangle = \sigma_a^2 \delta(t-t')\delta_{i,j}$ . The parameter  $D$  denotes the coupling strength and is fixed to  $D = 0.1$ .

I investigate the dynamics of Eqs. (3.3) and (3.4) in the same region of the signal periods and noise levels as in Figs. 3.1 and 3.2. Fig. 3.3 presents the dependence of  $Q$  on the noise intensity for  $T_s = 3.2 - (a)$  and  $T_s = 4.2 - (b)$ .

Under the action of weak noise the first element shows SR at any  $T_s$  and the transmission of the signal to the second element is observed starting from the SR-optimal noise. For standard SR a further evolution of  $Q$  with noise for both element should be a continuous decreasing of  $Q$ . The same is true for the elements coupled via their fast variables, but the inhibitor-coupled relaxation excitable elements demonstrate a large second peak. Numerical simulations have shown that the second resonance peak appears for driving periods  $T_s$  between 4.2 and 4.5 [Fig. 3.3(b)]. The nature of this peak is the noise-induced anti-phase stochastic cycle in the presence of the coupling. It has been shown recently that in a broad interval of noise amplitudes the anti-phase cycle dominates and results in a new type of coherence resonance [136]. The period of this cycle depends on the coupling strength and the noise amplitude which define the position of the second peak on the curve  $Q(\sigma_a^2)$  in Fig. 3.3(b). The influence of the stiffness is also essential because for  $\varepsilon > 0.001$  the second peak cannot be clearly observed, but the rate of  $Q(\sigma_a^2)$  decreasing is less than that for standard SR [Fig. 3.1]. A similar double maximum in the power spectral amplitude at the forcing frequency as a function of the noise intensity has been found recently but for an underdamped bistable system where two maxima are linked with two noise-induced motions: intrawell and interwell [119]. These results show that one can use inhibitor-coupled oscillators for frequency selection in Stochastic Resonance. It is noteworthy that a multi-peak *coherence* resonance has also been observed in coupled FHN models [137].

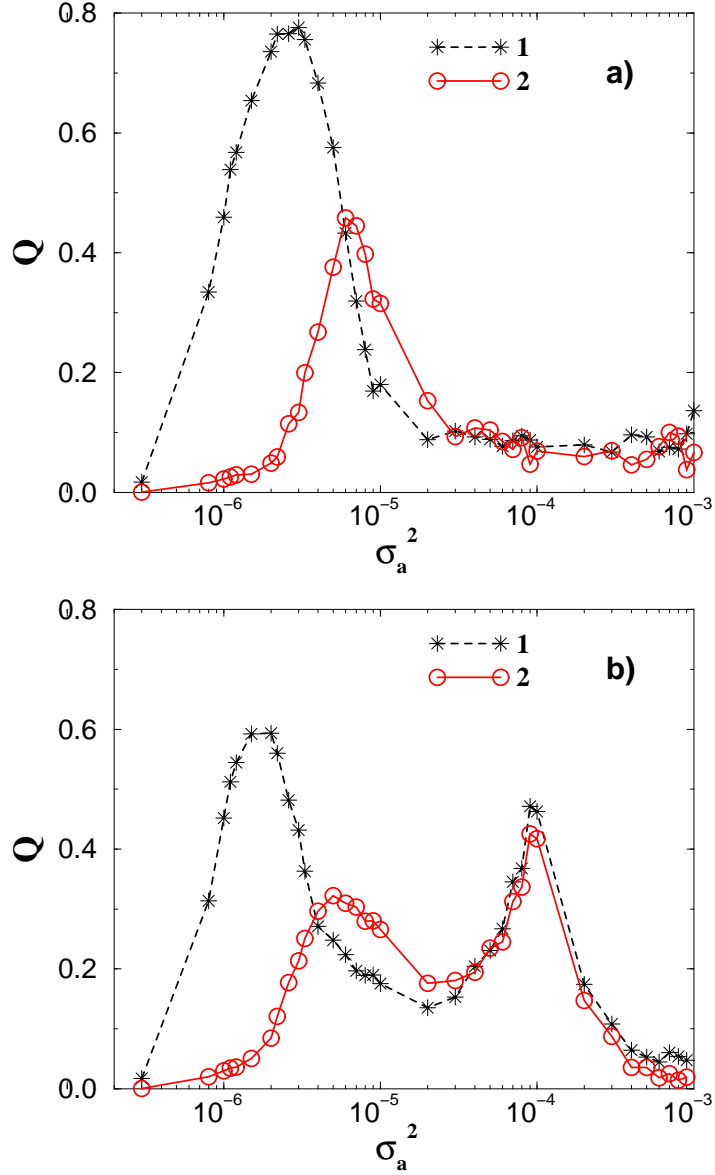


Figure 3.3: The linear response  $Q$  for two inhibitor-coupled FHN's (Eqs. (3.3) and (3.4)) as function of the noise intensity for signal periods  $T_s = 3.2$  (a) and  $T_s = 4.2$  (b). Other parameters are  $a = 1.02$ ,  $\varepsilon = 0.0001$ ,  $A_1 = 0.01$ ,  $A_2 = 0.0$  and  $D = 0.1$ .

### 3.4 Frequency-dependent Stochastic Resonance in a chain of three oscillators

Three identical coupled elements in a chain can demonstrate a richer set of regimes which depend on the configuration:

$$\varepsilon \frac{dx_{1,2,3}}{dt} = y_{1,2,3} - \frac{x_{1,2,3}^3}{3} + x_{1,2,3}, \quad (3.5)$$

$$\frac{dy_1}{dt} = a - x_1 + \xi_1(t) + A_1 \sin\left(\frac{2\pi}{T_s}t\right) + D(y_2 - y_1), \quad (3.6)$$

$$\frac{dy_2}{dt} = a - x_2 + \xi_2(t) + A_2 \sin\left(\frac{2\pi}{T_s}t\right) + D(y_1 - y_2) + D(y_3 - y_2), \quad (3.7)$$

$$\frac{dy_3}{dt} = a - x_3 + \xi_3(t) + D(y_2 - y_3), \quad (3.8)$$

where  $\langle \xi_i(t)\xi_j(t') \rangle = \sigma_a^2 \delta(t-t')\delta_{i,j}$ .

Let us analyze possible attractors in the autonomous system of three inhibitor-coupled identical oscillators. For a linear chain of oscillators whose bifurcation parameters are close to Hopf bifurcation, three main types of stable attractors occur [138]. The first is in anti-phase regime in which oscillators at the ends move in anti-phase with the middle one. The second type was called “dynamic trap” because the anti-phase motion of the end’s oscillators does not permit the firing of the middle one. The third type is not a single attractor but a family of attractors which may be designated as “ $n/2/n$ ”, where  $n = 3, 5, 7, \dots$ . The value of  $n$  depends on the coupling strength and the distance of  $a$  from the bifurcation value. The closer  $a$  is to 1.0 (for FHN model), the larger is the value “ $n$ ” and the stronger is the crowding of attractors. If the elements do not oscillate deterministically but are excited by noise, then the observed stochastic collective modes only partially resemble these types of regimes due to noise-dependent perturbations of trajectories. The attractors “ $n/2/n$ ” will be practically corrupted by noise. This type of multimodal distribution is not model-specific and was observed for auto-oscillating [139] and excitable [140] electronic arrays with dephasing (inhibitory) interactions.

Fig. 3.4 shows the distribution of interspike intervals (ISIs) for 3 coupled excitable elements without an external signal. It can be clearly seen that only two stochastic attractors are really manifested in the ISI distributions. In the dynamic trap, in which the first and the third oscillator are moved in average in anti-phase, their interspike intervals are around  $T \approx 3.0$  that is very close to the excursion time  $t_e = 3.2$ . Since the system is symmetric, the ISI histograms of the first and third element are identical. In this regime the ISI distribution for the middle element is very broad and polymodal. There are only infrequent realizations with very large ISI for the second element. In the anti-phase regime,

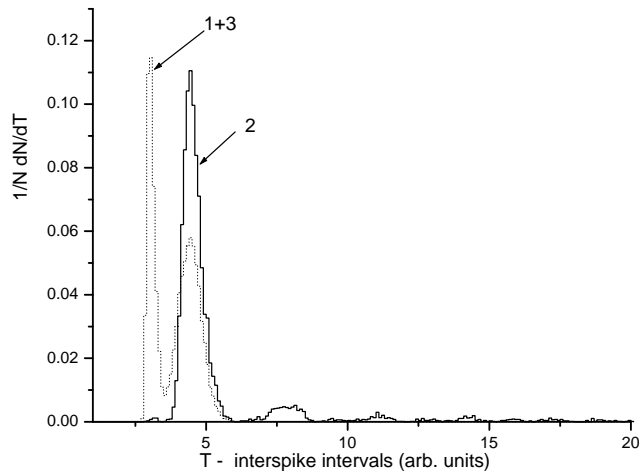


Figure 3.4: The ISI distributions for a chain of 3 coupled excitable elements (Eqs. (3.5) - (3.8)) and no signal ( $A_{1,2} = 0.0$ ). The ISI distributions of the first and the third (1+3) oscillator are denoted by a dashed line and the second one (2) by a solid line. The other parameters are  $a = 1.02$ ,  $D = 0.1$ ,  $\sigma_a^2 = 10^{-4}$  and  $\varepsilon = 0.0001$ .

in which the first and the third oscillator are moving in average in-phase but in anti-phase with middle oscillators, they all have the same average period about  $T_{anti} \approx 4.2$  under the given set of the other parameters. Fig. 3.5 shows typical selected time series of the inhibitor variables  $y(t)$  of the three coupled oscillators related to the two main phase regimes, anti-phase motion Fig. 3.5(a) and dynamic trap Fig. 3.5(b).

The life-times and periods of attractors depend on the coupling strength and noise values which may be adjusted to enhance (or to inhibit) the acceptance of a sinusoidal signal of a given period. To check this possibility, I calculate  $Q(\sigma_a^2)$  for different signal periods and present results which clearly reflect the specific modification of signal acceptance. I consider two cases:

*Case 1:* The harmonic signal with  $A_1 = 0.01$  is applied only to the first oscillator ( $A_2 = 0.0$ ). The corresponding dependencies of the linear response, measured for all three oscillators, are shown in Fig. 3.6 for different periods of the external signal  $T_s$ . As discussed above, we have in this system two noise-supported attractors: a dynamic trap ( $T = 3.0 - 3.6$ ) and an anti-phase attractor ( $T \approx 4.2$ ). These two time scales demonstrate themselves also in the frequency selectivity by signal processing. If the signal period  $T_s < 3.0$  (e.g.  $T_s = 2.8$ ) or  $T_s > 5.5$ , the behavior of  $Q_1(\sigma_a^2)$  is quite similar to that of isolated FHN and  $Q_2 \approx Q_3$  have only one peak as in the classical SR [Fig. 3.6(a) and (f)]. If the signal period is in the interval  $T_s \in [3.0, 3.4]$  then  $Q_1$  declines sharply in

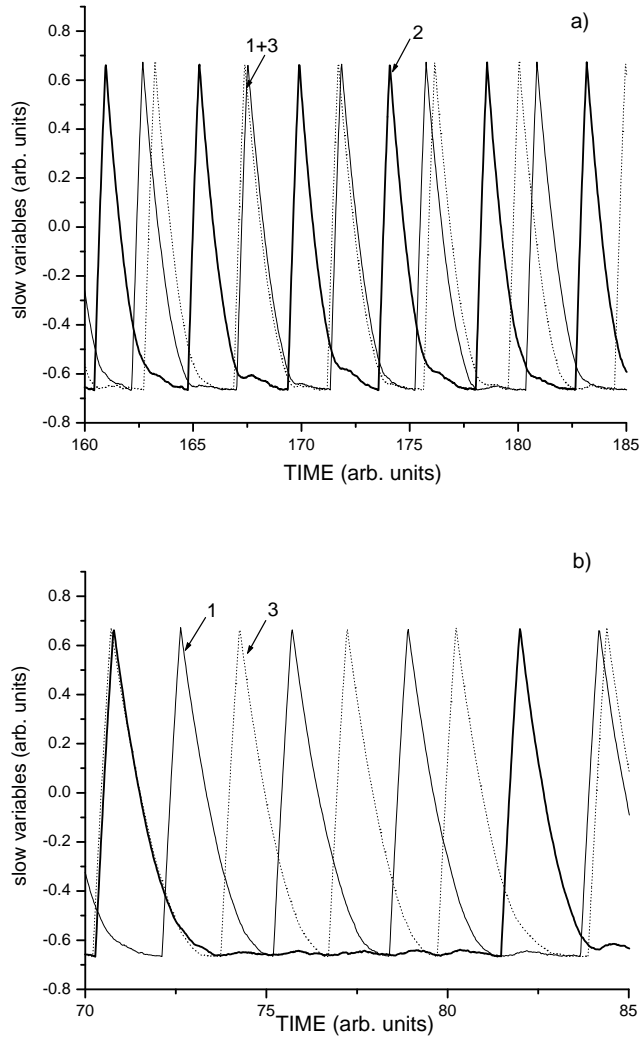


Figure 3.5: The time-series intervals selected from trajectory giving ISI distribution of Fig. 3.4. They present the anti-phase regime (a) and “dynamic trap” (b). The parameters are  $a = 1.02$ ,  $D = 0.1$ ,  $\sigma_a^2 = 10^{-4}$ ,  $\varepsilon = 0.0001$  and  $A_{1,2} = 0.0$  (no signal).

comparison with an isolated FHN in Fig. 3.1 but  $Q_3$  dramatically increases for noise amplitudes in the interval  $\sigma_a^2 \in [10^{-5}, 5 \times 10^{-5}]$  [Fig. 3.6(b), (c) and (d)], i.e. the signals with these periods easily penetrate through the middle element and are selectively manifested in the time series of the third oscillator. For  $T_s > 3.6 Q_3$  decreases again [Fig. 3.6(e)]. The reason for this phenomenon is the coincidence of the signal period with the average values of the interspike intervals of the stochastic dynamic trap [Fig. 3.5(b)]. In this regime the average ISI of the first and the third element are equal and their interspike distributions are significantly

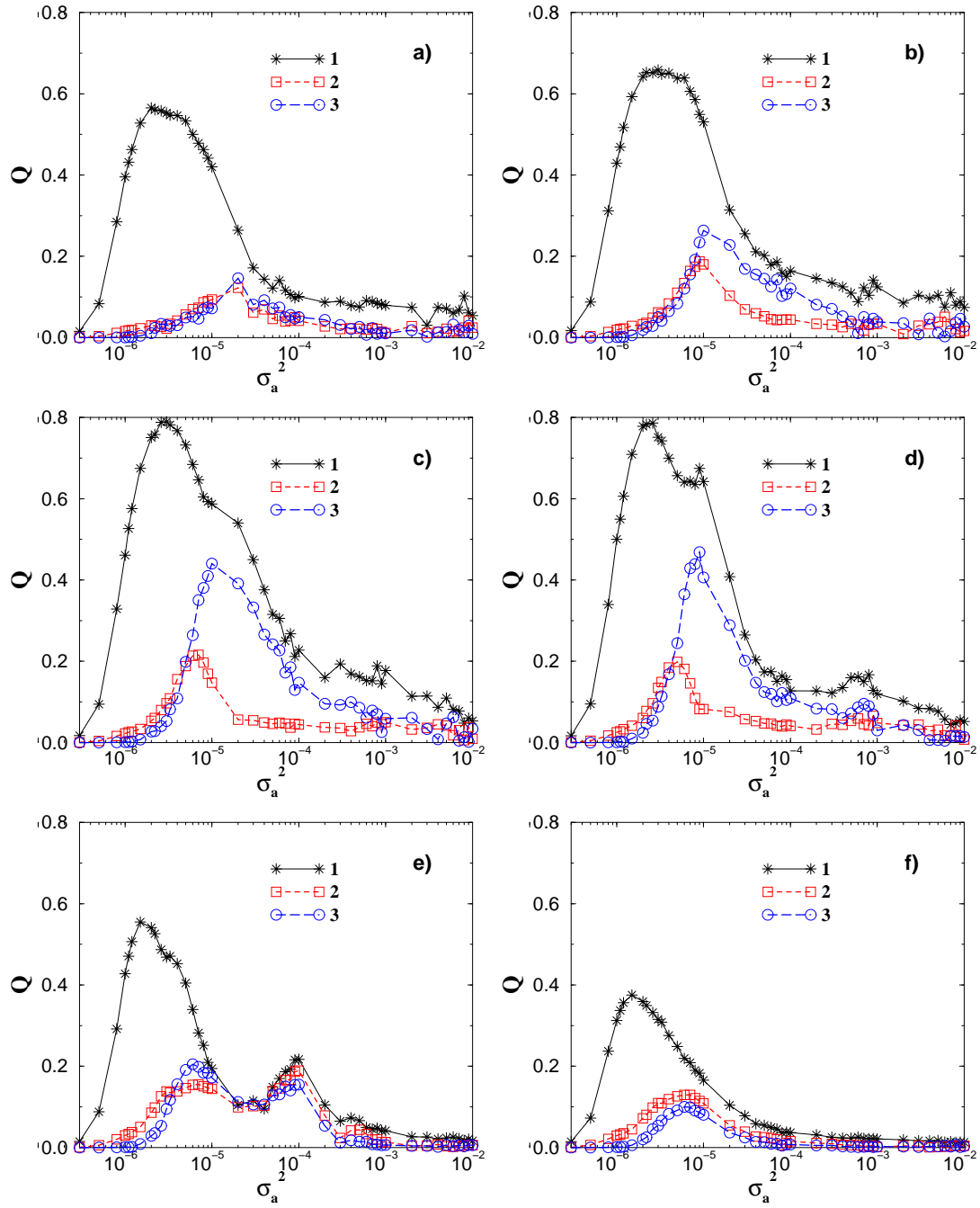


Figure 3.6: The dependencies of the linear response  $Q$  for a chain of 3 elements (Eqs. (3.5)-(3.8)) as a function of the noise intensity for different signal periods:  $T_s = 2.8$  (a), 3.0 (b), 3.2 (c), 3.4 (d), 4.5 (e), 6.0 (f);  $a = 1.02$ ,  $\varepsilon = 0.0001$ ,  $D = 0.1$ . The signal of the amplitude  $A_1 = 0.01$  is applied to the first oscillator only ( $A_2 = 0.0$ ).

narrower than that of the second element. Therefore, the signal manifestation in the behavior of the second oscillator is small for this interval of the signal period.

If the noise amplitude is larger than  $5 \times 10^{-6}$ , the average activation time of excitation is small and several stochastic attractors may occur, but the harmonic signal supports those which have a similar value of average period. The next stochastic attractor which has a noticeable life-time (not very sensitive to noise) under stronger noise is the anti-phase oscillation with the average period  $T_{anti} \approx 4.2$ . The second peak on the curves  $Q_i(\sigma_a^2)$  at  $T_s = 4.0-4.5$  at about  $\sigma_a^2 \approx 2 \times 10^{-4}$  is realized for all oscillators [Fig. 3.6(e)], because the average ISIs are the same for all elements in this regime [Fig. 3.5(a)]. All the three oscillators generate similar spike sequences and hence perform with nearly the same linear response  $Q$ . For the current model and the given set of other parameters, the distance between the ISIs of the two different phase regimes (anti-phase and dynamic trap) is not large [Fig. 3.4] and the selectivity of signal enhancement is limited by noise-induced transitions between these regimes.

*Case 2:* The harmonic signal is applied only to the middle element ( $A_1 = 0.0$  and  $A_2 = 0.015$ ). This example of the selective enlargement of  $Q(\sigma_a^2)$  is presented in Fig. 3.7(a,b). For  $T_s = 3.2$ , which corresponds to the maximal manifestation of the signal in the behavior of an isolated oscillator up to noise amplitude  $10^{-4}$  [Fig. 3.1], the function  $Q_2$  dramatically decreases if the noise is around  $10^{-5}$ . Such behavior reflects the absence of small ISIs in the time series of the second element after this noise value. The increase of signal period up to  $T_s = 4.5$  results in the appearance of the second peak on all curves  $Q_{1,2,3}(\sigma_a^2)$  and that is similar to Fig. 3.6(e) except that here  $Q_2$  is larger than  $Q_{1,3}$  because the signal is applied to the middle element of the chain.

Thus, the presence of a double resonant peak structure of  $Q(\sigma_a^2)$  is caused by the coexistence of two stochastic limit cycles which share the phase space due to the inhibitor exchange. In our model the distances between average periods of attractors are not large and therefore the amplitudes of the second peaks in the Figs. 3.3, 3.6 and 3.7 are noticeable but not so pronounced as compared with the standard SR peak which, however, is almost the same for any values of the external periods.

The attractors differ not only by periods but by phase relations as well; that opens the possibility for additional checking of our explanation by the simultaneous application of two harmonic subthreshold signals with appropriate phase shift. For instance, the second peak on the  $Q_{1,2,3}$  has a larger height if two signals are applied to the end's oscillators in-phase, but  $Q_{1,2,3}$  is almost negligible if the same signals are in anti-phase each other.

The manifestation of the described effects depends not only on the stiffness but on the other model parameters too: the coupling strength and the proximity of  $a$  to the bifurcation value. These studies have shown that the results are retained under a 2-fold changing of coupling and the difference ( $a - 1.0$ ).

*In summary,* I have demonstrated the frequency-selective response and in-

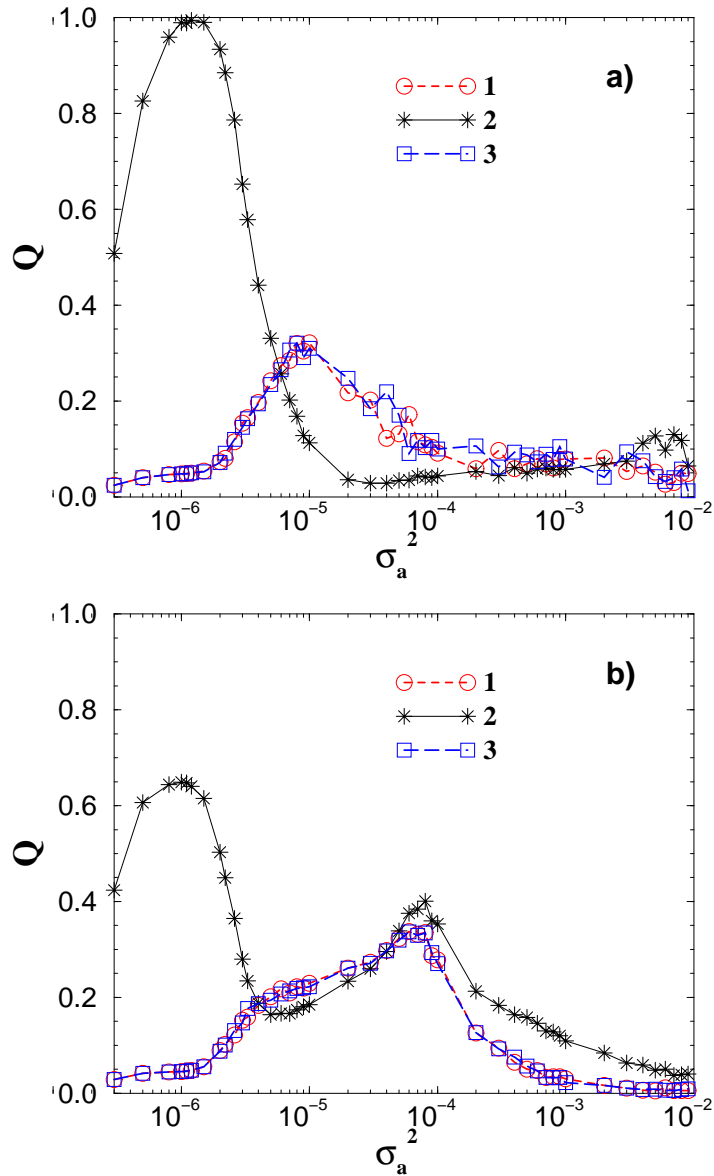


Figure 3.7: The linear response  $Q$  as a function of the noise intensity for signal periods  $T_s = 3.2$  (a) and  $T_s = 4.5$  (b).  $a = 1.02$ ,  $\varepsilon = 0.0001$ ,  $D = 0.1$ . The periodic signal  $A_2 = 0.015$  is applied only to the middle oscillator ( $A_1 = 0.0$ ).

formation propagation in a noisy system which consists of inhibitor-coupled excitable units and is driven by a subthreshold harmonic signal. The signals with periods from some intervals (e.g.  $T_s \in [4.0, 4.5]$ ) may be enhanced not only for small but also for larger noise which are typically ineffective for standard SR. The signals with shorter periods (e.g.  $T_s \in [3.0, 3.2]$ ), which are the most effective for SR, may be strongly inhibited under some noise levels in comparison with an iso-

lated FHN in Fig. 3.1. The background of the selectivity is the multi-rhythmicity generated by the inhibitor-coupling in combination with the high stiffness of elements which provides the fast transitions between stochastic attractors.

The mechanism of this selectivity can be explained by the appearance of new resonance frequencies of the coupled system which are caused by different phase relations of the oscillators and differ from the resonance frequency of an isolated FHN. Especially the resonance frequencies of the anti-phase and dynamic trap regime exhibit stable attractors in a noisy environment. By forcing one element of the network in resonance with these coupled dependent resonance frequencies, we observe an additional resonance peak in the SR curve besides the typical bell-shaped curve of standard SR. Another interesting phenomenon which I have explained is the masking of the information flow in the dynamic trap regime. In this effect, the last oscillator in the row shows a much better response at the signal frequency which was fed at the first oscillator of the row than the middle one. I believe that study of the frequency-selective SR and the masking of information flow in an array due to inhibitor-coupling can be useful for understanding of multi-frequency information exchange mechanisms in neural networks. Because of the generality of these effects for diffusive coupled activator-inhibitor oscillator arrays and not only to FHN systems, I expect that the findings can be applied also in other fields, e.g. in chemistry or biology.

It is important to note that these results contribute also to the study of fundamental synchronization phenomena [141]. In frames of this study SR can be considered as a synchronization-like phenomenon, in which optimal noise induces phase synchronization between output and input signal. In Ref. [142] it has been shown that in deterministic systems of coupled elements, synchronization can happen through the asynchronized region. The effect, considered here, demonstrates a synchronization-like behavior through the dynamic trap, and can be considered as a stochastic analogue of this kind of phase synchronization in deterministic systems.

The next chapter concerns a noise-induced phase transition to an excitable regime. The difference from to the previously-investigated noise-driven effects consists in the fact that the excitable property is evoked by noise itself and vanishes in the absence of noise.

# Chapter 4

## Noise-induced excitability and related effects

### 4.1 Phase transition to excitability generated by multiplicative noise

Recent investigations have shown that parametric noise is able to induce a *bona-fide transition* from an excitable to an oscillatory regime, via a renormalization of the parameters defining the local dynamics of the system [71, 72]. This mechanism has also been found responsible for inducing excitability in bistable [73, 74] and subexcitable [71, 101] media. In all those cases, however, noise has the expected role of increasing dynamical instability. In this chapter I show, on the other hand, that certain types of noise operate in the opposite direction of constructive influence, namely enhancing stability in the system. In particular, I demonstrate that random fluctuations can induce a transition from oscillatory to excitable behavior, by stabilizing a deterministically unstable fixed point of the dynamics, while preserving the overall phase space structure that leads to large amplitude pulses (but which will then be triggered only by above-threshold perturbations). In contrast to previous results on noise-induced excitability, spatial coupling is absolutely essential in this case, in order to prevent noise-driven oscillations from exciting the system and converting it back into an oscillator. In that sense, coupling plays here a role similar to that of standard phase transitions, suppressing fluctuations and coupling the stable regions. It prevents the system from visiting the whole available phase space and locks it close to the stable steady state (until a perturbation triggers an excitable spike). Noise-induced phase transitions between homogeneous phases have long been known to use the joint action of coupling and noise in this way [62, 65]; here I extend this fundamental mechanism to the field of excitable dynamics.

To demonstrate this noise-induced excitability (NIE) I consider a system of coupled FitzHugh-Nagumo (FHN) elements in the oscillating state and under

the action of multiplicative noise. The mechanism of a noise-induced phase transition is explained theoretically in the framework of a small-noise-expansion of the model, which extracts the systematic contribution of the multiplicative noise accounting for the excitability restoration. The excitable character of the noise-induced regime is demonstrated by showing the existence of Stochastic Resonance and wave propagation through the system in the following chapters 4.2 and 4.3.

### 4.1.1 The model with noise-induced excitability

I analyze the following set of  $N$  coupled FHN oscillators:

$$\frac{du_i}{dt} = \frac{1}{\varepsilon}(F(u_i) - v_i) + D_u(\bar{u}_i - u_i), \quad (4.1)$$

$$\frac{dv_i}{dt} = cu_i + d + v_i\xi_i(t) + D_v(\bar{v}_i - v_i), \quad (4.2)$$

where  $\bar{x}_i \equiv \frac{1}{N} \sum_{j=1}^N x_j$ ,  $x_i = u_i, v_i$  and the self-activation term of  $u_i$  is given by a piecewise linear approximation of the cubic function, used in the previous FHN models:

$$F(u) = \begin{cases} -1 - u + b & u \leq -\frac{1}{2} \\ u + b & -\frac{1}{2} < u < \frac{1}{1+a} \\ +1 - au + b & u \geq \frac{1}{1+a}. \end{cases}$$

I use this piecewise linear approximation of the cubic function in Eq. (4.1) instead of a cubic function as in the previous equations for the FHN model (e.g. Eq. (2.1)), in anticipation of a possible analytic approximation of the noise-induced excitability. An analytic approximation of the FHN model without the noise-induced phase transition to the excitability has been given in Ref. [88] for such a piecewise linear approximation of the cubic function. This approximation is based on a time-scale separation between fast and slow variable. Possibly one could find an analytic approximation of the NIE by a combination of the approximation suggested in Ref. [88] and the small-noise-expansion [62]. In a neural context,  $u(t)$  represents the membrane potential of the neuron and  $v(t)$  is related to the time-dependent conductance of the potassium channels in the membrane [18]. The dynamics of the activator variable  $u$  is much faster than that of the inhibitor  $v$ , as indicated by the small time-scale-ratio parameter  $\varepsilon$ . Coupling is considered in both the activator and the inhibitor and is taken to be global, although as I will show later in chapter 4.3, similar results are obtained for local diffusive coupling. The coupling strengths are denoted by  $D_u$  and  $D_v$ . Random fluctuations are represented by the  $\delta$ -correlated Gaussian noise  $\xi_i(t)$ , with zero mean and the correlation  $\langle \xi_i(t)\xi_j(t') \rangle = \sigma_m^2 \delta(t - t')\delta_{i,j}$ . This multiplicative noise term is interpreted in the Stratonovich sense [62].

### 4.1.2 Analytical description of the noise-induced phase transition

I have calculated the non-zero mean of the multiplicative noise term  $v_i \xi_i$  in Eq. (4.2) with help of the small-noise-expansion [62] (see also chapter 1.2.4) by  $\langle v_i \xi_i \rangle = (\sigma_m^2/2)v_i$ . Therefore, in the presence of fluctuations the effective local dynamic of the inhibitor variable is given by  $\dot{v}_i = cu_i + d + (\sigma_m^2/2)v_i$ , at first order in the noise intensity. The corresponding nullclines of an isolated oscillator for increasing multiplicative intensity are represented in the phase plane of Fig. 4.1. Without noise the nullcline for the slow variable  $v$  (curve 1) crosses the nullcline of the fast variable (inverted-N piecewise line) in its middle segment, so that the crossing point is an unstable steady state and the system exhibits an oscillatory behavior. An increase of the multiplicative noise intensity  $\sigma_m^2$  leads to a tilting and shifting of the  $v$ -nullcline [curves 2-4 in Fig. 4.1]. As a result, for large enough  $\sigma_m^2$  (in the present case for  $\sigma_m^2 \gtrsim 0.033$ ) the crossing occurs in the left segment of the  $u$ -nullcline and the fixed point becomes stable.

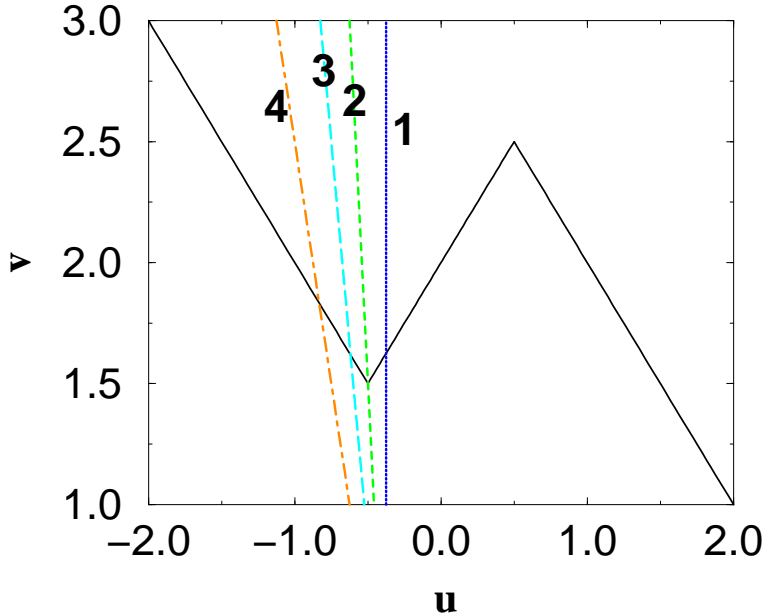


Figure 4.1: Nullclines of a single FHN oscillator in phase space. The inverted-N piecewise line corresponds to the noise-independent nullcline of the activator  $u$ . The other lines (1-4) describe the tilting of the inhibitor nullcline by increasing the noise intensity: 1 -  $\sigma_m^2 = 0.0$ , 2 -  $\sigma_m^2 = 0.0334$ , 3 -  $\sigma_m^2 = 0.06$ , 4 -  $\sigma_m^2 = 0.1$ . Other parameters are  $a = 1.0$ ,  $b = 2.0$ ,  $c = 0.2$  and  $d = 0.075$

Throughout this process, however, the overall phase space structure of the system is not changed, which allows perturbations of the noise-induced stable fixed point to excite large-amplitude excursions towards the right segment of the  $u$ -nullcline (excited branch). In particular, in an isolated oscillator, perturbations

due to the noise itself may induce a stochastic limit cycle which prevents the system from escaping out of the oscillatory regime. In other words, the transition to excitability cannot be observed in isolated oscillators, in spite of the renormalization of the dynamical parameters due to noise. In the presence of coupling, the weight of those oscillators that are not firing prevents these noise-induced excursions and leads to effective excitability.

### 4.1.3 Manifestation of the noise-induced phase transition in the time series

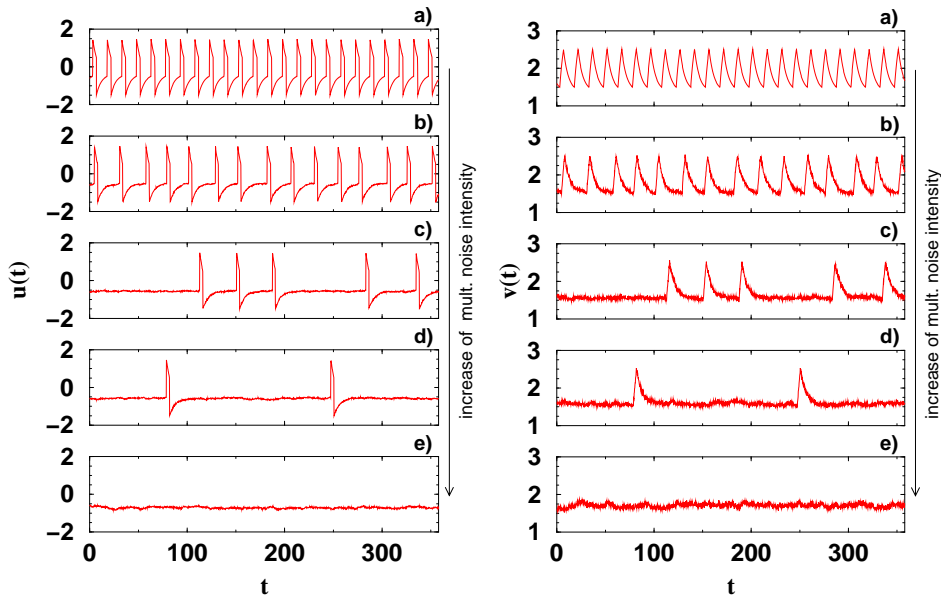


Figure 4.2: Time series of the mean field of the activator variable  $u$  (left) and the inhibitor variable  $v$  (right), with increasing multiplicative noise intensity: (a)  $\sigma_m^2 = 0.0$ , (b)  $\sigma_m^2 = 0.033$ , (c)  $\sigma_m^2 = 0.045$ , (d)  $\sigma_m^2 = 0.05$  and (e)  $\sigma_m^2 = 0.08$ . Other parameters are  $N = 500$ ,  $\varepsilon = 0.01$ ,  $a = 1.0$ ,  $b = 2.0$ ,  $c = 0.2$ ,  $d = 0.075$  and  $D_u = D_v = 100$ .

Figure 4.2 depicts the appearance of NIE, by plotting the time series of the activator's mean field,  $u(t) = (1/N) \sum_{i=1}^N u_i(t)$ , and the inhibitor's mean field,  $v(t) = (1/N) \sum_{i=1}^N v_i(t)$ . Because of the relatively large values of the coupling strengths (which nevertheless have the order of magnitude of  $\varepsilon^{-1}$ ), the time series of the single oscillators differs only very slightly from that of the mean field, i.e. the oscillators are synchronized. Figure 4.2(a) displays the regular self-sustained oscillations of the system without noise. Increasing the multiplicative noise intensity  $\sigma_m^2$  leads to an increase and randomization of the time interval between consecutive spikes, as seen in Figs. 4.2(b–d). Finally, for large enough noise no spike appears [Fig. 4.2(e)]. This corresponds to an oscillation suppression

due to multiplicative noise: the system stays at the noise-induced stable fixed point. But besides an oscillation suppression, the system also exhibits excitable properties when perturbations (other than the stabilizing noise) affect the system. As will be shown below, this noise-induced regime displays Stochastic Resonance when driven periodically (chapter 4.2), and wave propagation in the case of local coupling (chapter 4.3).

#### 4.1.4 The bifurcation diagram

The phase transition and the influence of the number of coupled FHN oscillators can be illustrated by the bifurcation diagrams Fig. 4.3. There the  $v$ -coordinates of intersection point of the trajectory with the inhibitor nullcline (slow variable  $v$ ) are plotted versus the multiplicative noise intensity  $\sigma_m^2$  as the control parameter. The tilting of the inhibitor nullcline due to multiplicative noise is taken into account by the small-noise-expansion [Fig. 4.1]. Thus, every point in the bifurcation diagrams denotes a crossing of the trajectory in the phase space with the line  $u = \frac{-d-(\sigma_m^2/2)v}{c}$ . Time series of 1000 time units were calculated for every parameter set, but the first 100 time units were excluded for the bifurcation diagrams to avoid transient states. Despite the stabilizing property of the multiplicative noise, one can clearly see the stochastic character of the NIE. For finite size the phase transition from the self-sustained (two branches in the bifurcation diagrams) to the noise-induced excitable regime (only one close to the stable fixed point) does not exhibit a sharp boundary and the boundary itself is influenced by the number of coupled FHN oscillators. In an ensemble of 100 coupled FHN oscillators [Fig. 4.3 (top)] one cannot find an explicit phase transition in the multiplicative noise range  $\sigma_m^2 \in [0.0, 0.1]$ . A system consisting of 300 FHN oscillators [Fig. 4.3 (middle)] undergoes the phase transition at  $\sigma_m^2$  between 0.074 and 0.076 and one with 500 FHN oscillators [Fig. 4.3 (bottom)] between 0.064 and 0.066. All the multiplicative noise intensities are greater than the boundary for the phase transition  $\sigma_m^2 \approx 0.033$  predicted by the small-noise-expansion. The reason is that the approximation considers the average systematic action of noise in first order and not the short-time fluctuations in individual oscillators. The dynamic of an individual oscillator in the coupled ensemble is depicted by the example of one selected oscillator in the bifurcation diagram. The fluctuations of an individual oscillator are larger than those of the mean field. The stochastic properties at the noise-induced stable fixed point also mask the phase transition and the oscillation suppression. This effect is especially pronounced in small ensembles, because small fluctuations lead to the reaching of the threshold of some oscillators. If several oscillators occasionally and simultaneously cross the threshold, they produce large spikes and also push the other oscillators above the threshold. As a result, a spike in the mean field can be observed. This is related to the problem, that one can not reliably distinguish a noise-perturbed self-sustained oscillating system and a noise stimulated excitable system by the

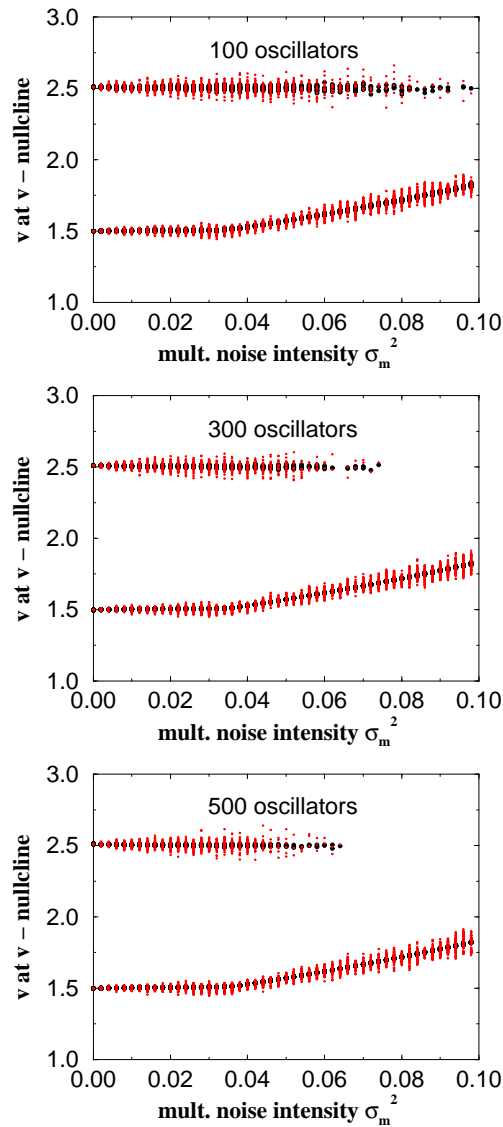


Figure 4.3: The finite size effect in bifurcation diagrams:  $v$ -intersection point of the trajectories with the  $v$ -nullcline versus multiplicative noise intensity  $\sigma_m^2$ . The bold filled circles denote the intersection point of the mean field of the inhibitor variable  $v$  and the small points that of an exemplary chosen oscillator. The number of coupled FHN oscillators is increased from 100 (top), 300 (middle) up to 500 (bottom). The other parameters are  $\varepsilon = 0.01$ ,  $a = 1.0$ ,  $b = 2.0$ ,  $c = 0.2$ ,  $d = 0.075$  and  $D_u = D_v = 100$  (same as in Fig. 4.2).

resulting time series. The probability of such an event decreases with an increase of oscillator numbers and larger threshold of excitation, i.e. larger multiplicative noise  $\sigma_m^2$ .

### 4.1.5 Phase diagrams

In order to describe quantitatively the transition towards excitability, I compute the relative resting time with respect to the whole measuring time. Due to the random character of the time series, I need to specify a measurement threshold. I define the resting time with two different conditions: weak as the interval during which every oscillator fulfills condition  $u_i < -0.5$  and strong, if  $u_i < -0.5$  and  $v_i \leq 1.85$ . The first weak requirement corresponds to the absence of spikes, and hence measures the noise-induced oscillation suppression, and the second checks additionally the absence of large excursions towards the left on the left branch of the  $u$ -nullcline. Such excursions would lead to a large excitation threshold and weaken the system's excitability. The threshold for the relative resting time is set to 0.98.

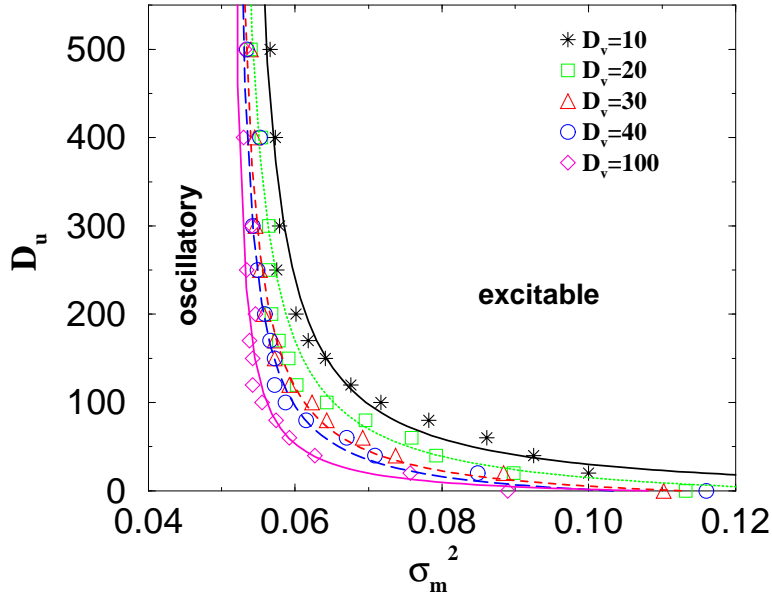


Figure 4.4: A phase diagram for the transition from a self-sustained oscillatory regime to NIE. Coupling strength  $D_u$  versus multiplicative noise intensity  $\sigma_m^2$  for 300 coupled elements and for different coupling strengths  $D_v$ . The excitable state is defined, if oscillators fulfill the condition  $u_i < -0.5$  for 98% of time. The solid lines denote an approximation of the boundary of phase transition.

According to the previous definitions, Figs. 4.4 and 4.5 display a phase diagram in the plane of parameters  $D_u - \sigma_m^2$  distinguishing the regions where the original oscillatory behavior and the noise-induced excitable (NIE) regime exist for different inhibitor coupling strengths  $D_v$ . The boundary at  $\sigma_m^2 \approx 0.06$  of the NIE corresponds basically to the condition  $u_i < -0.5$ , and the right one of the NIE balloon in Fig. 4.5 to  $v_i < 1.85$ . The difference in the boundary at  $\sigma_m^2 \approx 0.06$  between the weak and strong condition can be understood as follows:

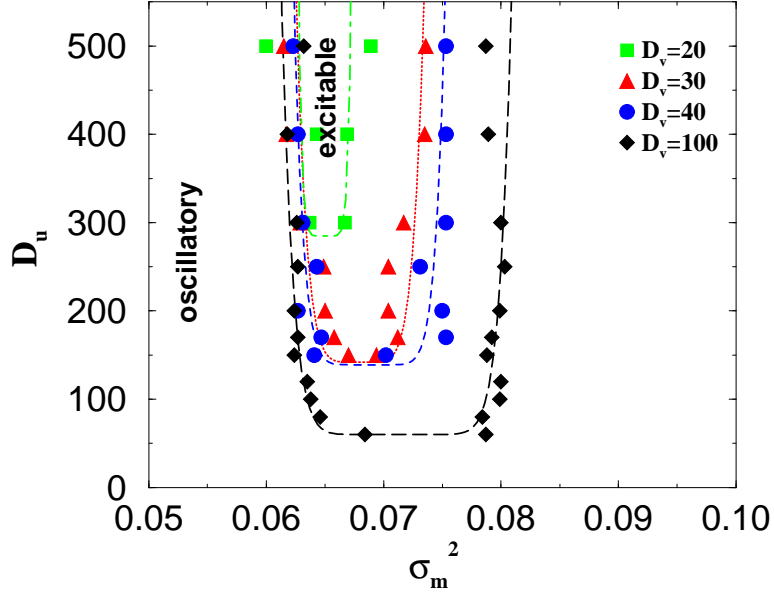


Figure 4.5: A phase diagram for the transition from a self-sustained oscillatory regime to NIE. Coupling strength  $D_u$  versus multiplicative noise intensity  $\sigma_m^2$  for 300 coupled elements and for different coupling strengths  $D_v$ . The excitable state is defined, if oscillators fulfill the condition  $u_i < -0.5$  and  $v_i \leq 1.85$  for 98% of time. The splines are fitted polynomials to approximate the boundary of phase transition. For inhibitor coupling  $D_v = 10$  no NIE can be observed in the depicted parameter plane  $D_u - \sigma_m^2$ .

The threshold for the relative resting time of 0.98 permits the oscillators to stay 2% of the time outside the resting conditions. Consequently some infrequent noise-stimulated spikes can occur in the NIE state. The NIE, defined with strong conditions, excludes a larger part of the trajectory of a spike because a significant fracture of the left branch of the activator nullcline ( $\dot{u}(t) = 0$ ) is outside of the additional strong condition  $v_i \leq 1.85$ , whereas the weak condition includes this nullcline completely. Hence, the strong condition excludes a part of the recovery time which is related to the movement on the left branch of the  $u$ -nullcline. The recovery time depicts a significant time of the spike cycle due to the relatively slow movement along this branch of the  $u$ -nullcline caused by the small time-scale separation factor  $\varepsilon = 0.01$ . As a result, the 98% threshold for the relative resting time admits more infrequent spikes at the weak NIE condition than at the strong one and so the boundary oscillatory  $\rightarrow$  NIE is slightly shifted to a higher multiplicative noise intensity  $\sigma_m^2$  in Fig. 4.5 then in Fig. 4.4. The NIE region shrinks in size as  $D_v$  decreases. In other words, minimum coupling strengths of both the activator and the inhibitor are required for the NIE regime to exist.

Figure 4.6 pictures the dependence of the transition to NIE on the number of coupled elements of the system. As in standard phase transitions, the region

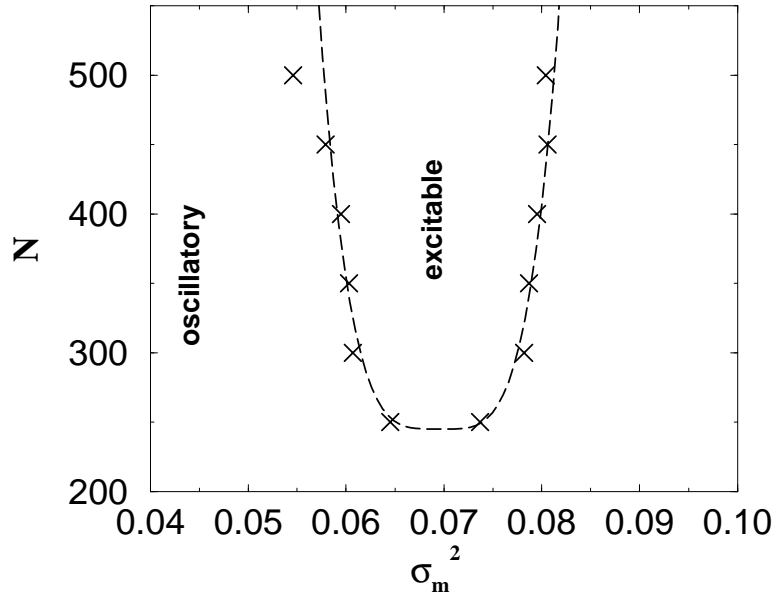


Figure 4.6: Phase diagram for the transition from a self-sustained oscillatory regime to NIE according to the strong definition. Number of coupled elements  $N$  versus multiplicative noise intensity  $\sigma_m^2$  for  $D_u = 416$  and  $D_v = 64$ .

of noise intensity values for which NIE exists becomes larger as the number of oscillators increases. We can also see that a minimum number of elements is needed to achieve the excitable regime (in the present case  $\sim 250$ ).

The strong condition of NIE is the proper measure for describing the excitable property with sufficiently small threshold and hence with a high sensitivity to perturbations. This treatment of NIE will be used in the following chapter for demonstrating typical effects in excitable systems in the noise-induced excitable system.

#### 4.1.6 Discussion of the short-time evolution

Van den Broeck et al. [67] have found analytically and numerically a noise-induced phase transition from a monostable (potential well at zero) to a bistable state (with two nonzero potential wells) on short time-scales in a single potential and argued that coupling of many systems leads to an enlargement of the time-scale on which the bistable state subsists. The particle initially in such a noise-induced bistable potential behaves for short times as in a deterministic bistable potential and tends to one nonzero potential well, while on longer time-scales one can observe a movement to zero and hence a monostable potential determines the dynamic. In contrast to that finding the noise-induced phase transition from oscillatory to excitable state does not demonstrate such short-time stability. Figure 4.7 depicts the time-dependent evaluation of the first

moment of the activator variable  $u$  (lower) and the inhibitor variable  $v$  (upper) of a single FHN oscillator. The average runs over 500 realizations and the common initial state is  $u(t = 0) = -0.71875$  and  $v(t = 0) = 1.71875$ , which is the noise-induced fixed point for the considered noise intensity  $\sigma_m^2 = 0.08$ , according to the small-noise-expansion. Following the idea of Van den Broeck et al. [67], short-time stability would lead to a persistence of the first moments in the vicinity of the noise-induced fixed point, but the single FHN oscillator leaves the initial state and simultaneously the noise-induced fixed point in the case  $\sigma_m^2 = 0.08$  (solid line). By comparing it with the deterministic undisturbed self-sustained oscillatory FHN ( $\sigma_m^2 = 0.0$  - dashed line), the FHN under the action of multiplicative noise leaves the vicinity of the noise-induced fixed point faster than the undisturbed FHN and so no noise-induced stability on short time-scales in single FHN can be observed.

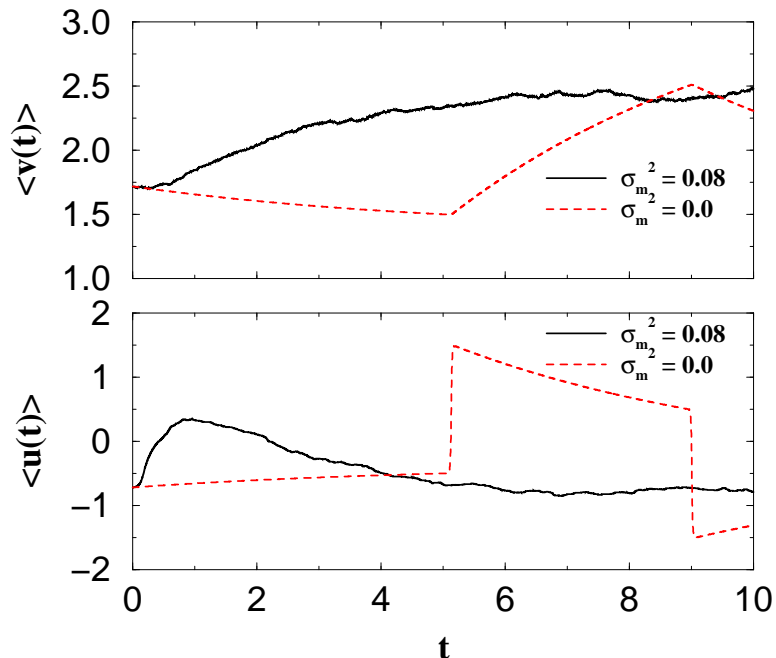


Figure 4.7: The first moments of the short-time evolution of the activator variable  $u$  (lower) and the corresponding inhibitor variable  $v$  of a single uncoupled FHN oscillator, starting from initial state  $u(t = 0) = -0.71875$  and  $v(t = 0) = 1.71875$ . The ensemble average  $\langle \cdot \rangle$  runs over 500 realizations. The parameters are:  $\varepsilon = 0.01$ ,  $a = 1.0$ ,  $b = 2.0$ ,  $c = 0.2$ ,  $d = 0.075$ ,  $D_u = D_v = 0.0$  and  $\sigma_m^2 = 0.0$  (dashed line), and  $0.08$  (solid line).

### 4.1.7 Influence of linear coordinate transformation

Additionally the question arises: what is the influence of the additive noise component on the phase transition? During the spike the inhibitor variable  $v$  occupies the range approximately between 1.5 and 2.5 [Figs. 4.1 and 4.2 (right)]. The noise-induced stable fixed point is located at  $v_0 \approx 1.7$ . Hence, these values of the inhibitor variable  $v$  lead to an additive noise component in the multiplicative noise term  $v_i \xi_i(t)$  in Eq. (4.2). To clarify the influence of this component a coordinate transformation  $v' = v - e$  is investigated which leads to a shift of the phase space in the  $v$  direction. For  $e \approx 1.7$  the noise-induced fixed point is shifted close to the  $v$  origin. The exact value of  $e$ , to set the fixed point to  $v'_0 = 0$ , depends on the multiplicative noise intensity  $\sigma_m^2$ . The coordinate transformation results in the following differential equations:

$$\frac{du_i}{dt} = \frac{1}{\varepsilon} (F(u_i) - v'_i + e) + D_u (\bar{u}_i - u_i) , \quad (4.3)$$

$$\frac{dv'_i}{dt} = cu_i + d + (v'_i + e)\xi_i(t) + D_v (\bar{v}'_i - v'_i) , \quad (4.4)$$

where  $\bar{x}_i \equiv \frac{1}{N} \sum_{j=1}^N x_j$ ,  $x_i = u_i, v'_i$  and the self-activation term of  $F(u_i)$  is unchanged compared to Eq. (4.1).

The multiplicative noise term  $(v'_i + e)\xi_i(t)$  in Eq. (4.4) has a non-zero mean given by  $\langle (v'_i + e)\xi_i \rangle = (\sigma_m^2/2)(v'_i + e)$  according to the small-noise-expansion [62] (see also chapter 1.2.4 and compare with chapter 4.1.2). Therefore, in the presence of fluctuations the effective local dynamics of the inhibitor variable are given by  $\dot{v}'_i = cu_i + d + (\sigma_m^2/2)(v'_i + e)$ , at first order in the noise intensity. The corresponding nullclines of an isolated oscillator for increasing multiplicative noise intensity are represented in the phase plane in Fig. 4.8 (lines 1 and 2 and the inverted-N piecewise line). The coordinate transformation with  $e = 1.71875$  leads to a translation of the whole phase space to lower  $v$  values [compare with Fig. 4.1] and the  $v$  coordinate of the noise-induced stable fixed point is zero for the shown noise intensity  $\sigma_m^2 = 0.08$  (intersection point between line (2) and the inverted-N piecewise line). The transformation does not influence the mechanism of NIE. The simultaneous action of noise upon  $(v'_i + e)$  is the important point in this consideration. If one would consider independent and uncorrelated noise for each part of the sum, i.e. one replaces  $(v'_i + e)\xi_i$  by  $v'_i \xi_i + e \zeta_i$  with  $\xi_i$  and  $\zeta_i$  Gaussian white noise with the same intensity  $\sigma_m^2$  but spatially and temporally uncorrelated, the effective local dynamics of the inhibitor variable would be given by  $\dot{v}'_i = cu_i + d + (\sigma_m^2/2)v'_i$  and one examines a totally different system without NIE. It is noteworthy that this replacement is not caused by the coordinate transformation, leads to a different system and is used only in this consideration. Although a sufficient noise intensity  $\sigma_m^2 = 0.08$  acts upon the FHN oscillators, the system remains self-sustainedly oscillatory because the unstable fixed point is left unstable [Fig. 4.8: intersection point between line (3) and inverted-N

piecewise line]. Numerical simulations have confirmed these results of the small-noise-expansion, that the noise has to act simultaneously on  $(v'_i + e)$  to reach NIE. These considerations show that additive noise is not able to cause a noise-induced phase transition from an oscillatory to an excitable state and only the systematic action of multiplicative noise results in the NIE.

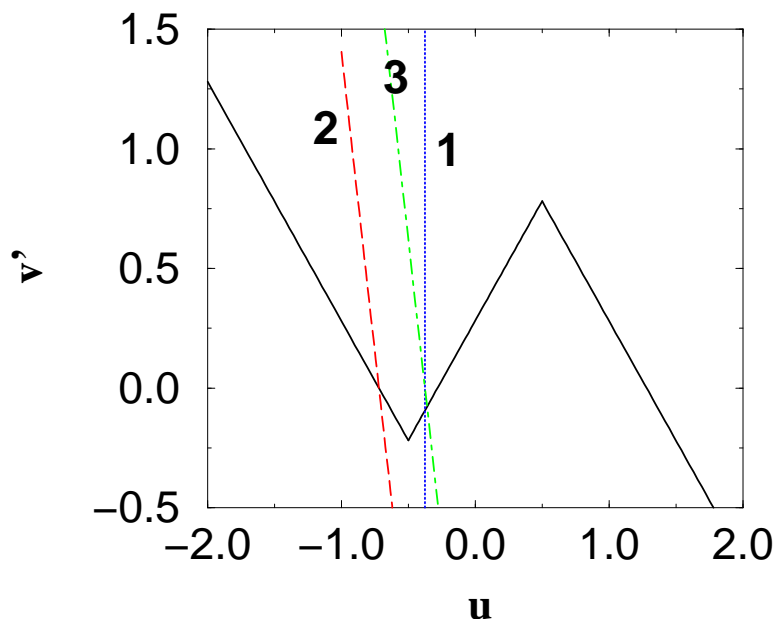


Figure 4.8: Nullclines of a single FHN oscillator after coordinate transformation with  $e = 1.71875$  in phase space. The inverted-N piecewise line corresponds to the noise-independent nullcline of the activator  $u$ . The lines (1 and 2) describe the tilting of the inhibitor nullcline by increasing the noise intensity:  $\sigma_m^2 = 0.0$  (1) and  $\sigma_m^2 = 0.08$  (2). The line (3) demonstrates the vanishing of NIE by splitting the multiplicative noise term  $(v'_i + e)\xi_i$  into two parts with independent noise sources with same noise intensity  $\sigma_m^2 = 0.08$ . Other parameters are  $a = 1.0$ ,  $b = 2.0$ ,  $c = 0.2$  and  $d = 0.075$ .

Next, I want to show the excitable properties, especially the threshold behavior, of the noise-induced excitable media by performing the Stochastic Resonance effect, as a typical effect in excitable systems.

## 4.2 Stochastic Resonance in noise-induced excitable systems

Defined as the enhanced response to an external signal for an optimal amount of noise, Stochastic Resonance (SR) has long been found in excitable media [30, 38, 143]. In order to show that the NIE regime possesses all immanent properties of excitable systems, I now examine the response of the system to external periodic driving and an additive source of noise. The dynamical behavior of the inhibitor is then given by:

$$\dot{v}_i = cu_i + d + v_i\xi_i(t) + D_v(\bar{v}_i - v_i) + \zeta_i(t) + A\cos\omega t, \quad (4.5)$$

where  $\zeta_i$  is a Gaussian white noise with intensity  $\sigma_a^2$ , the intensity of the multiplicative noise is taken large enough to make the system excitable, and the amplitude  $A$  of the external forcing is chosen small enough so that no excitation is produced in the absence of the additive noise. We are interested in the response of the system at the signal frequency  $\omega$  when the additive noise intensity  $\sigma_a^2$  is increased. Figure 4.9 displays the time series of the averaged activator (left) and the inhibitor (right) concentration for different additive noise intensities, superimposed with the periodic input signal (with rescaled amplitude for a better comparability with the output signal). In the absence of additive noise [Fig. 4.9(a)], the signal alone is too small to reach the excitation threshold, and the system remains at the noise-induced stable fixed point. When additive noise is added, spikes appear more and more frequently [Fig. 4.9(b) and (c)], until at an optimal noise intensity the spikes occur basically synchronously with the signal [Fig. 4.9(d)]. Further increase of additive noise destroys the synchronization effect [Fig. 4.9(e)].

To evaluate the linear response  $Q$  of the system at the input frequency  $\omega$  I extract the parameter  $Q$  from a signal  $\langle u_r \rangle$  as in [39, 110], where

$$\begin{aligned} Q_{sin} &= \frac{\omega}{2n\pi} \int_0^{\frac{2\pi n}{\omega}} 2\langle u_r(t) \rangle \sin(\omega t) dt \\ Q_{cos} &= \frac{\omega}{2n\pi} \int_0^{\frac{2\pi n}{\omega}} 2\langle u_r(t) \rangle \cos(\omega t) dt \\ Q &= \sqrt{Q_{sin}^2 + Q_{cos}^2}, \end{aligned}$$

when  $n$  is the number of periods  $T_s = \frac{2\pi}{\omega}$ , covered by the integration time.

In order to compute this quantity, I neglect subthreshold dynamics and replace the global signal by  $\langle u_r(t) \rangle = \Theta(\langle u \rangle - u_{\text{threshold}}) - 0.6\Theta(u_{\text{threshold}} - \langle u \rangle)$ , where  $\langle \dots \rangle$  denotes the average over the population and  $u_{\text{threshold}} = -0.45$ . The

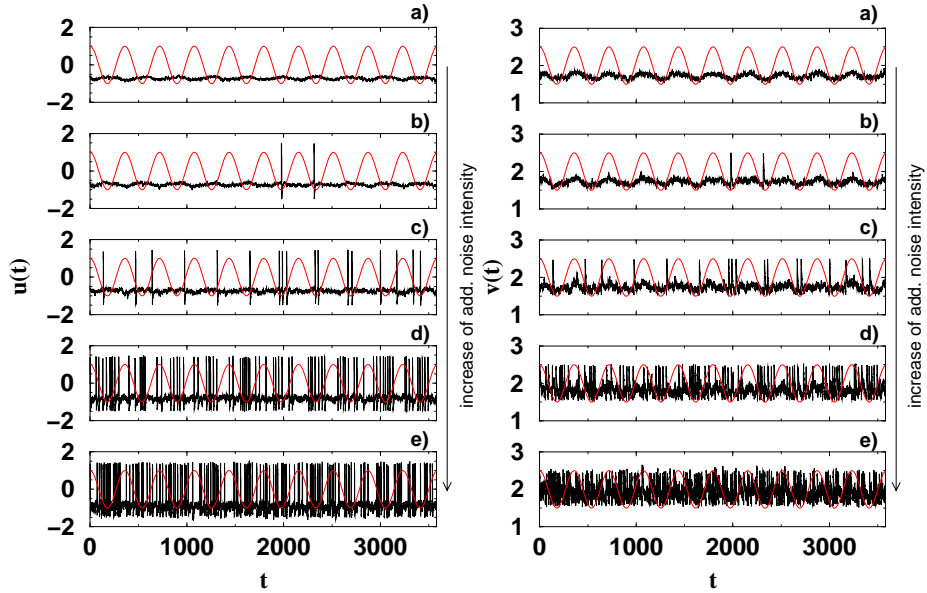


Figure 4.9: The time series of the average activator (left) and inhibitor (right) concentration for increased additive noise intensity and  $\sigma_m^2 = 0.08$ : (a)  $\sigma_a^2 = 0.0$ , (b)  $\sigma_a^2 = 0.1$ , (c)  $\sigma_a^2 = 0.5$ , (d)  $\sigma_a^2 = 2.0$ , and (e)  $\sigma_a^2 = 5.0$ . The parameters are  $D_u = 100$ ,  $D_v = 100$ ,  $A = 0.012$  and  $\omega = 0.0175$ . Other parameters are those of Fig. 4.2:  $\varepsilon = 0.01$ ,  $a = 1.0$ ,  $b = 2.0$ ,  $c = 0.2$  and  $d = 0.075$ .

numerical results are shown in Fig. 4.10 both with and without the multiplicative noise. The typical bell-shaped SR curve appears only in the presence of a suitable multiplicative noise intensity (i.e. in the NIE regime), whereas in the original self-sustained oscillatory regime (without multiplicative noise), the SR effect cannot be observed. The former behavior corresponds to a double stochastic effect [110, 144–146], because optimal response in the presence of additive noise occurs due to a property (excitability) which is induced by a second, multiplicative noise and can be classified as doubly Stochastic Resonance.

A smaller signal amplitude  $A = 0.005$  requires a smaller excitation threshold, i.e. lower multiplicative noise, and smaller additive noise for optimizing the linear response  $Q$  [Fig. 4.11]. The sensitivity of the system increases by decreasing the noise-induced threshold of excitation closer to the bifurcation point, see  $\sigma_m^2 = 0.068$  (square),  $\sigma_m^2 = 0.06$  (diamond) and  $\sigma_m^2 = 0.05$  (triangle). The resonance curve for  $\sigma_m^2 = 0.06$  (diamond) exceeds that of the original self-oscillatory system  $\sigma_m^2 = 0.0$  (crosses) and demonstrates the qualitative enhancement of the signal response due to the noise-induced phase transition considered. In this case,  $\sigma_m^2 = 0.06$  (diamond), the signal is not subthreshold because a small response without any additive noise (due to the logarithmic scaling only  $\sigma_a^2 = 0.01$  is shown as smallest value) appears but nevertheless additive noise can optimize the response. Similar signal constellations have been found as well in natural systems,

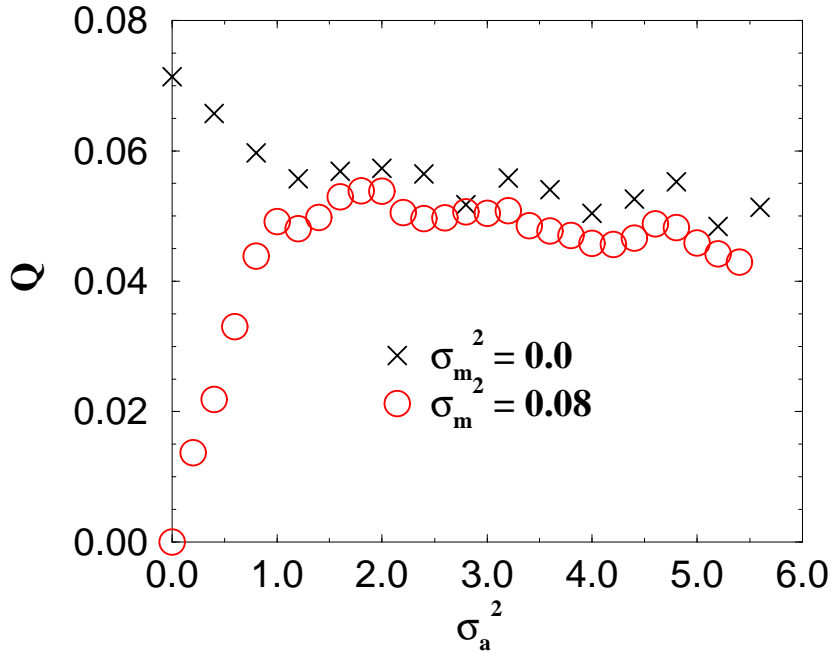


Figure 4.10: Response of the system, consisting of 500 oscillators, to the signal frequency  $\omega$  versus additive noise intensity, for  $\sigma_m^2 = 0.0$  (crosses) and  $\sigma_m^2 = 0.08$  (circles). Parameters are  $D_u = 100$ ,  $D_v = 100$ ,  $A = 0.012$  and  $\omega = 0.0175$ . Other parameters are those of Fig. 4.2:  $\varepsilon = 0.01$ ,  $a = 1.0$ ,  $b = 2.0$ ,  $c = 0.2$  and  $d = 0.075$ .

e.g. Ref. [6]. The curve  $\sigma_m^2 = 0.05$  (triangle) corresponds to the regime between regular self-sustained oscillatory and noise-induced excitable. According to the phase diagrams Figs. 4.4 - 4.6, this state is outside the noise-induced excitable regime but beyond the bifurcation point at  $\sigma_m^2 \approx 0.033$ . The rare self-excited spikes still remaining at this intermediate multiplicative noise intensity are suppressed during one half of the signal period and supported during the other one, and hence in the absence of additive noise a signal-modulated spike series results. In other words, the period signal switches the system synchronously from small-noise-stimulated dynamics during one half of the signal period to rest during the other one.

In order to investigate the signal processing in this intermediate region, I have calculated the response of the system to the signal frequency  $\omega$  by increasing the multiplicative noise intensity  $\sigma_m^2$  without additive noise ( $\sigma_a^2 = 0.0$ ) [Fig. 4.12]. A resonance curve, similar to a bell-shaped SR curve, demonstrates a significant enhancement of the signal processing compared to the deterministic situation  $\sigma_m^2 = 0.0$  at the beginning. The maximum  $\sigma_{m,max}^2 = 0.04$  is located close to the bifurcation point  $\sigma_m^2 \approx 0.033$  and demonstrates the very high sensitivity of the system in the vicinity of the phase transition. It is noteworthy that Fig. 4.12

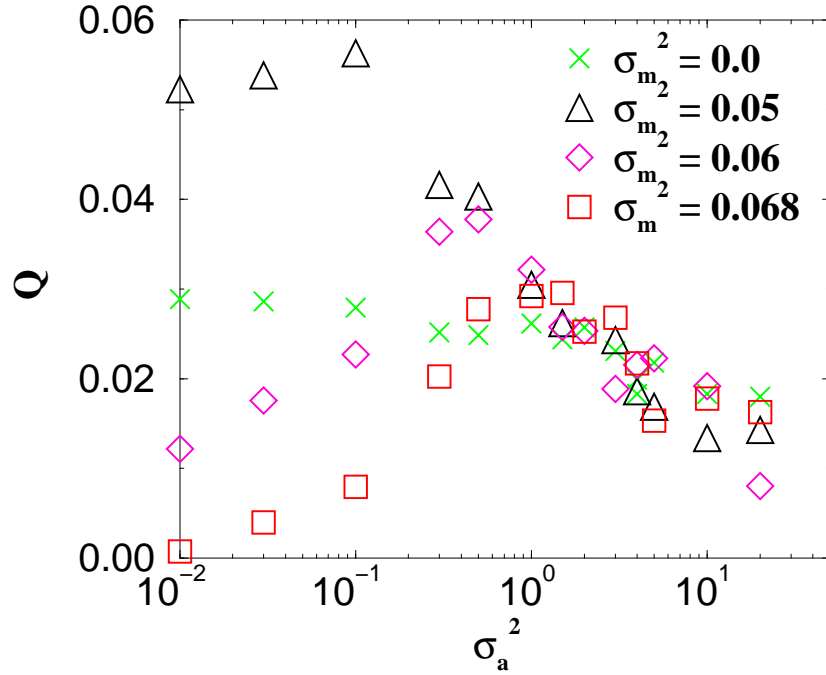


Figure 4.11: The response of the system, consisting of 500 oscillators, to the signal frequency  $\omega$  versus additive noise intensity (logarithmic scaling), for  $\sigma_m^2 = 0.0$  (crosses),  $\sigma_m^2 = 0.05$  (triangle),  $\sigma_m^2 = 0.06$  (diamond) and  $\sigma_m^2 = 0.068$  (square). Other parameters are  $D_u = 100$ ,  $D_v = 100$ ,  $A = 0.005$ ,  $\omega = 0.0175$ ,  $\varepsilon = 0.01$ ,  $a = 1.0$ ,  $b = 2.0$ ,  $c = 0.2$  and  $d = 0.075$ .

demonstrates only an effect similar to SR, but in contrast to SR, multiplicative noise plays the essential role and the systematic action of multiplicative noise leads to a qualitative changing of the system properties due to the noise-induced phase transition.

In the light of these results, one could speculate that sensory adaptation by noise in living organisms [6] can be possible even in oscillatory situations because parametric noise can suppress undesirable oscillations and enhances sensitivity to a signal.

I proceed in the next section with the demonstration of spatiotemporal pattern formation in a noise-induced excitable lattice as a further demonstration of the excitable properties.

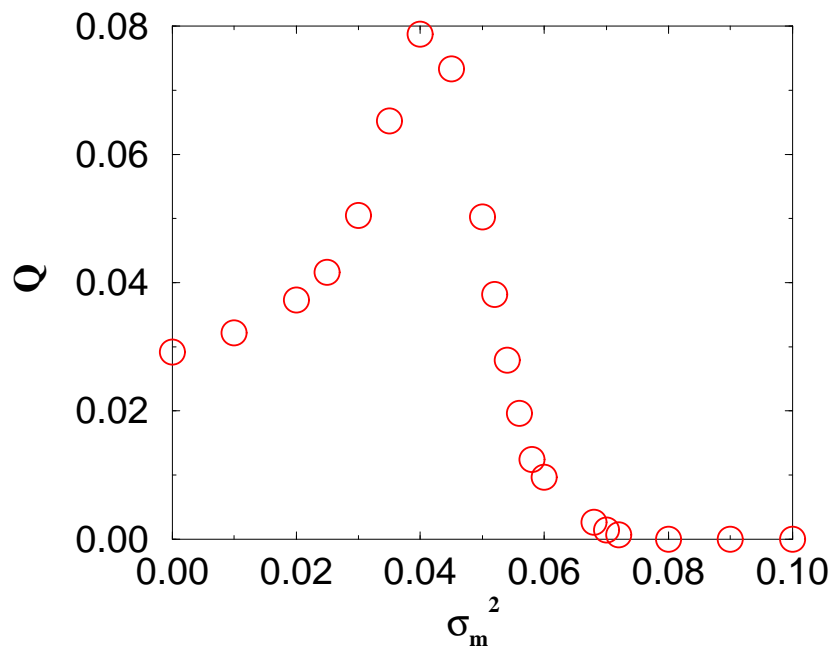


Figure 4.12: The response of the system to the signal frequency  $\omega$  versus multiplicative noise intensity without additive noise ( $\sigma_a^2 = 0.0$ ). Other parameters are  $D_u = 100$ ,  $D_v = 100$ ,  $A = 0.005$ ,  $\omega = 0.0175$ ,  $\varepsilon = 0.01$ ,  $a = 1.0$ ,  $b = 2.0$ ,  $c = 0.2$  and  $d = 0.075$ .

### 4.3 Signal propagation in a two-dimensional lattice of local coupled noise-induced excitable FitzHugh-Nagumo models

One of the main characteristics of excitable media is their ability to sustain lossless propagation of structures. This is, for instance, the way in which electrical pulses propagate through neural tissue in physiological systems [18]. The NIE regime reported here offers the possibility of a signal propagation through *oscillatory* media. Additionally, NIE allows the activation/deactivation of the excitable property, in such a way that information transmission can be controlled by multiplicative noise.

In order to verify that the NIE regime allows the propagation of excitable structures, I substitute the global coupling considered so far (Eqs. (4.1)–(4.2)) by a local diffusive coupling. Hence the coupling term in Eqs. (4.6)–(4.7) is now given by  $\bar{x}_i \equiv \frac{1}{\mathcal{N}} \sum_{j \in n.n} x_j$ , where the sum runs only over the  $\mathcal{N}$  nearest neighbors of site  $i$ , and  $x_i = u_i, v_i$ . In what follows I consider a 2-dimensional lattice with fixed or periodic boundary conditions:

$$\frac{du_i}{dt} = \frac{1}{\varepsilon} (F(u_i) - v_i) + D_u (\bar{u}_i - u_i) , \quad (4.6)$$

$$\frac{dv_i}{dt} = cu_i + d + v_i \xi_i(t) + D_v (\bar{v}_i - v_i) . \quad (4.7)$$

Additionally, the  $u$  - nullcline is now given by:

$$F(u) = \begin{cases} -1 - u + b & u \leq -\frac{1}{2} \\ gu + b + \frac{1}{2}(g - 1) & -\frac{1}{2} < u < \frac{1}{g} - \frac{1}{2} \\ +1 - au + b - \frac{1}{2} + a(\frac{1}{g} - \frac{1}{2}) & u \geq \frac{1}{g} - \frac{1}{2} , \end{cases}$$

to provide that the slope of its unstable middle branch decreases and the excursion time  $t_e$  becomes smaller. The dynamical equation of  $v$  with the multiplicative noise term, on the other hand, remains unchanged, and thus the noise-induced transition mechanism described above persists [Fig. 4.13].

Under these conditions, this system displays a noise-induced phase transition to excitability, as for global coupling, via the formation of clusters of stable elements [Fig. 4.14]. The color coding runs from black for  $u_i = -2.0$  to white for  $u_i = 6.0$  over 128 gray levels. These figures depict the transient state from a random initial condition to the excitable state. A random realization of the uniform distribution with  $u_i \in [-2.0, 6.0]$  and  $v_i \in [1.0, 3.0]$  is chosen as random initial conditions to demonstrate the strong attraction of the noise-induced fixed point. The  $200 \times 200$  FHN oscillators with periodic boundary conditions considered here occupy initially the whole phase space, shown in Fig. 4.13. The multiplicative noise with  $\sigma_m^2 = 0.072$  acts on every local coupled oscillator and no

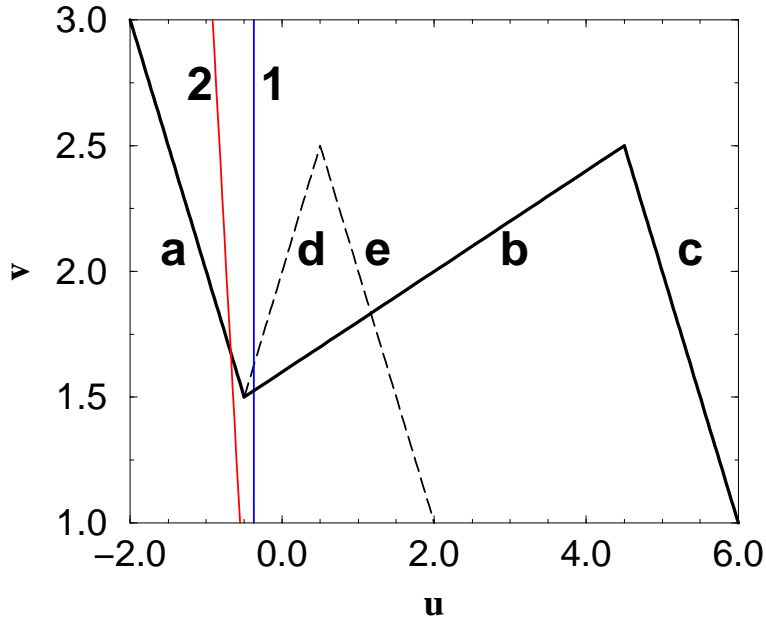


Figure 4.13: The nullclines of a single FHN oscillator. The inverted-N piecewise line (a,b and c) corresponds to the noise-independent nullcline of the activator  $u$  with the reduced middle slope  $g = 0.2$ . The dashed lines (d) and (e) denote the activator nullcline considered before [Fig. 4.1]. The lines (1) and (2) describe the tilting of the inhibitor nullcline by increasing the noise intensity:  $\sigma_m^2 = 0.0$  (1) and  $\sigma_m^2 = 0.072$  (2). Other parameters are  $a = 1.0$ ,  $b = 2.0$ ,  $c = 0.2$  and  $d = 0.075$ .

further influences are present here. In the first figures a formation and growth of local excited clusters can be observed (time  $t$  up to 0.2 time units) until the suppression of the spikes due to the coupling and the multiplicative noise dominates. In this situation from  $t = 0.6$  time units no spiking oscillator can be observed and every oscillator is attracted by the noise-induced fixed point.

In the NIE region (i.e. for large enough  $\sigma_m^2$ ), independently of the initial conditions every oscillator of the coupled ensemble moves to the NIE fixed point and remains there. As a consequence, the media can transmit an information signal. In this situation, the spatiotemporal response of the system to a plane wave perturbation is depicted in Fig. 4.15 (left column). The simulations start with uniform initial conditions  $u_i = -0.7$  and  $v_i = 1.7$  near the noise-induced fixed point at time  $t = 0.0$  and include periodic boundary conditions. After a transient state (as in Figs. 4.14), at time  $t = 10.0$  six rows of oscillators in the bottom are excited by setting these oscillators above the excitation threshold to  $u_i = -0.3$  and  $v_i = 1.3$ . Additionally the next 6 rows below the first one are set in a refractory state at  $u_i = -1.0$  and  $v_i = 2.0$  to suppress a bidirectional wave-front propagation in the lattice with periodic boundary conditions. All other

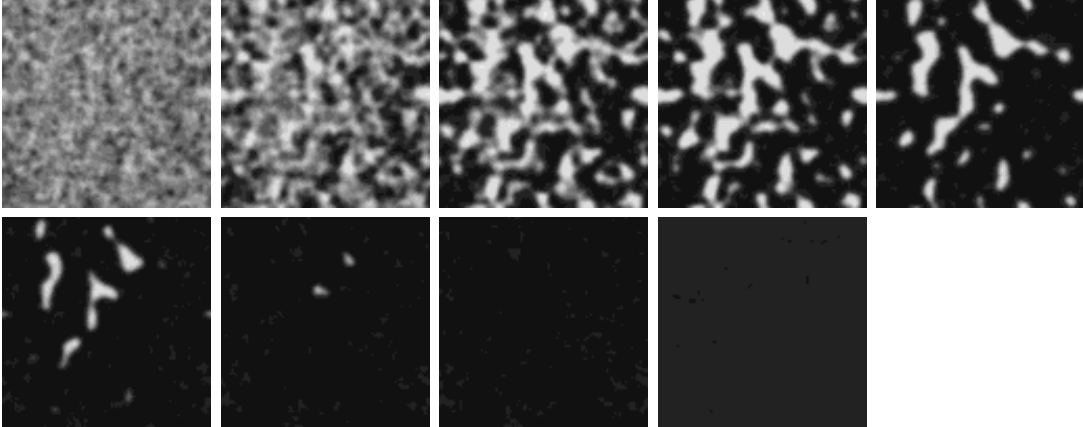


Figure 4.14: Snapshots of the activatory variable  $u$  of an array of  $200 \times 200$  FHN's during the unperturbed transition from a random initial condition at  $t = 0.0$  to the NIE state. The time increases from left to right and from top to bottom. First row:  $t = 0.05, 0.1, 0.15, 0.2$  and  $0.3$ , and second row:  $t = 0.4, 0.5, 0.6$ , and  $6.0$ . Other parameters are  $\varepsilon = 0.01$ ,  $a = 1.0$ ,  $b = 2.0$ ,  $c = 0.2$ ,  $d = 0.075$ ,  $g = 0.2$ ,  $D_u = 416$ ,  $D_v = 64$ , and  $\sigma_m^2 = 0.072$ .

oscillators outside the noted excitation area are not excited by this external signal. These stimulations persist only 0.7 time units and after this stimulation time all oscillators remain unperturbed. We observe a clear propagation of the plane wave. The wave front dies when it reenters the lattice on the bottom ( $t = 28$ ) because the refractory time of the oscillators is greater than the traveling time of the wave front across the  $600 \times 600$  lattice. The front hits oscillators far from the noise-induced fix-point and disappears. The lattice with this size is too small to observe a reproducing wave front with periodic boundaries. In larger lattices one would observe a permanent reproducing wave front.

The sensitivity and the feature of information transmission can be observed only in the noise-induced excitable regime Fig. 4.15 (left column) and not in the deterministic self-sustained oscillatory system Fig. 4.15 (right column). Both columns differ only by the multiplicative noise intensity (left:  $\sigma_m^2 = 0.072$ , hence the NIE regime and right:  $\sigma_m^2 = 0.0$ , the self-sustained oscillatory regime). All the other conditions like excitation, coupling and parameters are the same. In the self-sustained oscillatory regime Fig. 4.15 (right column) the small excitation is not large enough to initiate propagating and stable spikes. Only a phase shift is caused, but no propagation can be observed. The coupling leads to a reduction of the phase shift and hence to a loss of the information. The self-sustained oscillations appear at the time  $t = 18.8$  and  $t = 31.0$ , but they are not related to the information seeded by the initiated wave front and only destroy the information transmission.

Spiral wave propagation can also be demonstrated in this system [Fig. 4.16

(left)]. The initialization of the spiral was implemented similarly to the above-noted wave front with the difference that the stimulation takes place in the middle of the lattice and only half of the rows are excited as one can see in the first figure on the top left. In the absence of multiplicative noise, on the other hand, the system exhibits a synchronous self-sustained oscillatory behavior and no wave propagation can be observed [Fig. 4.16 (right)]. The self-sustained oscillations take place at about time  $t \approx 18$ ,  $t \approx 31$ , and  $t \approx 44$ . This means that the presence of multiplicative noise is crucial for information transmission in this system.

*In summary*, I have studied a different kind of phase transition in which the application of noise to an array of oscillating elements leads to the suppression of oscillations and induces excitability. The appearance of noise-induced excitability is a collective effect, and occurs via a phase transition due to the joint action of coupling and multiplicative noise. In contrast to standard phase transitions and other studies on excitable systems [71–74, 101], the increase of noise enhances the stability in the system and restores excitable properties. This noise-supported excitability displays characteristic properties of standard excitable media, such as Stochastic Resonance and wave propagation. Since SR relies on a property of the system which is in turn induced by noise, optimization of both noise sources is needed, and hence this effect is an example of a doubly stochastic phenomenon [144]. The interplay between excitable and oscillatory dynamics in noisy systems is a current important issue [102]. In particular, these theoretical findings suggest a possible mechanism to suppress undesirable global oscillations in neural networks (which are usually characteristic of abnormal medical conditions such as Parkinson’s disease or epilepsy), using the action of noise to restore excitability, which is the normal state of neural ensembles.

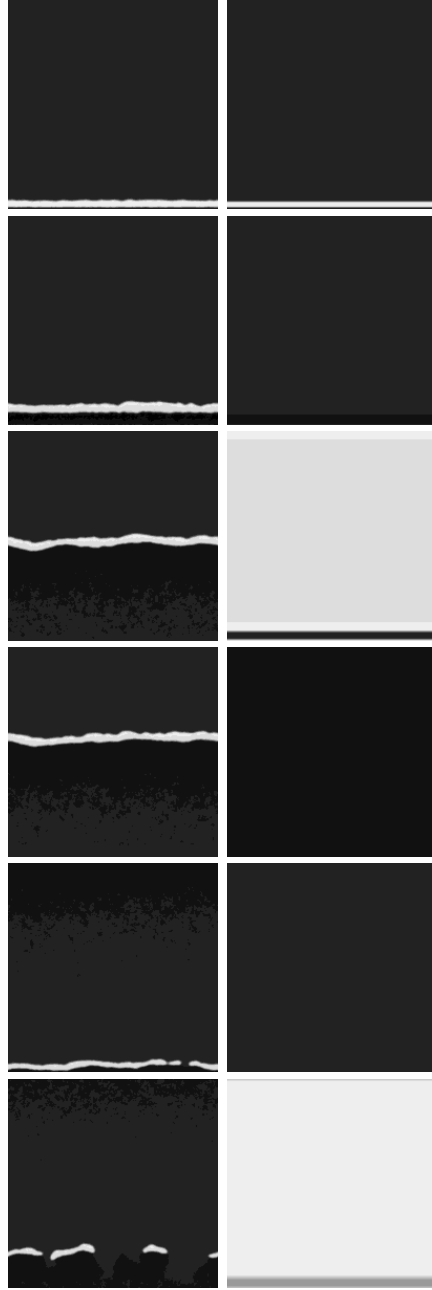


Figure 4.15: Snapshots of the activatory variable  $u$  for increasing time (from top to bottom). The left column shows the propagation of a wave front in an  $600 \times 600$  array at time steps 11.0, 12.0, 18.5, 20.0, 28.0, and 31.0 time units in the noise-induced excitable regime ( $\sigma_m^2 = 0.072$ ). The right column depicts the deterministic self-sustained oscillating regime ( $\sigma_m^2 = 0.0$ ) at the same time steps and demonstrates the necessity of the excitable property for the information transmission. Other common parameters are  $\varepsilon = 0.01$ ,  $a = 1.0$ ,  $b = 2.0$ ,  $c = 0.2$ ,  $d = 0.075$ ,  $g = 0.2$ ,  $D_u = 416$ , and  $D_v = 64$ .

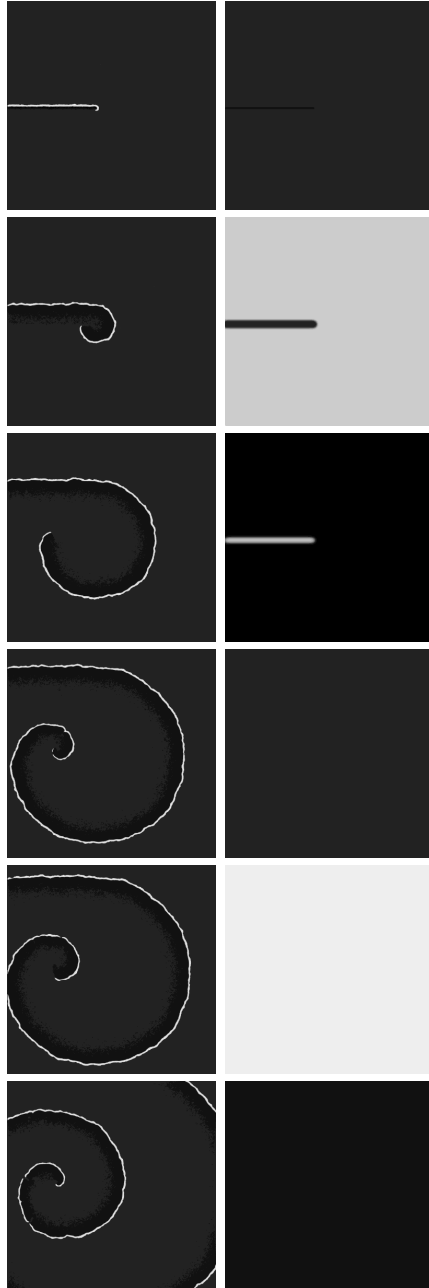


Figure 4.16: Snapshots of the activatory variable  $u$  for increasing time (from top to bottom). The left column shows the propagation of a spiral in an  $2600 \times 2600$  array at time steps 12, 18, 32, 42, 44, and 60 time units in the noise-induced excitable regime ( $\sigma_m^2 = 0.072$ ). The right column depicts the deterministic self-sustained oscillating regime ( $\sigma_m^2 = 0.0$ ) at the same time steps and demonstrates the necessity of the excitable property for the spiral formation. All the other conditions and parameters are the same in both columns and in Fig. 4.15.



# Chapter 5

## Conclusions and outlook

In this thesis I have investigated several new noise-induced phenomena in neural models with FitzHugh-Nagumo dynamics. The main results and the conclusions can be grouped into three parts.

**First,** I have investigated new resonance phenomena in excitable systems: the vibrational resonance (VR), vibrational propagation (VP) (chapter 2.1) and the Canard-enhanced Stochastic Resonance (chapter 2.2). The VR effect is a specification of SR in a single excitable element, where the additive noise term is replaced by a periodic signal with a fixed high frequency and a variable amplitude, i.e. the excitable element is subjected to a bichromatic signal. I have shown that an optimal amplitude of the high-frequency component of the signal can optimize signal processing of the low-frequency component, which encodes the information. This result has been observed in an excitable electronic circuit and has been confirmed by a numerical analysis of the FitzHugh-Nagumo model. The numerical simulations have shown that the VR effect is qualitatively independent of the frequency of the high-frequency component in the bichromatic signal. This frequency influences mainly the position of the resonance curve by increasing the high-frequency amplitude. I have also shown that in the presence of noise, high-frequency driving can substitute a fraction of the noise and, hence, can control the effect of Stochastic Resonance. This connection between SR and VR is reversible, i.e. additional additive noise can replace a part of the high-frequency driving in the VR effect and can help to reduce the needed input energy for an optimal signal processing. I have demonstrated that in spatially extended excitable media, the vibrational resonance mechanism enhances propagation of the low-frequency signal through the system using the high-frequency driving. The vibration propagation can be considered as the spatial extension of the vibrational resonance.

I have investigated the Canard-enhanced Stochastic Resonance, which is a combination of SR and VR in systems with Canard oscillations. Numerical simulations have shown a significant enhancement of the Stochastic Resonance curve

when the high-frequency component of the bichromatic periodic signal is in resonance with the Canard eigenfrequency, i.e. the optimization of the system response at the desired low frequency by increasing additive noise intensity. The effect shows a frequency selectivity and disappears in the region out of resonance with the Canard frequency. This phenomenon of Canard-enhanced SR could be found not only in the oscillatory regime, where the Canard oscillations are self-excited, but also in an excitable regime, i.e. where the subthreshold Canard oscillations are evoked by noise. This phenomenon is relevant in biology if the stiffness of the system is limited by the interval  $\varepsilon \in [0.01, 0.2]$  in order to get the observable periods of noise-induced Canard-like orbits. In this interval very small noise is necessary for a significant improvement of signal processing. It means, e.g. for neurons, the possibility of a new regulation of signal processing. In addition to the choice of the value of the bifurcation parameter, this regulation can control the signal transmission under a small noisy environment.

These theoretical findings should stimulate experimental work to find new possibilities of signal reception and propagation in systems which demonstrate Canard-like oscillations, especially in nonlinear chemical systems [127] or in biophysical models [115, 116]. Here one should mention the recent experimental observation of Canard oscillations in a diode laser system [147]. This experiment offers the opportunity to prove the Canard-enhanced SR experimentally. Moreover, the dynamic systems, which have some specific regime between excitable and oscillatory states, are not limited by the FHN with Canard phenomenon. Recently it has been shown that the modified Oregonator equations have three steady states and excitation occurs via resonance between damped HF oscillations around the stable fixed point and periodic perturbations with an appropriate tuning frequency [92]. A similar SR enhancement by HF signal may also be expected in this chemical system with low excitability.

**Second,** I have studied an effect of noise-induced signal processing in systems with complex attractors (chapter 3). I have demonstrated there a frequency selective response and information propagation in a noisy system which consists of inhibitor-coupled excitable units and is driven by a subthreshold harmonic signal. The mechanism of this selectivity can be explained by the appearance of new resonance frequencies of the coupled system which are caused by different phase relations of the oscillators and differ from the resonance frequency of an isolated FHN. The inhibitor-coupled system of two or three FHN oscillators offers a richer eigenfrequency spectrum than an isolated FHN oscillator. Especially the resonance frequencies of the anti-phase and dynamic trap regime exhibit stable attractors in a noisy environment. By forcing one element of the network in resonance with these coupling-dependent resonance frequencies, one observes an additional resonance peak in the SR curve besides the typical bell-shaped curve of standard SR. Another interesting phenomenon which I have explained is the

masking of the information flow in the dynamic trap regime. In this effect, the last oscillator in the row shows a much better response at the signal frequency which was fed to the first oscillator of the row, than the middle one. I believe that the study of the frequency-selective SR and the masking of information flow in an array due to inhibitor-coupling can be useful for understanding of multi-frequency information-exchange mechanisms in neural networks. Because of the generality of these effects for diffusive coupled activator-inhibitor oscillator arrays, I expect that these theoretical findings can be applied also in other fields, e.g. in chemistry or biology.

It is important to note that these results contribute also to the study of fundamental synchronization phenomena [141]. In frames of this study, SR can be considered as a synchronization-like phenomenon, in which optimal noise induces phase synchronization between output and input signal.

This research field can be continued in two directions. The first direction includes investigations of systems with more than three elements and in other spatial configurations than the chain (e.g. ring or two-dimensional networks). The problem arises that the number of complex attractors and consequently the number of eigenfrequencies increases rapidly. The growing number of attractors are located closer in the phase plane and so the coupled system can jump easily between them in a noisy environment. Due to these complications a clear frequency selectivity could disappear. The second direction is devoted to the consideration of an ensemble of non-identical coupled FHN oscillators. For instance, one could investigate a chain of three oscillators, where the middle element is in a self-sustained oscillatory regime, whereas the first and the last one are excitable. The dynamic trap regime could lead to a suppression of the self-sustained oscillations in the middle element, whereas a signal transmission at a certain resonance frequency from the first to the last elements survives. Such a set-up could be a possible mechanism to suppress undesirable oscillations in neural networks which are typical for abnormal medical conditions like Parkinson's disease or epilepsy. One could imagine that the middle self-sustained oscillator represents a diseased neuron which breaks up the information transmission between the healthy first and third neurons. The described frequency-selective SR effect in the dynamic trap regime could be a mechanism to suppress the undesirable oscillations of the diseased neuron and to restore the information flow. Additionally, this system acts as a filter due to the frequency selectivity. Only the resonance frequency of the "dynamic trap" regime can be transmitted.

**Third,** I have examined a new noise-induced phase transition from a self-sustained oscillatory regime to an excitable behavior and related effects which are enabled by this new phase transition (chapter 4). This noise-induced excitability includes inevitably an oscillation suppression by noise. The appearance of noise-induced excitability is a collective effect, and occurs via a phase transi-

tion due to the joint action of coupling and multiplicative noise. In contrast to standard phase transitions and other studies on excitable systems [71–74, 101], the increase of noise enhances the stability in the system and restores excitable properties.

This noise-supported excitability displays characteristic properties of standard excitable media, such as Stochastic Resonance, wave propagation and spatiotemporal pattern formation. Since SR relies on a property of the system which is in its turn induced by noise, optimization of both noise sources is needed, and hence this effect is an example of a doubly stochastic phenomenon [144]. With the help of the noise-induced excitability, I extend the system classes with a flexible and reliable information transmission ability to self-sustained oscillatory systems with an unstable fixed point.

These theoretical findings suggest a possible mechanism to suppress undesirable global oscillations in neural networks (which are usually characteristic of abnormal medical conditions such as Parkinson’s disease or epilepsy), using the action of noise to restore excitability, which is the normal state of neural ensembles. Alternatively, the deep brain stimulation [148, 149] with a permanent periodic high-frequency electrical signal ( $> 100Hz$ ) is already used to suppress such undesirable global oscillations in neural networks. The problem is, that the brain can adapt itself to this periodic signal and the oscillation-suppression effect of this method decreases. In consequence, the voltage has to be increased in time. This is a kind of addiction. To overcome this problem, one could use the new suggested method of oscillation suppression and reconstruction of excitable properties with help of the noise-induced phase transition described. In this way noise could help to reconstruct the sensitivity of neural ensembles for signaling without the negative addiction effect, because the noise consists of irregular random fluctuations and so the brain probably will not adapt itself so easily to the noise stimulation. Additionally, the noise-induced excitability offers the opportunity to enable or suppress the information transmission in a coupled system in a surprising way: an increase of noise enables information exchange, whereas a lack of noise hinders it. Furthermore, this noise-induced excitability could open an opportunity to control pacemaker dynamics, so that the pacemaker fires periodically only in the absence of noise and falls silent in a noisy surrounding. These theoretical findings contribute also to the investigation of the interplay between excitable and oscillatory dynamics in noisy systems which is a current important issue [102].

The investigation of NIE can be progressed in several different directions. First, an experimental realization of the noise-induced excitability is most desirable. To achieve this one should develop a theoretical description of the effect in the paradigmatic FitzHugh-Nagumo neural model to a more realistic model. This investigation should be carried out in close cooperation with experimentalists and neuroscientists. An experimental realization includes the challenge to build up and control a large ensemble of coupled elements. A more theoretical development

could concern itself with an analytical approximation of the noise-induced phase transition. To this aim one could use a combination of the small-noise-expansion and the two-state approximation for the FHN model given in Ref. [88]. The analytic approximation of the FHN model is based on a time-scale separation between fast and slow variables and is performed in a piecewise linear FHN model. Further it would be important to analyze the influence of correlations (spatial and / or temporal) between the noise sources in different coupled elements. The investigation of other noise-induced phase transitions has shown that the additional memory of colored noise is critical for these transitions [69, 70] and leads to a growing disorder in the system by increased correlation. I would expect that an increased correlation of noise leads to a reduction of the oscillation suppression and so to destruction of the noise-induced excitability. This investigation should clarify what, and which kind of correlation does still provide the phase transition before it vanishes.



# Acknowledgements

This work has been mainly done at the Institut für Physik der Universität Potsdam in close cooperation with Prof. Dr. J. Kurths. I would like to thank Prof. Dr. Kurths for creating an inspiring scientific environment, for numerous fruitful discussions and for providing me with his endless support. Several parts of this work have been carried out in cooperation with Prof. Dr. A. Zaikin. I am very grateful to Prof. Dr. Zaikin for helpful discussions and close collaboration.

I am very thankful to my close cooperation partners Prof. Dr. J. García-Ojalvo and Prof. Dr. E. Volkov for their patience and help in endless scientific discussions.

Let me thank the International Max Planck Research School on Biomimetic Systems, especially the Speaker of the School Prof. Dr. R. Lipowsky and the Coordinator Dr. A. Valleriani, for the interdisciplinary classes and discussions and all the lecturers and students there for the international and cooperative atmosphere. I am indebted to the State of Brandenburg for sponsoring the stipend which made possible my work at the IMPRS.

Let me kindly thank Prof. Dr. García-Ojalvo for hosting my stay at the University of Terrassa and for our very fruitful scientific collaboration.

My best acknowledgments go to Prof. Dr. García-Ojalvo, Prof. Dr. Kurths, Dr. M. Rosenblum, and Prof. Dr. Zaikin for their readiness to be referees of this work.

I have greatly appreciated the many enlightening discussions and fruitful cooperations which I have had with my colleagues. In particular, I am grateful to Dr. B. Blasius, R. Donner, Dr. F. Feudel, M. Gellert, Dr. N. Marwan, J. Ong, Prof. Dr. A. Pikovsky, Dr. Rosenblum, J. Schneider, Dr. U. Schwarz, Prof. Dr. N. Seehafer, Dr. F. Spahn, L. Zemanova, Dr. C. Zhou and many others.

Let me thank my colleagues and friends around the world for the valuable opportunity to discuss and collaborate with them: Prof. Dr. R. Bartlett, R. Bascones, H. Busch, Prof. Dr. L. Schimansky-Geier, Prof. Dr. P. Hänggi, C. Hänisch, Prof. Dr. J.M. Sancho, Dr. M. Zaks, and many others.

Especial thanks are due to all the Faculty staff for the technical assistance I was given throughout the project, especially I owe thanks to B. Nader and J. Tessmer, who helped a great deal with all the necessary official and technical requirements during the period of my stay in Potsdam.

I am very thankful to my parents and my brother for their contribution to the genesis of this work, through their loving support in more wonderful ways than a page can hold.

# Bibliography

- [1] C. W. Gardiner, *Handbook of Stochastic Methods: for Physics, Chemistry and the Natural Sciences*, Springer series in synergetics; 13, Springer, Berlin, 2 ed., 1997. 4. printing.
- [2] W. Horsthemke and R. Lefever, *Noise-Induced Transitions*, Springer, Berlin, 1984.
- [3] H. Haken, *Advanced synergetics: instability hierarchies of self-organizing systems and devices*, Springer series in synergetics; 20, Springer, Berlin, 1993. 3. printing.
- [4] G. Nicolis and I. Prigogine, *Self-organization in nonequilibrium systems: from dissipative structure to order through fluctuations*, A Wiley-Interscience publication, Wiley, New York, 1977. Repr.
- [5] R. Feistel and W. Ebeling, *Evolution of complex systems: self-organization, entropy and development*, Mathematics and its applications. East European Series; 30, Kluwer, Dordrecht, 1989.
- [6] D. F. Russell, L. A. Wilkens, and F. Moss, “Use of behavioural stochastic resonance by paddle fish for feeding,” *Nature* **402**, pp. 291–294, 1999.
- [7] R. Sarpeshkar, “Analog Versus Digital: Extrapolating from Electronics to Neurobiology,” *Neural Comput.* **10**(7), pp. 1601 – 1638, 1998.
- [8] T. Mori and S. Kai, “Noise-induced entrainment and stochastic resonance in human brain waves,” *Phys. Rev. Lett.* **88**, p. 218101, 2002.
- [9] A. Winfree, *The Geometry of Biological Time*, Springer, Berlin, 1980.
- [10] A. S. Mikhailov, *Foundations of Synergetics*, Springer, Berlin, 2nd ed., 1994.
- [11] L. Glass, “Synchronization and rhythmic processes in physiology,” *Nature* **410**, p. 277, 2001.
- [12] C. O. Weiss and R. Vilaseca, *Dynamics of lasers*, VCH, Weinheim, 1991.

- [13] B. Krauskopf, K. Schneider, J. Sieber, S. Wieczorek, and M. Wolfrum, “Excitability and self-pulsations near homoclinic bifurcations in semiconductor laser systems,” *Optic Comm.* **215**, pp. 367–379, 2003.
- [14] H. J. Wünsche, O. Brox, M. Radziunas, and F. Henneberger, “Excitability of a Semiconductor Laser by a Two-Mode Homoclinic Bifurcation,” *Phys. Rev. Lett.* **88**, p. 023901, 2002.
- [15] G. M. Shepherd, *Neurobiology*, Oxford University Press, New York, 1994.
- [16] R. Kapral and K. Showalter, *Chemical waves and patterns*, Kluwer Academic Publishers, Dordrecht, 1995.
- [17] A. Ganopolski and S. Rahmstorf, “Abrupt Glacial Climate Changes due to Stochastic Resonance,” *Phys. Rev. Lett.* **88**, p. 038501, 2002.
- [18] J. P. Keener and J. Sneyd, *Mathematical Physiology*, Springer, New York, 1998.
- [19] B. Lindner, J. García-Ojalvo, A. Neiman, and L. Schimansky-Geier, “Effects of noise in excitable systems,” *Phys. Rep.* **392**(6), pp. 321–424, 2004.
- [20] A. L. Hodgkin and A. F. Huxley, “A quantitative description of membrane current and its application to conduction and excitation in nerve,” *J. Physiol* **117**(4), pp. 500–544, 1952.
- [21] R. A. FitzHugh, “Impulses and physiological states in models of nerve membrane,” *Biophys. J.* **1**, pp. 445–466, 1961.
- [22] A. V. Holden, *Models of the stochastic activity of neurones*, Springer, Berlin, 1976.
- [23] L. M. Ricciardi, *Diffusion processes and related topics in biology*, Springer, Berlin, 1977.
- [24] C. Koch, *Biophysics of computation: information processing in single neurons*, Oxford Univ. Press, New York, NY, 1999.
- [25] E. R. Kandel, ed., *Principles of neural science*, Prentice-Hall, London, 1991.
- [26] J. Nagumo, S. Arimoto, and S. Yoshitawa, “An active pulse transmission line simulating nerve axon,” *Proc. IRE* **50**, p. 2061, 1962.
- [27] J. Grasman, *Asymptotic methods for relaxation oscillations and applications*, Springer, New York, 1987.

- [28] M. N. Shadlen and W. T. Newsome, “The Variable Discharge of Cortical Neurons: Implications for Connectivity, Computation, and Information Coding,” *J. Neurosci.* **18**, pp. 3870–3896, 1998.
- [29] J. Feng and B. Tirozzi, “Stochastic resonance tuned by correlations in neural models,” *Phys. Rev. E* **61**, pp. 4207–4211, 2000.
- [30] B. Lindner, *Coherence and Stochastic Resonance in Nonlinear Dynamical Systems*. PhD thesis, Humboldt-Universität zu Berlin, 2002.
- [31] S. Lee, A. Neiman, and S. Kim, “Coherence resonance in a Hodgkin-Huxley neuron,” *Phys. Rev. E* **57**, p. 3292, 1998.
- [32] A. Pikovsky and J. Kurths, “Coherence Resonance in a Noise-Driven Excitable System,” *Phys. Rev. Lett.* **78**, p. 775, 1997.
- [33] B. Lindner, L. Schimansky-Geier, and A. Longtin, “Maximizing spike train coherence or incoherence in the leaky integrate-and-fire model,” *Phys. Rev. E* **66**, p. 031916, 2002.
- [34] A. Longtin, “Autonomous stochastic resonance in bursting neurons,” *Phys. Rev. E* **55**, p. 868, 1997.
- [35] C. Palenzuela, R. Toral, C. Mirasso, O. Calvo, and J. Gunton, “Coherence resonance in chaotic systems,” *Europhys. Lett.* **56**(3), pp. 347–353, 2001.
- [36] J. L. A. Dubbeldam, B. Krauskopf, and D. Lenstra, “Excitability and coherence resonance in lasers with saturable absorber,” *Phys. Rev. E* **60**, pp. 6580–6588, 1999.
- [37] J. M. Buldú, J. García-Ojalvo, C. R. Mirasso, M. C. Torrent, and J. M. Sancho, “Effect of external noise correlation in optical coherence resonance,” *Phys. Rev. E* **64**, p. 051109, 2001.
- [38] K. Wiesenfeld, D. Pierson, E. Pantazelou, C. Dames, and F. Moss, “Stochastic Resonance on a circle,” *Phys. Rev. Lett.* **72**(14), pp. 2125–2129, 1994.
- [39] L. Gammaitoni, P. Hänggi, P. Jung, and F. Marchesoni, “Stochastic resonance,” *Rev. Mod. Phys.* **70**, p. 223, 1998.
- [40] P. Landa and P. McClintock, “Vibrational Resonance,” *J. Phys. A: Math. Gen* **33**, p. L433, 2000.
- [41] N. Stocks, N. Stei, and P. McClintock, “Stochastic resonance in monostable systems,” *J. Phys. A* **26**, p. 385, 1993.

- [42] Z. Gingl, L. B. Kiss, and F. Moss, “Non-dynamical stochastic resonance: theory and experiments with white and arbitrarily coloured noise,” *Europhys. Lett.* **29**(3), pp. 191–196, 1995.
- [43] T. Alarcón, A. Pérez-Madrid, and J. Rubí, “Stochastic resonance in non-potential systems,” *Phys. Rev. E* **57**(5), pp. 4979–4985, 1998.
- [44] R. Benzi, A. Sutera, and A. Vulpiani, “The mechanism of stochastic resonance,” *J. Phys. A* **14**, p. L453, 1981.
- [45] B. McNamara, K. Wiesenfeld, and R. Roy, “Observation of Stochastic Resonance in a Ring Laser,” *Phys. Rev. Lett.* **60**, pp. 2626–2629, 1988.
- [46] L. Gammaitoni, M. Martinelli, L. Pardi, and S. Santucci, “Observation of stochastic resonance in bistable electron-paramagnetic-resonance systems,” *Phys. Rev. Lett.* **67**, p. 1799, 1991.
- [47] R. Mantegna and B. Spagnolo, “Stochastic resonance in a tunnel diode,” *Phys. Rev. E* **49**, pp. R1792–R1795, 1994.
- [48] A. Simon and A. Libchaber, “Escape and synchronization of a Brownian particle,” *Phys. Rev. Lett.* **68**, pp. 3375–3378, 1992.
- [49] M. Dykman, T. Horita, and J. Ross, “Statistical distribution and stochastic resonance in a periodically driven chemical system,” *J. Chem. Phys.* **103**(3), pp. 966–972, 1995.
- [50] W. Hohmann, J. Müller, and F. W. Schneider, “Stochastic Resonance in Chemistry. 3. The Minimal-Bromate Reaction,” *J. Phys. Chem* **100**(13), pp. 5388–5392, 1996.
- [51] M. Riani and E. Simonotto, “Stochastic resonance in the perceptual interpretation of ambiguous figures: A neural network model,” *Phys. Rev. Lett.* **72**, pp. 3120–3123, 1994.
- [52] E. Simonotto, M. Riani, C. Seife, M. Roberts, J. Twitty, and F. Moss, “Visual perception of stochastic resonance,” *Phys. Rev. Lett.* **78**, p. 1186, 1997.
- [53] M. Usher and M. Feingold, “Stochastic resonance in the speed of memory retrieval,” *Biological Cybernetics* **83**, pp. L11–L16, 2000.
- [54] H. Haken, *Synergetics: an introduction; nonequilibrium phase transitions and self-organization in physics, chemistry, and biology*, Springer series in synergetics; 1, Springer, Berlin, 3 ed., 1983.
- [55] A. Zaikin, *Noise-induced transitions and resonant effects in nonlinear systems*, Universität Potsdam, Potsdam, 2002. State doctorate thesis.

- [56] I. Fedchenia, “Boundary stochastic problems, multistability in the presence of fluctuations and noise-induced phase transitions,” *Physica A* **125A**, pp. 577–590, 1984.
- [57] J. Smythe, F. Moss, and P. McClintock, “Observation of a Noise-Induced Phase Transition with an Analog Simulator,” *Phys. Rev. Lett.* **51**, pp. 1062–1065, 1983.
- [58] S. Kabashima and T. Kawakubo, “Observation of a noise-induced phase transition in a parametric oscillator,” *Phys. Lett.* **A70**, p. 375, 1970.
- [59] P. Landa and P. McClintock, “Changes in the Dynamical Behavior of Nonlinear Systems Induced by Noise,” *Phys. Reports.* **323**(1), pp. 1–80, 2000.
- [60] P. Landa and A. Zaikin, “Noise-induced phase transitions in a pendulum with a randomly vibrating suspension axis,” *Phys. Rev. E* **54**(4), pp. 3535–3544, 1996.
- [61] P. Landa, A. Zaikin, V. Ushakov, and J. Kurths, “Influence of Additive Noise on Transitions in Nonlinear Systems,” *Phys. Rev. E* **61**, p. 4809, 2000.
- [62] J. García-Ojalvo and J. M. Sancho, *Noise in Spatially Extended Systems*, Springer, New York, 1999.
- [63] A. Mikhailov, “Noise-induced phase transition in a biological system with diffusion,” *Phys. Lett. A* **73**, p. 143, 1979.
- [64] J. García-Ojalvo, A. Hernández-Machado, and J. Sancho, “Effects of external noise on the Swift-Hohenberg equation,” *Phys. Rev. Lett.* **71**, p. 1542, 1993.
- [65] C. Van den Broeck, J. M. R. Parrondo, and R. Toral, “Noise-induced Nonequilibrium phase transition,” *Phys. Rev. Lett.* **73**, p. 3395, 1994.
- [66] J. García-Ojalvo, J. M. R. Parrondo, J. M. Sancho, and C. Van den Broeck, “Reentrant transition induced by multiplicative noise in the time-dependent Ginzburg–Landau model,” *Phys. Rev. E* **54**, p. 6918, 1996.
- [67] C. Van den Broeck, J. M. R. Parrondo, R. Toral, and R. Kawai, “Nonequilibrium phase transitions induced by multiplicative noise,” *Phys. Rev. E* **55**(4), pp. 4084–4094, 1997.
- [68] J. García-Ojalvo, J. Sancho, and L. Ramírez-Piscina, “A nonequilibrium phase transition with colored noise,” *Phys. Lett. A* **168**, pp. 35–39, 1992.

- [69] S. Mangioni, R. Deza, H. S. Wio, and R. Toral, “Disordering effects of color in nonequilibrium phase transitions induced by multiplicative noise,” *Phys. Rev. Lett.* **79**, p. 2389, 1997.
- [70] S. Mangioni, R. Deza, R. Toral, and H. Wio, “Nonequilibrium phase transitions induced by multiplicative noise: Effects of self-correlation,” *Phys. Rev. E* **61**, p. 223, 2000.
- [71] S. Alonso, I. Sendiña-Nadal, V. Pérez-Muñuzuri, J. M. Sancho, and F. Sagués, “Regular Wave Propagation Out of Noise in Chemical Active Media,” *Phys. Rev. Lett.* **87**, p. 078302, 2001.
- [72] J. García-Ojalvo, F. Sagués, J. M. Sancho, and L. Schimansky-Geier, “Noise-enhanced excitability in bistable activator-inhibitor media,” *Phys. Rev. E* **65**, p. 011105, 2001.
- [73] J. García-Ojalvo and L. Schimansky-Geier, “Excitable Structures in Stochastic Bistable Media,” *Journal of Statistical Physics* **101**, p. 473, 2000.
- [74] R. Báscones, J. García-Ojalvo, and J. Sancho, “Pulse propagation sustained by noise in arrays of bistable electronic circuits,” *Phys. Rev. E* **65**, p. 061108, 2002.
- [75] E. Ullner, A. Zaikin, J. García-Ojalvo, and J. Kurths, “Noise-Induced Excitability in Oscillatory Media,” *Phys. Rev. Lett.* **91**(18), pp. 180601–1–180601–4, 2003.
- [76] G. M. Shepherd, ed., *The synaptic organization of the brain*, Oxford University Press, New York, 3 ed., 1990.
- [77] V. Mironov and V. Sokolov, “Detection of broadband phase-code-modulated two-frequency signals through calculation of their cross-correlation function,” *Radiotekhnika i elektronika* **41**, p. 1501, 1996. (in Russian).
- [78] D. Su, M. Chiu, and C. Chen, “Simple two-frequency laser,” *Precision Engineering-journal* **18**, p. 161, 1996.
- [79] J. Victor and M. Conte, “Two-frequency analysis of interactions elicited by Vernier stimuli,” *Visual Neuroscience* **17**, p. 959, 2000.
- [80] C.-W. Cho, Y. Liu, W. N. Cobb, T. K. Henthorn, K. Lillehei, U. Christians, and K.-Y. Ng, “Ultrasound-Induced Mild Hyperthermia as a Novel Approach to Increase Drug Uptake in Brain Microvessel Endothelial Cells,” *Pharm. Res.* **19**(8), pp. 1123–1129, 2002.

- [81] J. Karnes and H. Burton, “Continuous therapeutic ultrasound accelerates repair of contraction-induced skeletal muscle damage in rats,” *Arch. Phys. Med. Rehabil.* **83**, pp. 1–4, 2002.
- [82] O. Schläfer, T. Onyeche, H. Bormann, C. Schröder, and M. Sievers, “Ultrasound stimulation of micro-organisms for enhanced biodegradation,” *Ultrasonics* **40**, pp. 25–29, 2002.
- [83] R. Feng, Y. Zhao, C. Zhu, and T. Mason, “Enhancement of ultrasonic cavitation yield by multi-frequency sonication,” *Ultrason. Sonochem.* **9**(5), p. 231, 2002.
- [84] A. Longtin and D. R. Chialvo, “Stochastic and Deterministic Resonances for Excitable Systems,” *Phys. Rev. Lett.* **81**(18), pp. 4012–4015, 1998.
- [85] S. R. Massanés and C. J. P. Vicente, “Nonadiabatic resonance in a noisy Fitzhugh-Nagumo neuron model,” *Phys. Rev. E* **59**(4), pp. 4490–4497, 1999.
- [86] T. Kanamaru, T. Horita, and Y. Okabe, “Stochastic resonance for superimposed periodic pulse train,” *Phys. Lett. A* **255**, pp. 23–30, 1999.
- [87] H. E. Plesser and T. Geisel, “Markov analysis of stochastic resonance in a periodically driven integrate-and-fire neuron,” *Phys. Rev. E* **59**(6), pp. 7008–7017, 1999.
- [88] B. Lindner and L. Schimansky-Geier, “Coherence and stochastic resonance in a two-state system,” *Phys. Rev. E* **61**, p. 6103, 2000.
- [89] C. Zhou, J. Kurths, and B. Hu, “Frequency and phase locking of noise-sustained oscillations in coupled excitable systems: Array-enhanced resonances,” *Phys. Rev. E* **67**, pp. 030101–1–030101–4, 2003.
- [90] A. Fuliński, “Active Transport in Biological Membranes and Stochastic Resonances,” *Phys. Rev. Lett.* **79**(24), pp. 4926–4929, 1997.
- [91] E. M. Izhikevich, “Resonate-and-fire neurons,” *Neural Networks* **14**, pp. 883–894, 2001.
- [92] P. Parmananda, H. Mahara, T. Amemiya, and T. Yamaguchi, “Resonance Induced Pacemakers: A New Class of Organizing Centers for Wave Propagation in Excitable Media,” *Phys. Rev. Lett.* **87**, p. 238302, 2001.
- [93] F. Liu, J. Wang, and W. Wang, “Frequency sensitivity in weak signal detection,” *Phys. Rev. E* **59**(3), pp. 3453–3460, 1999.

- [94] E. Volkov, E. Ullner, A. Zaikin, and J. Kurths, “Oscillatory amplification of stochastic resonance in excitable systems,” *Phys. Rev. E* **68**, pp. 026214–1–026214–7, 2003.
- [95] E. I. Volkov and M. N. Stolyarov, “Birhythmicity in a system of two coupled identical oscillators,” *Phys. Lett. A* **159**, pp. 61–66, 1991.
- [96] E. I. Volkov and M. N. Stolyarov, “Temporal variability in a system of coupled mitotic timers,” *Biol. Cybern.* **71**, pp. 451–459, 1994.
- [97] B. Kerner and V. Osipov, “Self-organization in active distributed media: scenarios for the spontaneous formation and evolution of dissipative structures,” *Soviet Physics - Uspekhi* **33**(9), pp. 679–719, 1990.
- [98] D. Ruwisch, M. Bode, D. Volkov, and E. Volkov, “Collective modes of three coupled relaxation oscillators: the influence of detuning,” *Int. J. Bifurcation and Chaos* **9**(10), pp. 1969–1981, 1999.
- [99] V. Vanag, L. Yang, M. Dolnik, A. Zhabotinky, and I. Epstein, “Oscillatory cluster patterns in a homogeneous chemical system with global feedback,” *Nature* **406**, pp. 389–391, 2000.
- [100] V. Castets, E. Dulos, J. Boissonade, and P. D. Kepper, “Experimental evidence of a sustained standing Turing-type nonequilibrium chemical pattern,” *Phys. Rev. Lett.* **64**(24), pp. 2953–2956, 1990.
- [101] S. Kádár, J. Wang, and K. Showalter, “Noise-supported traveling waves in sub-excitable media,” *Nature* **391**, p. 770, 1998.
- [102] J. M. Vilar, H. Y. Kueh, N. Barkai, and S. Leibler, “Mechanisms of noise-resistance in genetic oscillators,” *Proc. Natl. Acad. Sci. U.S.A.* **99**(9), pp. 5988–5992, 2002.
- [103] J. K. Douglass, L. Wilkens, E. Pantazelou, and F. Moss, “Noise enhancement of information transfer in crayfish mechanoreceptors by stochastic resonance,” *Nature* **365**, pp. 337–340, 1993.
- [104] S. Sinha, “Noise-free stochastic resonance in simple chaotic systems,” *Physica A* **270**, p. 204, 1999.
- [105] A. Maksimov, “On the subharmonic emission of gas bubbles under two-frequency excitation,” *Ultrasonics* **35**, p. 79, 1997.
- [106] V. Gherm, N. Zernov, B. Lundborg, and A. Vastberg, “The two-frequency coherence function for the fluctuating ionosphere: Narrowband pulse propagation,” *Journ. of Atmospheric and Solar-terrestrial physics* **59**, p. 1831, 1997.

- [107] Y. Yu, W. Wang, J. Wang, and F. Liu, “Resonance-enhanced signal detection and transduction in the Hodgkin-Huxley neuronal systems,” *Phys. Rev. E* **63**, p. 021907, 2001.
- [108] S. Kádár, J. Wang, and K. Showalter, *Nature* **391**, 770 (1998); J. García-Ojalvo and L. Schimansky-Geier, *J. Stat. Phys.* **101**, 473 (2000); J. García-Ojalvo, F. Sagués, J.M. Sancho, and L. Schimansky-Geier, *Phys. Rev. E* **65**, 011105 (2002).
- [109] M. Löcher, D. Cigna, and E.R. Hunt, *Phys. Rev. Lett.* **80**, 5212 (1998); J.F. Lindner, S. Chandramouli, A.R. Bulsara, M. Löcher, and W.L. Ditto, *Phys. Rev. Lett.* **81**, 5048 (1998); J. García-Ojalvo, A.M. Lacasta, F. Sagués, and J.M. Sancho, *Europhys. Lett.* **50**, 427 (2000).
- [110] A. Zaikin, J. García-Ojalvo, L. Schimansky-Geier, and J. Kurths, “Noise induced propagation in monostable media,” *Phys. Rev. Lett.* **88**, p. 010601, 2002.
- [111] D. Barkley, M. Kness, and L. S. Tuckerman, “Spiral-wave dynamics in a simple model of excitable media: The transition from simple to compound rotation,” *Phys. Rev. A* **42**, pp. 2489–2492, 1990.
- [112] M. Abramowitz and I. A. Stegun, *Handbook of Mathematical functions with Formulas, Graphics, and Mathematical Tables*, Dover Publication, Inc., New York, N.Y., 1972.
- [113] C. Heneghan, C. C. Chow, T. T. Imhoff, S. B. Lowen, and M. C. Teich, “Information measures quantifying aperiodic stochastic resonance,” *Phys. Rev. E* **54**(3), pp. 2228–2231, 1996.
- [114] V. A. Makarov, V. I. Nekorkin, and M. G. Velarde, “Spiking Behavior in a Noise-Driven System Combining Oscillatory and Excitatory Properties,” *Phys. Rev. Lett.* **86**(15), pp. 3431–3434, 2001.
- [115] S. M. Baer and T. Erneux, “Singular Hopf bifurcation to relaxation oscillations,” *SIAM J. Appl. Math.* **46**, pp. 721–737, 1986.
- [116] S. Schuster and M. Marhl, “Bifurcation Analysis of Calcium Oscillations: Time-Scale Separation, Canards, and Frequency Lowering,” *J. Biol. Systems* **9**, pp. 291–314, 2001.
- [117] P. Glendinning, *Stability, instability and chaos: an introduction to the theory of nonlinear differential equations*, Cambridge University Press, Cambridge, 1996.
- [118] F. Dumortier and R. Roussarie, “Canard cycles and center manifolds,” *Mem. Am. Math. Soc.* **577**, p. 1, 1996.

- [119] L. Alfonsi, L. Gammaitoni, S. Santucci, and A. Bulsara, “Intrawell stochastic resonance versus interwell stochastic resonance in underdamped bistable systems,” *Phys. Rev. E* **62**(1), p. 299, 2000.
- [120] M. Inchiosa, V. In, A. Bulsara, K. Wiesenfeld, T. Heath, and M. Choi, “Stochastic dynamics in a two-dimensional oscillator near a saddle-node bifurcation,” *Phys. Rev. E* **63**, p. 066114, 2001.
- [121] J. Acebrón, W. Rappel, and A. Bulsara, “Cooperative dynamics in a class of coupled two-dimensional oscillators,” *Phys. Rev. E* **67**, p. 016210, 2003.
- [122] E. Ullner, A. Zaikin, J. García-Ojalvo, R. Báscones, and J. Kurths, “Vibrational resonance and vibrational propagation in excitable systems,” *Phys. Lett. A* **312**, pp. 348–354, 2003.
- [123] J. Das and H. Busse, “Analysis of the dynamics of relaxation type oscillation in glycolysis of yeast extracts,” *Biophys. J.* **60**, pp. 369–379, 1991.
- [124] S. Girard, A. Luckhoff, J. Lechleiter, J. Sneyd, and D. Clapham, “Two-dimensional model of calcium waves reproduces the patterns observed in *Xenopus* oocytes,” *Biophys. J.* **61**, pp. 509–517, 1992.
- [125] H. Mahara, T. Yamaguchi, and Y. Amagishi, “A numerical study of the decomposition of chemical waves in a closed system,” *Chem. Phys. Lett.* **317**, pp. 23–28, 2000.
- [126] P. Parmananda, C. H. Mena, and G. Baier, “Resonant forcing of a silent Hodgkin-Huxley neuron,” *Phys. Rev. E* **66**, p. 047202, 2002.
- [127] M. Brons and J. Sturis, “Explosion of limit cycles and chaotic waves in a simple nonlinear chemical system,” *Phys. Rev. E* **64**, p. 026209, 2001.
- [128] H. Gang, H. Haken, and X. Fagen, “Stochastic Resonance with Sensitive Frequency Dependence in Globally Coupled Continuous Systems,” *Phys. Rev. Lett.* **77**, pp. 1925–1928, 1996.
- [129] J. F. Lindner, B. J. Breen, M. E. Wills, A. Bulsara, and W. Ditto, “Monostable array-enhanced stochastic resonance,” *Phys. Rev. E* **63**, p. 051107, 2001.
- [130] H. Meinhardt, *Models of Biological Pattern Formation*, Academic Press, New York, 1982.
- [131] I. Lengyel and I. Epstein, “Modeling of Turing structures in the chlorite-iodide-malonic acid-starch reaction system,” *Science* **251**, pp. 650–652, 1991.

- [132] V. V. Astakhov, B. P. Bezruchko, E. N. Erastova, and E. P. Seleznev, “Modes of oscillation and their evolution in dissipatively coupled Feigenbaum systems,” *Soviet Physics - Technical Physics* **35**(10), pp. 1122–1127, 1990.
- [133] A. Sherman and J. Rinzel, “Rhythmogenic Effects of Weak Electrotonic Coupling in Neuronal Models,” *Proc. Natl. Acad. Sci. U.S.A* **89**, pp. 2471–2474, 1992.
- [134] G. S. Cymbalyuk, E. V. Nikolaev, and R. M. Borisyuk, “In-phase and antiphase self-oscillations in a model of two electrically coupled pacemakers,” *Biol. Cybern* **71**(2), pp. 153–160, 1994.
- [135] D. Postnov, S. K. Han, and H. Kook, “Synchronization of diffusively coupled oscillators near the homoclinic bifurcation,” *Phys. Rev. E* **60**, pp. 2799–2807, 1999.
- [136] E. Volkov, M. Stolyarov, A. Zaikin, and J. Kurths, “Coherence resonance and polymodality in inhibitory coupled excitable oscillators,” *Phys. Rev. E* **67**, pp. 66202–1–66202–7, 2003.
- [137] Y. Horikawa, “Coherence resonance with multiple peaks in a coupled FitzHugh-Nagumo model,” *Phys. Rev. E* **64**, pp. 031905–1–031905–6, 2001.
- [138] E. I. Volkov and M. N. Stolyarov, “Temporal variability generated by coupled mitotic timers,” *J. Biol. Systems* **3**, pp. 63–78, 1995.
- [139] E. I. Volkov and D. V. Volkov, “Multirhythmicity generated by slow variable diffusion in a ring of relaxation oscillators noise induced abnormal interspike variability,” *Phys. Rev. E* **65**, pp. 046232–1–046232–13, 2002.
- [140] D. E. Postnov, O. V. Sosnovtseva, S. K. Han, and W. S. Kim, “Noise-induced multimode behavior in excitable systems,” *Phys. Rev. E* **66**, pp. 16205–16209, 2002.
- [141] A. Pikovsky, M. Rosenblum, and J. Kurths, *Synchronization. A Universal Concept in Nonlinear Sciences*, Cambridge University Press, Cambridge, 2001.
- [142] Z. Zheng, G. Hu, and B. Hu, “Phase Slips and Phase Synchronization of Coupled Oscillators,” *Phys. Rev. Lett.* **81**(24), pp. 5318–5321, 1998.
- [143] F. Moss, J. Douglass, L. Wilkens, D. Pierson, and E. Pantazelou, “Stochastic resonance in an Electronic FitzHugh-Nagumo Model,” *Ann. N. Y. Acad. Sci.* **706**, p. 26, 1993.

- [144] A. Zaikin, “Doubly stochastic effects,” *Fluctuations and Noise Letters* **2**, pp. L157–L169, 2002.
- [145] A. Zaikin, J. García-Ojalvo, R. Báscones, E. Ullner, and J. Kurths, “Doubly stochastic coherence via noise-induced symmetry in bistable neural models,” *Phys. Rev. Lett.* **90**, p. 030601, 2003.
- [146] A. Zaikin, J. Kurths, and L. Schimansky-Geier, “Doubly Stochastic Resonance,” *Phys. Rev. Lett.* **85**(2), p. 227, 2000.
- [147] F. Marino, G. Catalán, P. Sánchez, S. Balle, and O. Piro, “Thermo-Optical ”Canard Orbits” and Excitable Limit Cycles,” *Phys. Rev. Lett.* **92**(7), pp. 073901–1–073901–4, 2004.
- [148] A. Benabid, P. Pollak, C. Gervason, D. Hoffmann, D. Gao, M. Hommel, J. Perret, and J. de Rougemont, “Long-term suppression of tremor by chronic stimulation of the ventral intermediate thalamic nucleus,” *Lancet* **337**, pp. 403–406, 1991.
- [149] S. Blond, D. Caparros-Lefebvre, F. Parker, R. Assaker, H. Petit, J.-D. Guieu, and J.-L. Christiaens, “Control of tremor and involuntary movement disorders by chronic stereotactic stimulation of the ventral intermediate thalamic nucleus,” *J. Neurosurg.* **77**(1), p. 62, 1992.

# Appendix A

## Noise-Induced Excitability in Oscillatory Media

E. ULLNER, A. ZAIKIN, J. GARCÍA-OJALVO AND J. KURTHS, Noise-Induced Excitability in Oscillatory Media. *Physical Review Letters* 91 (18), 2003, 180601.  
DOI: [10.1103/PhysRevLett.91.180601](https://doi.org/10.1103/PhysRevLett.91.180601)



## Noise-Induced Excitability in Oscillatory Media

E. Ullner,<sup>1</sup> A. Zaikin,<sup>1</sup> J. García-Ojalvo,<sup>2,3</sup> and J. Kurths<sup>1</sup>

<sup>1</sup>*Institut für Physik, Potsdam Universität, Am Neuen Palais 10, D-14469 Potsdam, Germany*

<sup>2</sup>*Center for Applied Mathematics, Cornell University, 657 Rhodes Hall, Ithaca, New York 14853, USA*

<sup>3</sup>*Departament de Física i Enginyeria Nuclear, Universitat Politècnica de Catalunya, Colom 11, E-08222 Terrassa, Spain*

(Received 28 May 2003; published 31 October 2003)

A noise-induced phase transition to excitability is reported in oscillatory media with FitzHugh-Nagumo dynamics. This transition takes place via a noise-induced stabilization of a deterministically unstable fixed point of the local dynamics, while the overall phase-space structure of the system is maintained. Spatial coupling is required to prevent oscillations through suppression of fluctuations (via clustering in the case of local coupling). Thus, the joint action of coupling and noise leads to a different type of phase transition and results in a stabilization of the system. The resulting regime is shown to display characteristic traits of excitable media, such as stochastic resonance and wave propagation. This effect thus allows the transmission of signals through an otherwise globally oscillating medium.

DOI: 10.1103/PhysRevLett.91.180601

PACS numbers: 05.40.-a, 05.70.Fh

Excitable systems are highly sensitive to perturbations, which trigger large-amplitude spiking responses above a small threshold. Noise, in particular, exerts an important influence in their dynamics. An optimal amount of noise, e.g., induces in them a coherent output in the form of roughly periodic spike trains, provided the random fluctuations are large enough to excite the system as soon as the refractory time from the previous spike is over (but not so large that the phase-space structure is destroyed) [1]. This effect, known as coherence resonance, has been observed in physical, chemical, and biological systems [2], making them behave effectively as oscillators.

Further investigations have shown that parametric noise is able to induce a bona fide transition from an excitable to an oscillatory regime, via a renormalization of the parameters defining the local dynamics of the system [3,4]. This mechanism has also been found responsible for inducing excitability in bistable [5,6] and subexcitable [3,7] media. In all those cases, however, noise has the expected role of increasing dynamical instability. In this Letter we show, on the other hand, that certain types of noise operate in the opposite direction of constructive influence, namely, enhancing stability in the system. In particular, we demonstrate that random fluctuations can induce a transition from oscillatory to excitable behavior, by stabilizing a deterministically unstable fixed point of the dynamics, while preserving the overall phase-space structure that leads to large-amplitude pulses (but which will then be triggered only by above-threshold perturbations). In contrast to previous results on noise-induced excitability, spatial coupling is absolutely essential in this case, in order to prevent noise-driven oscillations from exciting the system and converting it back in an oscillator. In that sense, the coupling plays a role similar to that of standard phase transitions, suppressing fluctuations and coupling the stable regions. It prevents the system from visiting the whole available phase space and locks it close to the stable steady state

(until a perturbation triggers an excitable spike). Noise-induced phase transitions between homogeneous phases have long been known to use the joint action of coupling and noise in this way [8,9]; here we extend this fundamental mechanism to the field of excitable dynamics.

To demonstrate this noise-induced excitability (NIE) we consider a system of coupled FitzHugh-Nagumo (FHN) elements in the oscillating state and under the action of multiplicative noise. The mechanism of a noise-induced phase transition is explained theoretically in the framework of a small-noise expansion, which extracts the systematic contribution of the multiplicative noise accounting for the excitability restoration. The excitable character of the noise-induced regime is demonstrated by showing the existence of stochastic resonance and wave propagation through the system.

*Model.*—We analyze the following set of  $N$  coupled FHN oscillators:

$$\dot{u}_i = \frac{1}{\varepsilon} (F(u_i) - v_i) + D_u(\bar{u}_i - u_i), \quad (1)$$

$$\dot{v}_i = cu_i + d + v_i\xi_i + D_v(\bar{v}_i - v_i), \quad (2)$$

where  $\bar{x}_i \equiv \frac{1}{N} \sum_{j=1}^N x_j$ ,  $x_i = u_i, v_i$ , and  $F(u)$  is given by

$$F(u) = \begin{cases} -1 - u + b, & u \leq -\frac{1}{2}, \\ u + b, & -\frac{1}{2} < u < \frac{1}{1+a}, \\ +1 - au + b, & u \geq \frac{1}{1+a}. \end{cases}$$

In a neural context,  $u(t)$  represents the membrane potential of the neuron and  $v(t)$  is related to the time-dependent conductance of the potassium channels in the membrane [10]. The dynamics of the activator variable  $u$  is much faster than that of the inhibitor  $v$ , as indicated by the small time-scale-ratio parameter  $\varepsilon$ . Coupling is considered in both the activator and the inhibitor and is taken to be global, although as we will show later, similar

results are obtained for local diffusive coupling. Random fluctuations are represented by the  $\delta$ -correlated Gaussian noise  $\xi_i(t)$ , with zero mean and the correlation  $\langle \xi_i(t)\xi_j(t') \rangle = \sigma_m^2 \delta(t-t')\delta_{i,j}$ . This multiplicative noise term is interpreted in the Stratonovich sense [9].

*Phase transition to excitability.*—The multiplicative noise term  $v_i \xi_i$  in Eq. (2) has a nonzero mean given by  $\langle v_i \xi_i \rangle = (\sigma_m^2/2)v_i$  [9]. Therefore, in the presence of fluctuations the effective local dynamics of the inhibitor variable is given by  $\dot{v}_i = cu_i + d + (\sigma_m^2/2)v_i$ , at first order in the noise intensity. The corresponding nullclines of an isolated oscillator for increasing multiplicative intensity are represented in the phase plane of Fig. 1 (left panel). Without noise the nullcline for the slow variable  $v$  (curve 1) crosses the nullcline of the fast variable (inverted-N piecewise line) in its middle segment, so that the crossing point is an unstable steady state and the system exhibits an oscillatory behavior. An increase of the multiplicative noise intensity  $\sigma_m^2$  leads to a tilting and shifting of the  $v$  nullcline [curves 2–4 in Fig. 1 (left panel)]. As a result, for large enough  $\sigma_m^2$  (here for  $\sigma_m^2 \geq 0.033$ ) the crossing occurs in the left segment of the  $u$  nullcline and the fixed point becomes stable. Throughout this process, however, the overall phase-space structure of the system is not changed, which allows perturbations of the noise-induced stable fixed point to excite large-amplitude excursions towards the right segment of the  $u$  nullcline (excited branch). In particular, in an isolated oscillator, perturbations due to the noise itself may induce a stochastic limit cycle which prevents the system from escaping out of the oscillatory regime, i.e., the transition to excitability cannot be observed in isolated oscillators, in spite of the renormalization of the dynamical param-

eters due to noise. In the presence of coupling, the weight of those oscillators that are not firing prevents these noise-induced excursions and leads to effective excitability.

Figure 1 (right panel) depicts the appearance of NIE, by plotting the time series of the activator's mean field,  $u(t) = (1/N)\sum_{i=1}^N u_i(t)$  for a system of 500 coupled elements, with the coupling strengths  $D_u = 100$  and  $D_v = 100$  and the time-scale-ratio parameter fixed to  $\varepsilon = 0.01$ . Because of the relatively large values of the coupling strengths (which nevertheless have the order of magnitude of  $\varepsilon^{-1}$ ), the time series of the single oscillators differs only very slightly from that of the mean field, i.e., the oscillators are synchronized. Figure 1(a) displays the regular self-sustained oscillations of the system without noise. Increasing the noise intensity  $\sigma_m^2$  leads to an increase and randomization of the time interval between consecutive spikes, as seen in Figs. 1(b)–1(d). Finally, for large enough noise no spike appears [Fig. 1(e)]. This corresponds to an oscillation suppression due to multiplicative noise: the system stays at the noise-induced stable fixed point. But besides an oscillation suppression, the system also exhibits excitable properties when perturbations (other than the stabilizing noise) affect the system. As shown below, this noise-induced regime displays stochastic resonance when driven periodically and wave propagation by local coupling.

In order to describe quantitatively the transition towards excitability, we compute the relative resting time with respect to the whole measuring time. Because of the random character of the time series, we need to specify a measurement threshold. We define the resting time as the interval during which every oscillator fulfills the conditions  $u_i < -0.5$  and  $v_i \leq 1.85$ . The first requirement corresponds to the absence of spikes, and the second checks the absence of large excursions towards the left on the left branch of the  $u$  nullcline. Such excursions would lead to a large excitation threshold and weaken the system's excitability. The threshold for the relative resting time is set to 0.98.

According to the previous definitions, Fig. 2(a) displays a phase diagram in the plane of parameters  $D_u - \sigma_m^2$  distinguishing the regions where the original oscillatory behavior and the NIE regime exist. The left boundary of the NIE balloon corresponds basically to the condition  $u_i < -0.5$  and the right one to  $v_i < 1.85$ . The NIE region shrinks in size as  $D_v$  decreases (results not shown). In other words, minimum coupling strengths of both the activator and the inhibitor are required for the NIE regime to exist. Figure 2(b) pictures the dependence of the transition to NIE on the number of coupled elements of the system. As in standard phase transitions, the region of noise intensity values for which NIE exists becomes larger as the number of oscillators increases. We can also see that a minimum number of elements is needed (in the present case  $\sim 250$ ).

*Stochastic resonance in NIE.*—Defined as the enhanced response to an external signal for an optimal

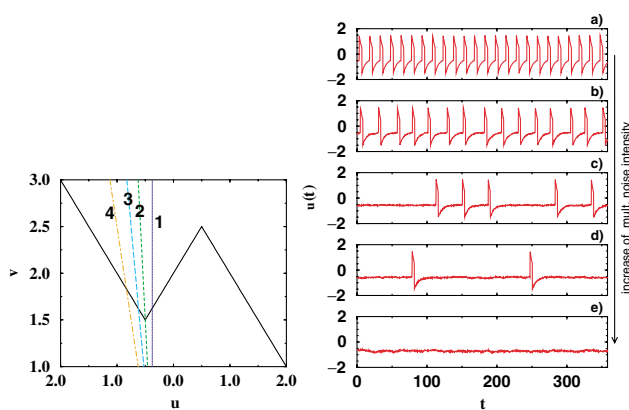


FIG. 1 (color online). Left panel: nullclines of a single FHN oscillator in phase space. The inverted-N piecewise line corresponds to the noise independent nullcline of the activator  $u$ . The other lines (1–4) describe the tilting of the inhibitor nullcline by increasing the noise intensity: 1— $\sigma_m^2 = 0.0$ ; 2— $\sigma_m^2 = 0.0334$ ; 3— $\sigma_m^2 = 0.06$ ; 4— $\sigma_m^2 = 0.1$ . Right panel: time series of the mean field of the fast variable  $u$  with increasing the multiplicative noise intensity: (a)  $\sigma_m^2 = 0.0$ ; (b)  $\sigma_m^2 = 0.033$ ; (c)  $\sigma_m^2 = 0.045$ ; (d)  $\sigma_m^2 = 0.05$ ; and (e)  $\sigma_m^2 = 0.08$ . Other parameters are  $a = 1.0$ ,  $b = 2.0$ ,  $c = 0.2$ , and  $d = 0.075$ .

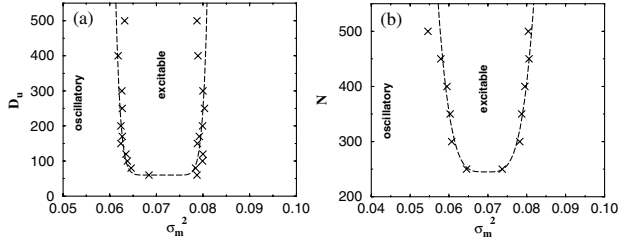


FIG. 2. Phase diagram for the transition from a self-sustained oscillatory regime to NIE. (a) Coupling strength  $D_u$  versus multiplicative noise intensity  $\sigma_m^2$  for 300 coupled elements. (b) Number of coupled elements  $N$  versus multiplicative noise intensity  $\sigma_m^2$  for  $D_u = 416$  and  $D_v = 64$ .

amount of noise, stochastic resonance (SR) has long been found in excitable media [11–13]. In order to show that the NIE regime possesses all immanent properties of excitable systems, we now examine the response of the system to external periodic driving and an additive source of noise. The behavior of the inhibitor is then given by

$$\dot{v}_i = cu_i + d + v_i \xi_i + D_v(\bar{v}_i - v_i) + \zeta_i + f \cos \omega_f t, \quad (3)$$

where  $\zeta_i$  is a Gaussian white noise with intensity  $\sigma_a^2$ , the intensity of the multiplicative noise is taken large enough to make the system excitable, and the amplitude  $f$  of the external forcing is chosen small enough so that no excitation is produced in the absence of the additive noise. We are interested in the response of the system at the signal frequency  $\omega_f$  when the additive noise intensity  $\sigma_a^2$  is increased. Figure 3 (left panel) displays the time series of the averaged activator concentration for different additive noise intensities, superimposed with the periodic input signal (with enlarged amplitude for a better comparability with the output signal). In the absence of additive noise [Fig. 3(a)], the signal alone is too small, and the system remains at the noise-induced stable fixed point. When additive noise is added, spikes appear more and more frequently, until at an optimal noise intensity the spikes occur basically synchronously with the signal [Figs. 3(b)–3(d)]. Further increase of additive noise destroys the synchronization effect [Fig. 3(e)].

To evaluate the linear response  $Q$  of the system at the input frequency  $\omega_f$  we extract the parameter  $Q$  from a signal  $\langle u_r \rangle$  as in [14,15]. In order to compute this quantity, we neglect subthreshold dynamics and replace the global signal by  $\langle u_r(t) \rangle = \Theta(\langle u \rangle - u_{\text{th}}) - 0.6\Theta(u_{\text{th}} - \langle u \rangle)$ , where  $\langle \dots \rangle$  denotes the average over the population and  $u_{\text{th}} = -0.45$ . The numerical results are shown in Fig. 3 (right panel) both with and without the multiplicative noise. The typical bell-shaped SR curve appears only in the presence of a suitable multiplicative noise intensity (i.e., in the NIE regime), whereas in the original self-sustained oscillatory regime ( $\sigma_m^2 = 0.0$ ), the SR effect cannot be observed. The former behavior corresponds to a double stochastic effect [15–18], because optimal response in the presence of additive noise occurs due to a

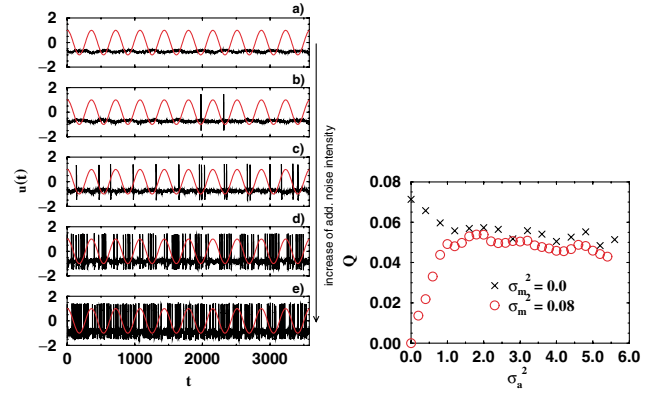


FIG. 3 (color online). Left panel: time series of the average activator concentration for increasing additive noise intensity and  $\sigma_m^2 = 0.08$ : (a)  $\sigma_a^2 = 0.0$ ; (b)  $\sigma_a^2 = 0.1$ ; (c)  $\sigma_a^2 = 0.5$ ; (d)  $\sigma_a^2 = 2.0$ ; and (e)  $\sigma_a^2 = 5.0$ . Right panel: response of the system to the signal frequency versus additive noise intensity, for  $\sigma_m^2 = 0.08$  (circles) and  $\sigma_m^2 = 0.0$  (crosses). Parameters are  $D_u = 100$ ,  $D_v = 100$ ,  $f = 0.012$ , and  $\omega_f = 0.0175$ . Other parameters are those of Fig. 1.

property (excitability) which is induced by a second, multiplicative noise. In light of these results, one could speculate that sensory adaptation by noise in living organisms [19] can be possible even in oscillatory situations because parametric noise can suppress undesirable oscillations.

*Wave propagation in NIE.*—One of the main characteristics of excitable media is their ability to sustain propagation of structures. This is, e.g., the way in which electrical pulses propagate through neural tissue in physiological systems [10]. The NIE regime reported here offers the possibility of a signal propagation through oscillatory media. Additionally, NIE allows the activation/deactivation of the excitable property so that information transport can be controlled by multiplicative noise.

In order to verify that the NIE regime allows the propagation of excitable structures, we substitute the global coupling considered so far by a local diffusive coupling. Hence the coupling term in Eqs. (1) and (2) is now given by  $\bar{x}_i \equiv \frac{1}{\mathcal{N}} \sum_{j \in n,n} x_j$ , where the sum runs only over the  $\mathcal{N}$  nearest neighbors of site  $i$ . In what follows we consider a 2-dimensional lattice with fixed boundary conditions. Additionally, the  $u$  nullcline is now given by

$$F(u) = \begin{cases} -1 - u + b, & u \leq -\frac{1}{2}, \\ gu + b + \frac{1}{2}(g-1), & -\frac{1}{2} < u < \frac{1}{g} - \frac{1}{2}, \\ +1 - au + b - \frac{1}{2} + a(\frac{1}{g} - \frac{1}{2}), & u \geq \frac{1}{g} - \frac{1}{2}, \end{cases}$$

in such a way that the slope of its unstable middle branch decreases, so that the refractory time becomes smaller. The dynamical equation of  $v$ , on the other hand, is unchanged from Eq. (2), and thus the noise-induced transition mechanism described above persists. Under these conditions, this system displays a noise-induced phase

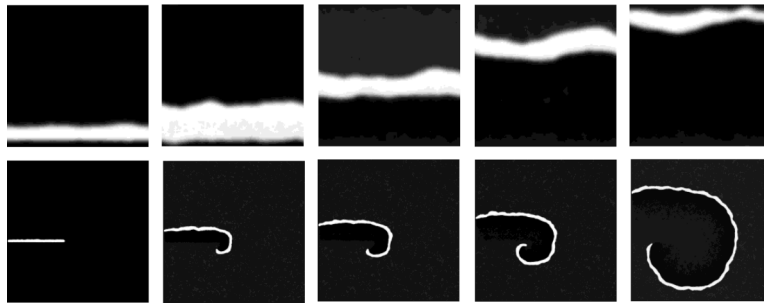


FIG. 4. Snapshots of the activatory variable  $u$  for increasing time (from left to right). The upper row shows the propagation of a plane wave front in an  $130 \times 130$  array at time steps 10.9, 11.5, 12.3, 13.4, and 14.2 time units. The lower row shows spiral wave propagation in a  $1000 \times 1000$  array at time steps 11.0, 13.5, 14.5, 16.0, and 21.0 time units. Parameters are  $\varepsilon = 0.01$ ,  $a = 1.0$ ,  $b = 2.0$ ,  $c = 0.2$ ,  $d = 0.075$ ,  $g = 0.2$ ,  $D_u = 416$ ,  $D_v = 64$ , and  $\sigma_m^2 = 0.072$ .

transition to excitability, as for global coupling, but in this case via the formation of clusters of stable elements. In the NIE region (i.e., for large enough  $\sigma_m^2$ ), independently of the initial conditions every oscillator of the coupled ensemble moves to the NIE fixed point and remains there. In this situation, the spatiotemporal response of the system to a plane-wave perturbation is depicted in Fig. 4 (upper row). We observe a clear propagation of the plane wave from bottom to top. Spiral wave propagation can also be seen in Fig. 4 (lower row). In the absence of multiplicative noise, on the other hand, the system exhibits a synchronous self-sustained oscillatory behavior and no wave propagation can be observed. This means that the presence of multiplicative noise is crucial for information transmission in this system.

In summary, we have studied a different kind of phase transition in which the application of noise to an array of oscillating elements leads to the suppression of oscillations and induces excitability. The appearance of noise-induced excitability is a collective effect and occurs via a phase transition due to the joint action of coupling and multiplicative noise. In contrast to standard phase transitions and other studies on excitable systems [3–7], the increase of noise enhances the stability in the system and restores excitable properties. This noise-supported excitability displays characteristic properties of standard excitable media, such as stochastic resonance and wave propagation. Since SR relies on a property of the system which is in turn induced by noise, optimization of both noise sources is needed, and hence this effect is an example of a doubly stochastic phenomenon [16]. The interplay between excitable and oscillatory dynamics in noisy systems is a current important issue [20]. In particular, these theoretical findings suggest a possible mechanism to suppress undesirable global oscillations in neural networks (which are usually characteristic of abnormal medical conditions such as Parkinson's disease or epilepsy), using the action of noise to restore excitability, which is the normal state of neuronal ensembles.

E. U. acknowledges the International MP Research School on Biomimetic systems, E. U. and A. Z. CESCA-

CEPBA (the EC IHP Program No. HPRI-1999-CT-00071), J. G. O. DGES (Spain, BFM2001-2159 and BFM2002-04369), and J. K. SFB 555 (Germany).

- 
- [1] A. Pikovsky and J. Kurths, *Phys. Rev. Lett.* **78**, 775 (1997).
  - [2] B. Lindner *et al.*, *Phys. Rep.* (to be published).
  - [3] S. Alonso *et al.*, *Phys. Rev. Lett.* **87**, 078302 (2001).
  - [4] J. García-Ojalvo, F. Sagués, J. M. Sancho, and L. Schimansky-Geier, *Phys. Rev. E* **65**, 011105 (2002).
  - [5] J. García-Ojalvo and L. Schimansky-Geier, *J. Stat. Phys.* **101**, 473 (2000).
  - [6] R. Báscones, J. García-Ojalvo, and J. M. Sancho, *Phys. Rev. E* **65**, 061108 (2002).
  - [7] S. Kádár, J. Wang, and K. Showalter, *Nature (London)* **391**, 770 (1998).
  - [8] C. Van den Broeck, J. M. R. Parrondo, and R. Toral, *Phys. Rev. Lett.* **73**, 3395 (1994).
  - [9] J. García-Ojalvo and J. M. Sancho, *Noise in Spatially Extended Systems* (Springer, New York, 1999).
  - [10] J. Keener and J. Snyder, *Mathematical Physiology* (Springer, New York, 1998).
  - [11] F. Moss *et al.*, *Ann. N.Y. Acad. Sci.* **706**, 26 (1993).
  - [12] K. Wiesenfeld *et al.*, *Phys. Rev. Lett.* **72**, 2125 (1994).
  - [13] B. Lindner, *Coherence and Stochastic Resonance in Nonlinear Dynamical Systems* (Logos-Verlag, Berlin, 2002).
  - [14] L. Gammaitoni, P. Hänggi, P. Jung, and F. Marchesoni, *Rev. Mod. Phys.* **70**, 223 (1998).
  - [15] A. Zaikin, J. García-Ojalvo, L. Schimansky-Geier, and J. Kurths, *Phys. Rev. Lett.* **88**, 010601 (2002).
  - [16] A. Zaikin, *Fluctuations and Noise Letters* **2**, L157 (2002).
  - [17] A. Zaikin, J. García-Ojalvo, R. Báscones, E. Ullner, and J. Kurths, *Phys. Rev. Lett.* **90**, 030601 (2003).
  - [18] A. Zaikin, J. Kurths, and L. Schimansky-Geier, *Phys. Rev. Lett.* **85**, 227 (2000).
  - [19] D. Russell, L. Wilkens, and F. Moss, *Nature (London)* **402**, 291 (1999).
  - [20] J. M. G. Vilar *et al.*, *Proc. Natl. Acad. Sci. U.S.A.* **99**, 5988 (2002).

# Appendix B

## Vibrational resonance and vibrational propagation in excitable systems

E. ULLNER, A. ZAIKIN, J. GARCÍA-OJALVO, R. BÁSCONES AND J. KURTHS,  
Vibrational resonance and vibrational propagation in excitable systems. *Physics Letters A* 312, 2003, 348–354.

DOI: 10.1016/S0375-9601(03)00681-9





ELSEVIER

Available online at [www.sciencedirect.com](http://www.sciencedirect.com)

SCIENCE @ DIRECT®

Physics Letters A 312 (2003) 348–354

PHYSICS LETTERS A

[www.elsevier.com/locate/pla](http://www.elsevier.com/locate/pla)

# Vibrational resonance and vibrational propagation in excitable systems

E. Ullner<sup>a</sup>, A. Zaikin<sup>a</sup>, J. García-Ojalvo<sup>b,c,\*</sup>, R. Báscones<sup>b</sup>, J. Kurths<sup>a</sup>

<sup>a</sup> *Institut für Physik, Potsdam Universität, Am Neuen Palais 10, D-14469 Potsdam, Germany*

<sup>b</sup> *Departament de Física i Enginyeria Nuclear, Universitat Politècnica de Catalunya, Colom 11, E-08222 Terrassa, Spain*

<sup>c</sup> *Center for Applied Mathematics, Cornell University, Ithaca, NY 14853, USA*

Received 5 December 2002; received in revised form 11 April 2003; accepted 14 April 2003

Communicated by C.R. Doering

## Abstract

We report the occurrence of vibrational resonance in excitable systems. Namely, we show that an optimal amplitude of the high-frequency driving enhances the response of an excitable system to a low-frequency signal. The phenomenon is confirmed in an excitable electronic circuit and in the FitzHugh–Nagumo model. In this last case we also analyze the influence of additive noise and the interplay between stochastic and vibrational resonance. Additionally, we show that this effect can be extended to spatially extended excitable media, taking the form of an enhanced propagation of the low-frequency signal.

© 2003 Elsevier Science B.V. All rights reserved.

## 1. Introduction

Signal detection by nonlinear systems can be considerably affected by external influences. The most relevant example of this fact is stochastic resonance (SR), where the response of a nonlinear system to a weak deterministic signal is enhanced by external random fluctuations [1]. Initially reported in bistable systems [2], SR has been found in many models and even natural systems [3,4], including excitable media [5].

In bistable systems, it has been shown that the role of noise in improving the quality of signal detection can be played by other types of driving, such

as a chaotic signal [6] or a high-frequency periodic force [7]. In the latter case, known as *vibrational resonance* (VR), the system is under the action of a two-frequency signal. Such bichromatic signals are pervasive in many different fields, including brain dynamics [8], where, for instance, bursting neurons may exhibit two widely different time scales, and telecommunications [9], where information carriers are usually high-frequency waves modulated by a low-frequency signal that encodes the data. Two-frequency signals are also of interest in several other fields, such as laser physics [10], acoustics [11], neuroscience [12], and physics of the ionosphere [13]. The beneficial role of high-frequency (ultrasonic) driving has already been reported as increased drug uptake by brain cells [14], acceleration of bone and muscle repairing [15], and resonantly enhanced biodegradation of micro-orga-

\* Corresponding author.

E-mail address: [jordi.g.ojalvo@upc.es](mailto:jordi.g.ojalvo@upc.es) (J. García-Ojalvo).



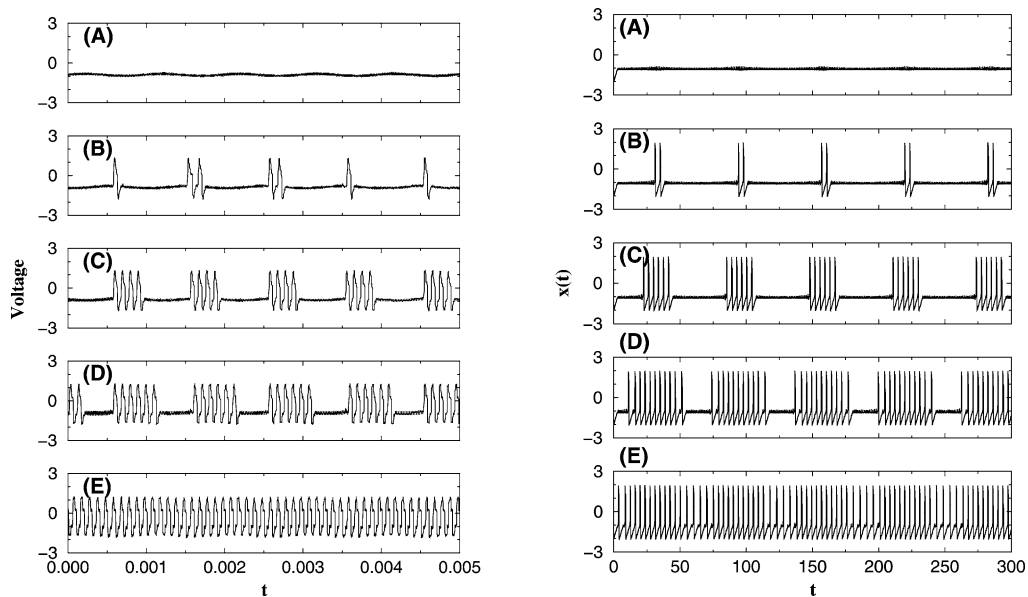


Fig. 2. Left: experimental results exhibiting vibrational resonance in the excitable electronic circuit of Fig. 1 under the action of a bichromatic signal. The voltage drop at the 1 nF condenser is plotted for different amplitudes of the high-frequency harmonic forcing: (A) 0.435 V, (B) 0.465 V, (C) 0.66 V, (D) 0.985 V, and (E) 1.385 V. The amplitude of the low-frequency component is fixed to 1.3 V. Right: corresponding regimes obtained by numerical simulations of the FitzHugh–Nagumo model for different HF amplitudes: (A)  $B = 0.05$ , (B)  $B = 0.0505$ , (C)  $B = 0.055$ , (D)  $B = 0.065$ , and (E)  $B = 0.07$ .

condenser. For a small enough amplitude of the HF component the total signal is below threshold, and hence there are no spikes in the system output, as shown in regime A of Fig. 2 (left). By increasing slightly the amplitude of the HF component, spikes start to appear at the low frequency (regime B). In this regime processing of the information (which is encoded in the LF signal) begins to occur, but can be considerably improved by further increasing the number of spikes per half period of the LF signal, since in this way the energy contained at this frequency is also increased. This happens in regimes C and D, which show the optimal detection of the LF signal. With further increase of the HF amplitude (regime E), the system fires immediately after reaching the stable point, so that the output mainly contains only the own frequency of the excitable system. Hence the LF component basically disappears from the system output, and signal processing is degraded again. This is a manifestation of vibrational resonance in an excitable medium, where an intermediate amplitude of a high-frequency driving leads to a resonant response at the low-frequency signal.

### 3. Vibrational resonance in the FitzHugh–Nagumo model

Next we show that the behavior reported in the previous section is not particular to the experimental system considered, but is a generic property of excitable systems. To that end we study numerically the FitzHugh–Nagumo (FHN) model, which is a paradigmatic model describing the behavior of firing spikes in neural activity [24], and in general the activator–inhibitor dynamics of excitable media [25]. In the presence of two harmonic signals, this model is defined by the following set of coupled equations:

$$\varepsilon \frac{dx}{dt} = x - \frac{x^3}{3} - y, \quad (1)$$

$$\frac{dy}{dt} = x + a + A \cos(\omega t) + B \cos(\Omega t) + \xi(t), \quad (2)$$

where  $x(t)$  is the activator variable (representing the membrane potential in the neural case) and  $y(t)$  is the inhibitor (related to the conductivity of the potassium channels existing in the neuron membrane [24]). The value of the time scale ratio  $\varepsilon = 0.01$  is chosen so that

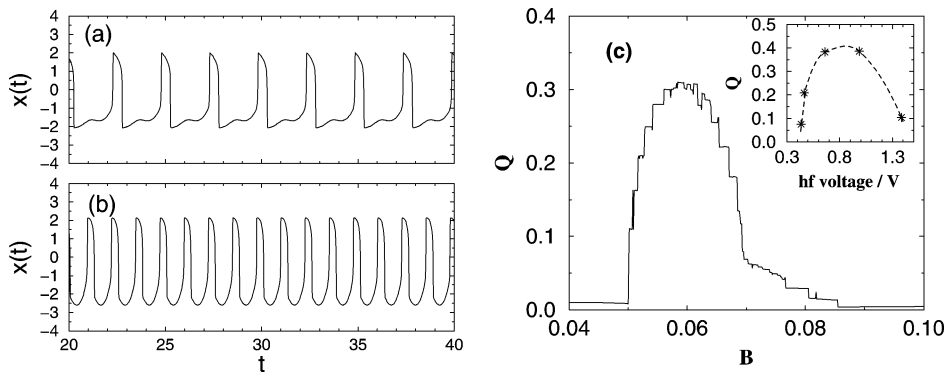


Fig. 3. (a) Oscillations exhibited by the bichromatically forced FHN model (1)–(2) at a frequency close to the own frequency of the system, and (b) at the driving high-frequency. The amplitude of the HF forcing is  $B = 0.1$  and  $10$ , respectively. (c) Response  $Q$  of the system at the low frequency  $\omega$  vs. the amplitude  $B$  of the high-frequency input signal. The inset shows the corresponding figure for the electronic circuit results presented in Fig. 2 (left).

the activator evolves much faster than the inhibitor. Under these conditions the system is excitable for  $a > 1$  [26]; we choose  $a = 1.05$ .  $\xi(t)$  is a Gaussian white noise with zero mean and correlation  $\langle \xi(t)\xi(t') \rangle = \sigma_a^2 \delta(t - t')$ . The terms  $A \cos(\omega t)$  and  $B \cos(\Omega t)$  stand for the low- and high-frequency components of the external signal, respectively. In what follows we will chose  $A = 0.01$ , so that the system is below the excitation threshold (which is  $A_{\text{thr}} \approx 0.075$  for  $B = 0$ ), and  $\Omega \gg \omega$ , in particular  $\Omega = 5$  and  $\omega = 0.1$ . In Eq. (2) we have considered no phase shift between the two driving signals, but it can be checked that the existence of an arbitrary phase shift does not alter the results that follow. To integrate model (1)–(2) we have used Heun's algorithm [27].

First we consider the noise-free case  $\sigma_a = 0$  and, mimicking the electronic implementation described in the previous section, we fix the amplitude of the LF signal component and increase the HF amplitude. The different regimes exhibited by the FHN model under these conditions are shown in Fig. 2 (right). These regimes closely resemble the preceding observations made in the electronic circuit (compare left and right plots in the figure). As in that case, an increase of the HF amplitude  $B$  initially improves (regimes A–D) and finally degrades (regime E) signal processing at the low frequency, in what constitutes another case of vibrational resonance. Several additional aspects of the system behavior can be found in this model with respect to the electronic implementation. For

instance, in regime E (Fig. 2 right) it is clearly seen that the intervals between spikes are not constant. This happens when the amplitude of the HF force is such that the system starts to fire asynchronously with respect to the signal. In this case, during one half of the signal period the system has to wait some time before spiking, whereas in the other half period the system can fire sooner once it reaches the stable point. This happens because in the latter case the time during which the signal is above threshold is larger, while the waiting time is close to the half period of the high-frequency force. Increasing the amplitude  $B$  further leads to a very regular spiking, as in the regime E of the electronic circuit (see also Fig. 3(a)). Finally, for large enough values of  $B$  we obtain a new regime that has not been observed in the circuit. In this regime, the oscillations happen with a frequency different from the own frequency of the system (i.e., the one related to the intrinsic time scale of the spiking behavior), but correspond in fact to the high-frequency component ( $\Omega = 5$  in this case). This regime is depicted in Fig. 3(b), where it is compared with the above mentioned case where each spike follows the previous one almost periodically with the system internal frequency (Fig. 3(a)).

The VR effect illustrated in Fig. 2 can be quantified by computing the response  $Q$  of the system (i.e., the component from the Fourier spectrum) at the signal frequency  $\omega$ , which is given by  $Q = \sqrt{Q_{\text{sin}}^2 + Q_{\text{cos}}^2}$ ,

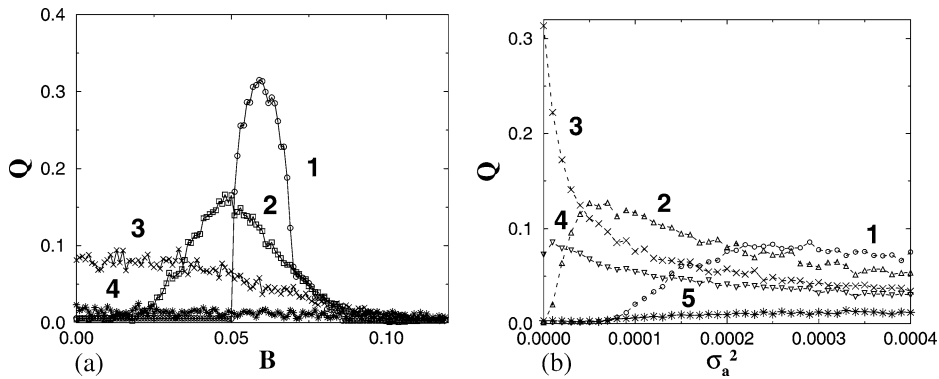


Fig. 4. Response of the system at the low frequency  $\omega$  in the presence of additive noise: (a) versus the HF amplitude  $B$  for different intensities of additive noise (curve 1:  $\sigma_a^2 = 0$ , curve 2:  $\sigma_a^2 = 0.05 \times 10^{-3}$ , curve 3:  $\sigma_a^2 = 0.25 \times 10^{-3}$ , curve 4:  $\sigma_a^2 = 3 \times 10^{-3}$ ; and (b) versus the noise intensity  $\sigma_a^2$  for different amplitudes (curve 1:  $B = 0$ , curve 2:  $B = 0.04$ , curve 3:  $B = 0.06$ , curve 4:  $B = 0.07$ , curve 5:  $B = 0.1$ ).

where

$$Q_{\sin} = \frac{\omega}{\pi n} \int_0^{2\pi n/\omega} y(t) \sin(\omega t) dt,$$

$$Q_{\cos} = \frac{\omega}{\pi n} \int_0^{2\pi n/\omega} y(t) \cos(\omega t) dt. \quad (3)$$

The dependence of this response on the amplitude of the high-frequency driving (Fig. 3(c)) displays a resonant form with a clearly defined maximum at  $B \sim 0.06$ , similarly to what happens in SR. The staircase form of this dependence is caused by the abrupt discrete appearance of new spikes in the spike train as the forcing amplitude increases. The staircase pattern persists (although its shape may change) when the frequency ratio between the two periodic signal changes, even when this ratio is incommensurate. We have checked that the resonance displayed in Fig. 3(c) persists for a wide range of values of the high-frequency around  $\Omega = 5.0$  (the values tested cover the range 2.0–17.0). However, due to the additional interplay between the HF signal and sub-threshold oscillations, the position and amplitude of the resonance peak vary with the value of the high frequency. This behavior constitutes a difference with respect to the standard SR effect, and could be useful for determining the system’s natural selectivity of special frequency components from the white noise when SR occurs.

So far we have not considered the influence of noise in the behavior of the FHN model. In order to study

the interplay of VR and SR in this system, we now increase the intensity  $\sigma_a^2$  of additive noise in the system. Fig. 4(a) shows that by adding noise to the system the response dependence is shifted to the left and decreased. Hence, with increasing noise the maximum of the response is achieved for a smaller value of  $B$  (compare curves 1 and 2 in Fig. 4(a)). This fact could be relevant for an efficient information processing, because natural fluctuations or noise (unavoidably present in experimental systems) are able to replace a fraction of the high-frequency driving and help to reduce the necessary input energy. If the noise intensity is too large, VR disappears (curve 4 in Fig. 4(a)). Next we analyze the response of the system as a function of noise intensity for varying amplitude  $B$  of the HF forcing (see Fig. 4(b)). For no HF amplitude (curve 1 in the figure) standard SR is found. Adding then a high-frequency driving to the signal improves SR, because the resonance curve is shifted to lower values of  $\sigma_a^2$  and is increased (curve 2 in Fig. 4(b)). Hence the amount of noise needed for an optimal signal processing is smaller. We can thus interpret that a high-frequency driving allows us to control stochastic resonance. Further increase of  $B$  to the value which corresponds to the optimal amplitude  $B = 0.06$  in the noise-free case leads only to a monotonous decrease of the quality of signal processing with increasing noise intensity  $\sigma_a^2$ , shown as curve 3 in Fig. 4(b) (but its value at zero noise is the largest one among all curves, as expected from the optimal driving amplitude – compare the values at  $\sigma_a^2 = 0$  of all the curves in Fig. 4(b) with curve 1 in Fig. 4(a)). For even larger values of  $B$ , signal

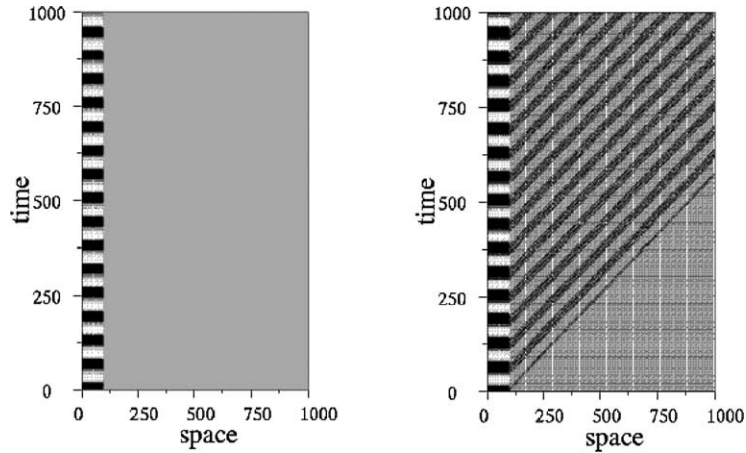


Fig. 5. Resonant vibrational propagation in an excitable medium. A chain of coupled oscillators (Eqs. (4)) is represented along the horizontal axis  $z$ . Time evolution goes from bottom to top. Left: without HF vibration ( $B = 0$ ); right: with HF vibration ( $B = 1.6$ ). The first 100 oscillators ( $i < i_{\text{ex}}$ ) are always driven by the low-frequency signal. An increase of high-frequency vibration leads to propagation of the information LF signal.

processing has very bad quality for all intensities of additive noise (curves 4 and 5).

#### 4. Resonant vibrational propagation

When excitable systems are coupled spatially in an extended medium, excitation pulses are able to propagate through the system in a very efficient way. Consequently, it is interesting to analyze whether the phenomenon of vibrational resonance can be generalized to the case of spatially extended systems. To that end we consider a chain of coupled excitable oscillators, whose behavior we represent now by the Barkley model [28]:

$$\begin{aligned} \frac{du_i}{dt} &= \frac{1}{\epsilon} u_i (1 - u_i) \left( u_i - \frac{v_i + b}{a} \right) \\ &+ \frac{D}{\Delta x} \sum_{j \in N(i)} c_{ij} u_j + A_i \cos(\omega t) + B \cos(\Omega t), \\ \frac{dv_i}{dt} &= cu_i - v_i, \end{aligned} \tag{4}$$

where  $i$  is the cell index along the chain, and we take  $A_i = 0$  for  $i > i_{\text{ex}}$ . In what follows we used the following values for the model parameters:  $\epsilon = 0.01$ ,  $a = 0.85$ ,  $b = 0.18$ , and  $c = 0.7$  (for which the system operates locally in an excitable regime) and the coupling strength is taken  $D = 0.05$ . The

weight coefficients  $c_{ij}$  correspond to the first-order discretization of the Laplacian operator [29] with  $\Delta x = 0.25$ . Every oscillator in the chain is driven by a high-frequency signal  $B \cos(\Omega t)$ , with  $\Omega = 5.0$ , and the oscillators with  $i < i_{\text{ex}}$  are additionally under the action of the low-frequency information-carrying signal  $A \cos(\omega t)$ , with  $\omega = 0.1$  and  $A = 3.0$ .

The behavior of this extended system is illustrated in Fig. 5. When no high-frequency vibration ( $B = 0$ ) is applied to the oscillators the signal is unable to propagate for the coupling strength chosen (Fig. 5 left). However, if we now apply a HF vibration ( $B = 1.6$ ) to all oscillators in the chain, the LF information-carrying signal propagates through the whole chain of oscillators as a train of pulses (Fig. 5 right). The mechanism of this effect is based on the occurrence of VR in single oscillators, but now the input of each oscillator (for  $i > i_{\text{ex}}$ ) comes from the output of the previous element in the chain. Hence, the effect of VR in excitable oscillators can be observed in spatially extended systems as a resonant *vibrational propagation*.

#### 5. Conclusions

We have studied several aspects of the dynamical response of excitable systems to bichromatic signals with two very different frequencies. We have demon-

strated the existence of two phenomena: vibrational resonance in zero-dimensional systems and resonant vibrational propagation in spatially extended media. Experimental results obtained in an excitable electronic circuit have been confirmed by a numerical analysis of the FitzHugh–Nagumo model. In particular, it has been shown that an optimal amplitude of the high-frequency component of the signal can optimize signal processing of the low-frequency component, which encodes the information. We have also shown that in the presence of noise high-frequency driving can substitute a fraction of the noise and hence control the effect of stochastic resonance. In spatially extended excitable media, vibrational resonance enhances propagation of the low-frequency signal through the system by means of the action of the high-frequency driving. We have reported vibrational resonance and resonant vibrational propagation in simple systems and paradigmatic models, and have studied these effects in a general framework, hence we expect that these findings will be relevant for different fields, including communication technologies, optics, chemistry, neuroscience, and medicine. Given the ubiquity of two-frequency signals in neural systems, mentioned already in the introduction, this result could be of special interest in the study of the activity of neuron ensembles, and in general in wave propagation in excitable activatory–inhibitory systems.

## Acknowledgements

A.Z. acknowledges financial support from CESCACEPBA through the EC IHP Program (HPRI-1999-CT-00071), and from the Microgravity Application Program/Biotechnology of the European Space Agency (ESA). J.G.O. was supported by the Ministerio de Ciencia y Tecnología (Spain, under projects BFM2001-2159 and BFM 2002-04369), E.U. by the International MP Research School on Biomimetic systems, and J.K. by SFB 555 (Germany).

## References

- [1] L. Gammaitoni, P. Hänggi, P. Jung, F. Marchesoni, *Rev. Mod. Phys.* 70 (1998) 223.
- [2] R. Benzi, A. Sutera, A. Vulpiani, *J. Phys. A* 14 (1981) L453.
- [3] B. McNamara, K. Wiesenfeld, R. Roy, *Phys. Rev. Lett.* 60 (1988) 2626.
- [4] J. Douglass, L. Wilkens, L. Pantazelou, *Nature* 365 (1993) 337.
- [5] K. Wiesenfeld, D. Pierson, E. Pantazelou, C. Dames, F. Moss, *Phys. Rev. Lett.* 72 (1994) 2125.
- [6] S. Sinha, *Physica A* 270 (1999) 204.
- [7] P. Landa, P. McClintock, *J. Phys. A: Math. Gen.* 33 (2000) L433.
- [8] G.M. Shepherd, *The Synaptic Organization of the Brain*, Oxford Univ. Press, 1990.
- [9] V. Mironov, V. Sokolov, *Radiotekh. Electron.* 41 (1996) 1501 (in Russian).
- [10] D. Su, M. Chiu, C. Chen, *Prec. Eng.* 18 (1996) 161.
- [11] A. Maksimov, *Ultrasonics* 35 (1997) 79.
- [12] J. Victor, M. Conte, *Visual Neurosci.* 17 (2000) 959.
- [13] V. Gherm, N. Zernov, B. Lundborg, A. Vastberg, *J. Atmos. Solar–Terrestrial Phys.* 59 (1997) 1831.
- [14] C.W. Cho, Y. Liu, W.N. Cobb, T.K. Henthorn, K. Lillehei, U. Christians, K.Y. Ng, *Pharm. Res.* 19 (2002) 1123.
- [15] J.L. Karnes, H.W. Burton, *Arch. Phys. Med. Rehabil.* 83 (2002) 1.
- [16] O. Schlafer, T. Onyeche, H. Bormann, C. Schroder, M. Sievers, *Ultrasonics* 40 (2002) 25.
- [17] R. Feng, Y. Zhao, C. Zhu, T.J. Mason, *Ultrason. Sonochem.* 9 (2002) 231.
- [18] Y. Yu, W. Wang, J. Wang, F. Liu, *Phys. Rev. E* 63 (2001) 021907.
- [19] P. Parmananda, H. Mahara, T. Amemiya, T. Yamaguchi, *Phys. Rev. Lett.* 87 (2001) 238302.
- [20] S. Kádár, J. Wang, K. Showalter, *Nature* 391 (1998) 770; J. García-Ojalvo, L. Schimansky-Geier, *J. Stat. Phys.* 101 (2000) 473; J. García-Ojalvo, F. Sagués, J.M. Sancho, L. Schimansky-Geier, *Phys. Rev. E* 65 (2002) 011105.
- [21] M. Löcher, D. Cigna, E.R. Hunt, *Phys. Rev. Lett.* 80 (1998) 5212; J.F. Lindner, S. Chandramouli, A.R. Bulsara, M. Löcher, W.L. Ditto, *Phys. Rev. Lett.* 81 (1998) 5048; J. García-Ojalvo, A.M. Lacasta, F. Sagués, J.M. Sancho, *Europhys. Lett.* 50 (2000) 427.
- [22] A. Zaikin, J. García-Ojalvo, L. Schimansky-Geier, J. Kurths, *Phys. Rev. Lett.* 88 (2002) 010601.
- [23] R. Báscones, J. García-Ojalvo, J.M. Sancho, *Phys. Rev. E* 65 (2002) 061108.
- [24] J. Keener, *J. Snyder, Mathematical Physiology*, Springer, New York, 1998.
- [25] A.S. Mikhailov, *Foundations of Synergetics*, 2nd Edition, Springer, Berlin, 1994.
- [26] A. Pikovsky, J. Kurths, *Phys. Rev. Lett.* 78 (1997) 775.
- [27] J. García-Ojalvo, J.M. Sancho, *Noise in Spatially Extended Systems*, Springer, New York, 1999.
- [28] D. Barkley, M. Kness, L.S. Tuckerman, *Phys. Rev. A* 42 (1990) 2489.
- [29] M. Abramowitz, I.A. Stegun, *Handbook of Mathematical Functions*, Dover, New York, 1972.



# Appendix C

## Oscillatory amplification of stochastic resonance in excitable systems

E.I. VOLKOV, E. ULLNER, A.A. ZAIKIN AND J. KURTHS, Oscillatory amplification of stochastic resonance in excitable systems. *Physical Review E* 68, 2003, 026214.

DOI: [10.1103/PhysRevE.68.026214](https://doi.org/10.1103/PhysRevE.68.026214)



## Oscillatory amplification of stochastic resonance in excitable systems

E. I. Volkov,<sup>1</sup> E. Ullner,<sup>2</sup> A. A. Zaikin,<sup>2</sup> and J. Kurths<sup>2</sup>

<sup>1</sup>*Department of Theoretical Physics, Lebedev Physical Institute, Leninskii 53, Russia*

<sup>2</sup>*Institut für Physik, Potsdam Universität, Am Neuen Palais 10, D-14469 Potsdam, Germany*

(Received 12 December 2002; published 22 August 2003)

We study systems which combine both oscillatory and excitable properties, and hence intrinsically possess two internal frequencies, responsible for standard spiking and for small amplitude oscillatory limit cycles (Canard orbits). We show that in such a system the effect of stochastic resonance can be amplified by application of an additional high-frequency signal, which is in resonance with the oscillatory frequency. It is important that for this amplification one needs much lower noise intensities as for conventional stochastic resonance in excitable systems.

DOI: 10.1103/PhysRevE.68.026214

PACS number(s): 05.45.-a, 05.40.Ca

### I. INTRODUCTION

The response of an excitable system to an external signal is a key effect of information processing in a single excitable oscillator or networks of excitable elements. Several intriguing phenomena have been found in the study of this effect. One of the most interesting and counterintuitive effect is stochastic resonance (SR) [1], initially found in bistable systems [2], and later confirmed in a large variety of physical [1] or biological systems [3], including also noise-induced structures [4] and excitable systems [5]. In SR an optimal amount of noise, acting upon an excitable system, increases the quality of the signal received via noise-induced synchronization [6]. Noteworthy, SR has been also found not only in excitable neural systems itself [7] or brain processing area [8], but also in the behavior of the whole organisms [9]. In spatially extended systems SR manifests itself in the signal transmission, resulted in a noise-induced propagation in bistable [10], excitable [11], or monostable systems [12,13].

In SR a part of the noise energy is used for constructive purposes, to cause a form of synchronization between input and output signals. Several investigations have been performed to find possibilities for the amplification of this effect. Array-enhanced SR has been considered in Refs. [14,15], where it has been shown that embedding of the processing element in a network of elements with optimal coupling and noisy strength [16] can improve the signal. This effect is closely connected and sometimes conceptually indistinguishable from spatiotemporal SR [17] or SR in extended bistable systems [18]. Another possibility to amplify the SR effect has been exploited in Ref. [15] by application of noninvasive control of SR. In this case, the external feedback has enhanced the response of a noisy system to a monochromatic signal. Finally, there were investigations, which have shown that with internal colored noise the SR effect can be enhanced in systems with a large memory time [19].

In this paper we study the SR effect in another class of systems, which differs to already explored ones by the fact that this class possesses properties of both oscillatory and excitable behavior. As a paradigmatic model for such systems we consider the famous FitzHugh-Nagumo (FHN) oscillator, known for its simplicity and rather realistic simulation of neural activity.

Generally, the FHN model is tuned to exhibit either an oscillatory behavior with strongly nonlinear oscillations in the system or an excitable behavior with a stable fix point, and the feature that relatively small perturbations can lead to a large excursion (excursion loop or spike) [20,5,21]. In contrast to this we are interested in a FHN model that is tuned to have both oscillatory and excitatory properties. Such dynamics takes place in FHN-like models [22] or in biophysical models [23,24], if their parameters are chosen in the region of the so-called “Canard” bifurcation [25,26]. In these works a Canard solution is a solution of a singular perturbed system which passes close to a bifurcation point and follows a repelling slow manifold for a considerable amount of time.

For the FHN model the Canard phenomenon means that there are quasiharmonic oscillations with small amplitude and small periods (see Fig. 1). The parameter region between pure excitable and oscillatory cases is typically very narrow if the stiffness of the oscillator is large ( $\varepsilon \ll 1$ ). But the value of stiffness is not obligatory large and is defined by the kinetic parameters of the specific models. A crucial feature of Canard-like behavior is that a very small change in the control parameter may lead to a large difference in the trajec-

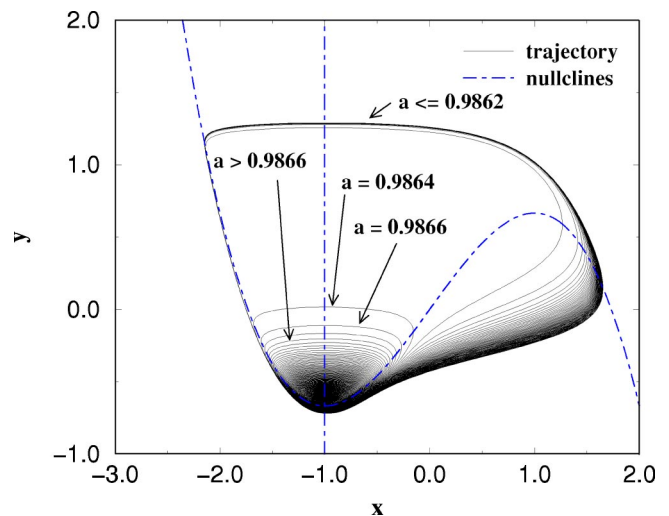


FIG. 1. The dependence of the trajectories and the appearance of Canard trajectories on the parameter  $a$  in the FHN model without noise and without driving forces.

ries and hence produce oscillations with different frequencies. This change can be also induced by the action of noise, if the system possesses Canard-like oscillations.

The idea to use a system with several intrinsic frequencies as a signal receiver in the presence of noise has been already reported in the literature. For example, in a bistable underdamped system, stochastic resonance may happen both due to intrawell as well as interwell motion [27]. Further on, it was described that nonadiabatic resonance under the action of a high frequency can exist in a noisy excitable system [28]. In all these works, the improvement of a signal processing occurs due to the resonance interplay between an incoming periodic signal and one of the internal frequencies of the oscillating system. In contrast to this case, we consider here the situation in which an additional high-frequency signal improves the detection of a low-frequency signal; i.e., it is crucial that the system is under the action of multifrequency signal. A similar problem formulation was studied in Ref. [29], where it was shown that adding a high-frequency signal may help the detection of a low-frequency signal and leads to a heterodyning effect in a two-dimensional oscillator with one internal frequency near a saddle-node bifurcation. However, this effect occurs due to the action of a resonant high-frequency signal on a detection threshold near a saddle-node bifurcation (see also a case of coupled oscillators [30]), whereas in our case we investigate a noisy system with two different internal frequencies under the action of a two-frequency signal, and the resonance effect at one higher internal frequency leads to the amplification of stochastic resonance at another low frequency.

We consider FHN system under the action of a subthreshold bichromatic signal, which consists of two parts: the first one has the frequency of an investigated signal, and the second one has a higher frequency. We demonstrate the effect of SR amplification, when the higher frequency is in resonance with the frequency of the Canard oscillations of our system. Noteworthy, two-frequency signals are widely used in communications [31], neuroscience [32], laser physics [33], or acoustics [34]. Additionally, the beneficial role of high-frequency (HF) driving has been already found in several biological phenomena, such as increased drug uptake by brain cells [35], improvement of bone and muscle healing [36], or enhanced biodegradation of microorganisms [37]. The effect, presented in this paper, is also closely connected to vibrational resonance (VR) in excitable systems [38], where the high-frequency driving acts as noise and improves the signal processing. VR demonstrates a resonancelike behavior with respect to the amplitude of the HF signal. In contrast to VR, in Canard-enhanced SR it is crucial that not the amplitude but *the frequency* of the HF signal should be in resonance with the oscillatory behavior of a system.

## II. THE MODEL

We study the following FHN model:

$$\varepsilon \dot{x}(t) = x(t) - \frac{x(t)^3}{3} - y(t), \quad (1)$$

$$\dot{y}(t) = x(t) + a + \xi(t) + F_{ext}(t), \quad (2)$$

where  $\xi(t)$  is Gaussian white noise of the intensity  $\langle \xi(t)\xi(t') \rangle = \sigma_a^2 \delta(t-t')$  and the parameter  $a$  determines the behavior of the system. For  $a > 1.0$  the FHN model is excitable, and for  $a < 1.0$  it shows an oscillatory behavior. At the bifurcation point  $a = 1.0$  the stability of the only fix point  $x_f = -a$ ,  $y_f = (a^3/3) - a$  will be changed. Between these two cases an intermediate behavior can appear. For values of the parameter  $a$  slightly beyond the bifurcation point, small oscillations near the unstable fix point are existing instead of large spikes. To illustrate this, in Fig. 1 trajectories in the phase space of the FHN system without driving force and noise are plotted in dependence on the parameter  $a$ . For  $a \leq 0.9862$  and  $\varepsilon = 0.1$ , the FHN model oscillates on the well-known big excursion loop. In the intermediate parameter region  $0.9864 \leq a < 1$  and  $\varepsilon = 0.1$ , there is also an oscillatory behavior but the loops (Canard-trajectories) in the phase space are much smaller than the excursion loops. Between both possible traces is a clear gap, so that both of these kinds of oscillations can be easily distinguished.

The Canard trajectories exist also for smaller  $\varepsilon$ -like 0.01, but the intermediate parameter region of  $a$  (where Canard oscillations exist) tends to zero for decreasing  $\varepsilon$ , and the period of subthreshold oscillations near the bifurcation point is  $T_{sth} \approx 2\pi\sqrt{\varepsilon}$  [22]. Hence, for  $\varepsilon = 0.01$  the subthreshold oscillations are very fast, and so the trajectory loops are very small. In the following, we fix the parameter  $\varepsilon = 0.1$  to have a system with a significant intermediate region where Canard oscillations exist. Similar values of  $\varepsilon$  (parameter to separate a slow and a fast moving variable) were used also in different papers for the modeling of natural processes [39–41], and so our choice has natural links. In spite of the fact that frequently used harmonic and singular approximations of FHN studies are very suitable for the mathematical tractability of the model behavior, in the real processes the stiffness is in between these two limit cases.

An important fact of the treatment of the Canard oscillations is that a very small change in the parameter  $a$  leads to a large difference in the trajectories. This change in the parameter  $a$  can be caused by some instantaneous influence of noise. Beside the expected case for the parameter  $a$  typical for the Canard phenomenon, Canard-like trajectories can be observed also in the excitable regime  $a > 1$  close to the bifurcation point if the FHN system is forced by additive noise  $\xi(t)$ . This can be easily seen in Fig. 2, where trajectories in the phase space were plotted for the parameters  $\varepsilon = 0.1$ ,  $a = 1.01$ ,  $\sigma_a^2 = 0.0004$  (in the excitable regime), and there is no periodic driving forces. Only the noise drives the FHN system and leads to the Canard-like trajectories and the spikes, and therefore, again the FHN system behaves with two different frequencies of the two cycles, which can be certainly used in signal processing.

These different trajectories manifest themselves in a poly-modal interspike interval histogram (ISIH) not only when the parameter  $a$  is chosen from the interval corresponding to the Canard orbits (as in Ref. [22]) but for  $a$  which provides an excitable regime (see Fig. 3). We have chosen the most pro-

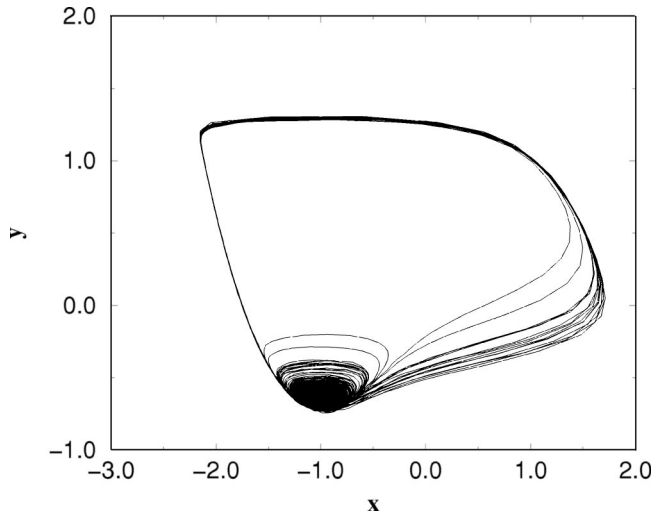


FIG. 2. Occurrence of spike and Canard trajectories in a noise driven FHN model in the excitable regime.

nounced examples of ISIH polymodality but this type of distribution is preserved in some intervals of the essential parameters:  $a \in [1.0 - 1.05], \epsilon \in [0.2 - 0.02]$  under the appropriate noise amplitudes.

Next we add a driving force  $F_{ext}(t) = b \cos(\omega t)$  and investigate the response of the periodic driven system at the input frequency. To evaluate the amplitude of the input frequency in the output signal, we calculate the Fourier coefficient  $Q$  for the input frequency  $\omega$ . We use the  $Q$  parameter instead of the power spectrum because we are interested in the transport of the information encoded in the frequency  $\omega$ . For this task the  $Q$  parameter is a much more compact tool than the power spectrum [1,12]:

$$Q_{\sin} = \frac{\omega}{2n\pi} \int_0^{2\pi n/\omega} 2x(t) \sin(\omega t) dt,$$

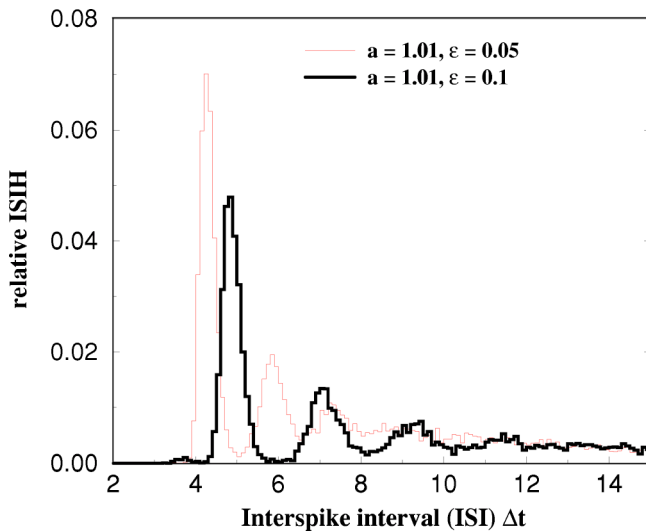


FIG. 3. ISIH in a noise driven excitable FHN model. The parameters are  $a = 1.01, \epsilon = 0.1$ .

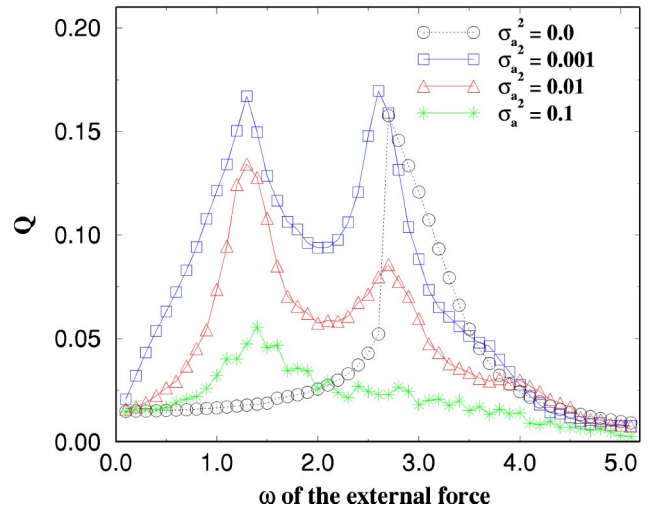


FIG. 4. Resonances for the periodically driven ( $b=0.03$ ) FHN system in the excitable regime ( $a=1.01$ ) under the influence of different noise intensities.

$$Q_{\cos} = \frac{\omega}{2n\pi} \int_0^{2\pi n/\omega} 2x(t) \cos(\omega t) dt,$$

$$Q = \sqrt{Q_{\sin}^2 + Q_{\cos}^2}.$$

First we look for the resonance frequencies of the system to find both internal frequencies (Canard frequency and frequency of the spiking behavior). Therefore we calculate the  $Q$  parameter versus the circle frequency of the driving force. We consider three cases: (a)  $a = 1.01$ , FHN in a monostable excitable regime; (b)  $a = 1.0$ , FHN at the bifurcation point; (c)  $a = 0.998$ , FHN in an oscillatory regime with small Canard oscillations around the unstable fix point and small amplitudes compared with the amplitude of a spike. The amplitude of the periodic driving force is chosen small enough so that the system needs noise to reach the threshold and to produce a spike. Figures 4–6 show the dependence of the  $Q$

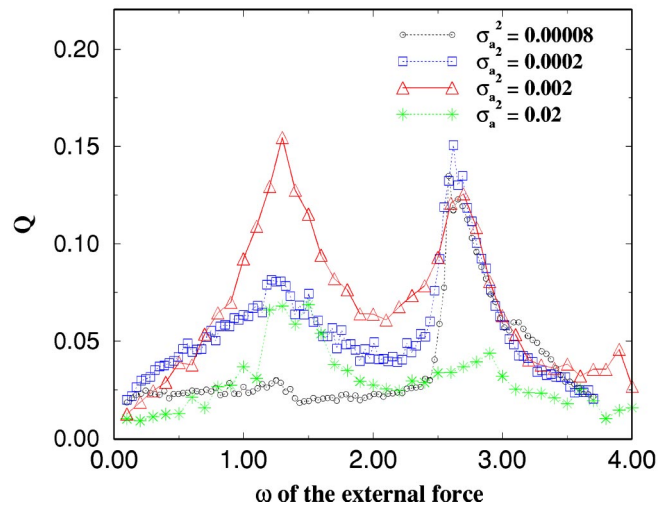


FIG. 5. Resonances for the periodically driven ( $b=0.02$ ) FHN system at the bifurcation point ( $a=1.0$ ) under the influence of different noise intensities.

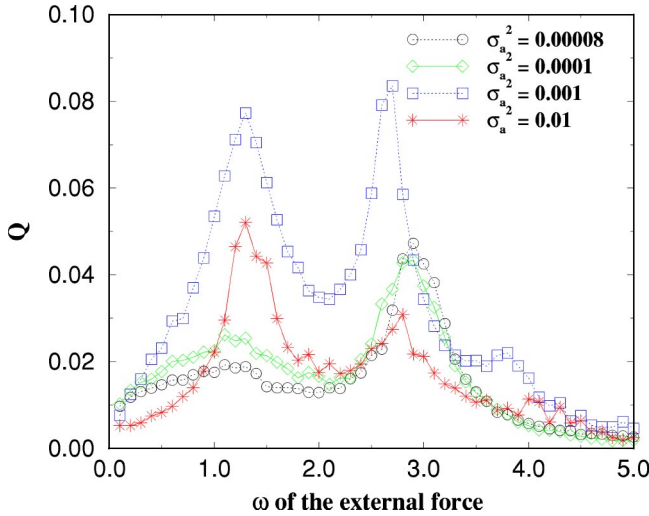


FIG. 6. Resonances for the periodically driven ( $b=0.01$ ) FHN system in the oscillatory regime ( $a=0.998$ ) under the influence of different noise intensities.

parameter on the input frequency for these three cases and various noise intensities  $\sigma_a^2$ . The  $Q$  parameter refers to the variable input frequency and measures the amplitude of the input frequency in the output signal.

The first peak in Figs. 4–6 at  $\omega=1.3$  corresponds to a period length of  $T=4.83$  and is caused by the firing of a spike. The second peak at about  $\omega=2.6$ – $2.9$  is caused by the Canard oscillations near the fix point  $x_f, y_f$  with a small amplitude compared with the big spike. In opposition to the resonance frequency of the spike, the position of the Canard resonance frequency  $\Omega_C$  depends on the parameter  $a$  and the noise intensity  $\sigma_a^2$ . This can be also easily seen in the phase space in Figs. 1 and 2. The trace of the spikes is very stable and narrow, and so the time for one round-trip during a spike is independent of the parameter  $a$  and the noise, while the traces for the Canard oscillations fill a much wider area in the phase space. Hence we can observe a shifting of the Canard-resonance frequency by changing  $a$  and  $\sigma_a^2$ . It is important to note that a peak at the Canard frequency exists even for smaller noise intensities, when the peak at the spiking frequency is not yet pronounced. This explains the fact that adding the driving force at this Canard frequency can be successfully used in the improvement of a signal receiving, even if the information is carried by another low frequency.

Noteworthy, similar high-frequency resonance has been described recently in the Hodgkin-Huxley model [42] and it was proposed in the “resonate-and-fire” neuron model [43], but its background is the oscillatory convergence to the rest state instead of the Canard phenomenon. For a more stiff FHN oscillator, only the low-frequency peak in ISIH is observed, and its coherency is maximal if the period is equal to the time of cycle excursion as it has been shown in Ref. [28].

### III. ENHANCEMENT OF STOCHASTIC RESONANCE

With the knowledge of the Canard-resonance frequency, we demonstrate that the response of the system to a given input frequency is improved. We force the FHN system with

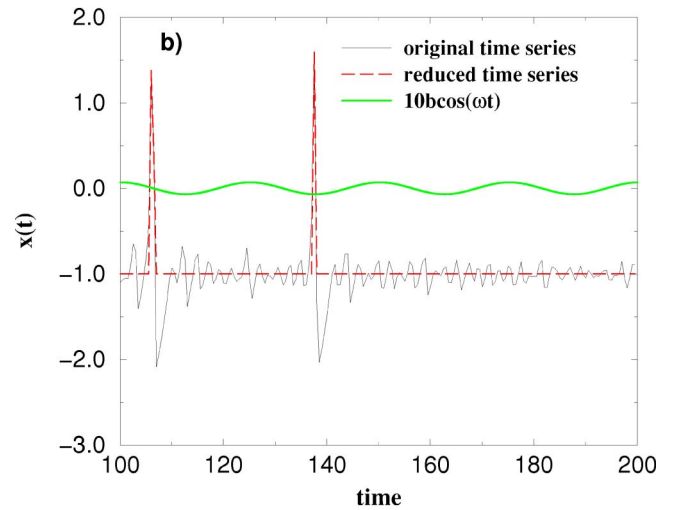
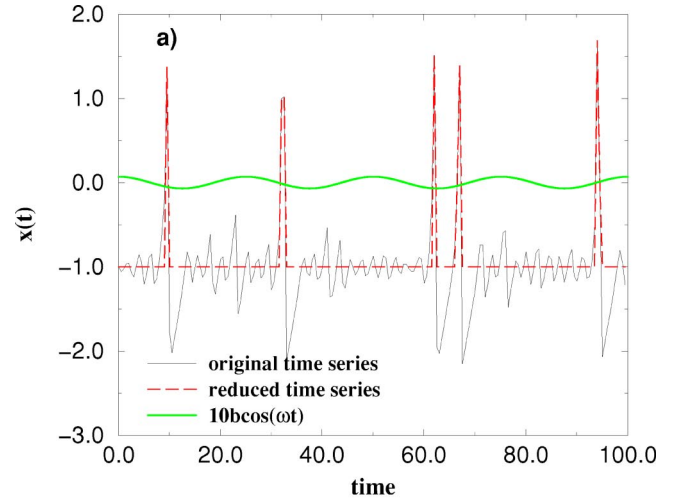


FIG. 7. Time series of the  $x(t)$  variable for the excitable FHN system driven by additive noise and two periodic forces. The high-frequency input signal is in resonance with the Canard frequency (a) and out of resonance with the Canard frequency (b). For a better recognition of the signal processing with the low-frequency input signal, this periodic input signal is also plotted (with a ten times higher amplitude than in the model).

two different but fixed frequencies,

$$F_{ext}(t) = b\cos(\omega t) + C\cos(\Omega t).$$

The basic idea is that the information is stored in a low-frequency input signal with a circle frequency  $\omega$  and an amplitude  $b$ . The additional high-frequency input signal  $C\cos(\Omega t)$  and the noise helps to reach the threshold, so both are necessary to produce a spike. The amplitude of both periodic input signals are chosen small enough that they cannot produce a spike without noise. A similar situation was in the study of the vibrational resonance [38]. But the setup of the parameters in Ref. [38] did not allow use of the Canard resonance in the signal processing.

In Fig. 7, two typical time series of the  $x$  variable are plotted for the parameters  $\varepsilon=0.1$ ,  $a=1.01$ ,  $\sigma_a^2=0.000375$ ,

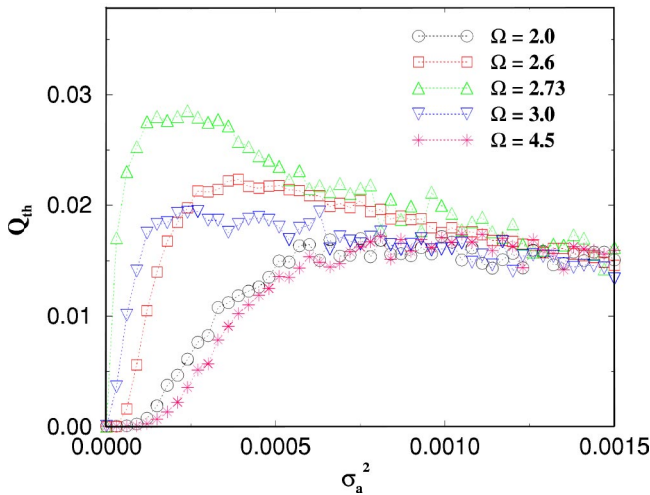


FIG. 8. Signal processing at the low-frequency ( $\omega$ ) input signal versus the noise intensity for various frequencies of the high-frequency input signals  $\Omega$  for the FHN system in the excitable regime. Parameters:  $a = 1.01$ ,  $b = 0.007$ ,  $C = 0.025$ , and  $\omega = 0.251$ . The Canard-resonance frequency is  $\Omega_C = 2.73$ , see Fig. 4.

$C = 0.025$ ,  $b = 0.007$ ,  $\omega = 0.251$ , and  $\Omega = 2.73$  for Fig. 7(a) and  $\Omega = 2.0$ , respectively, for Fig. 7(b). The difference between these two figures is the frequency  $\Omega$  of the high-frequency input signal: the first one shows the case of resonant forcing with the Canard frequency ( $\Omega = \Omega_C$ ) and the second one corresponds to the forcing out of the Canard frequency ( $\Omega \neq \Omega_C$ ). As an important result, the amplitudes of the small oscillations around the fix point in the original time series  $x(t)$  are different. Because of the resonance between the external high-frequency force and the noise-induced small amplitude oscillations in the Canard-resonant case, these small oscillations are enhanced by amplitude and the FHN in this regime can easier reach the threshold of the firing with the help of noise. As a result, we can observe the behavior that is more synchronized with the low-frequency input signal.

In natural systems with such a spiking behaviorlike neurons, only the spikes themselves are important for the information transport. As shown above, small Canard oscillations near the fix point are very important for the behavior of the FHN itself, but not for the information transport. To evaluate the information transport, we calculate again the response of the system,  $Q_{th}$ , but replace the original time series  $x(t)$  by a reduced time series without oscillations around the fix point. In this way we consider only the spikes for the information transport. To distinguish between a spike and the sub-threshold oscillations, we set the threshold of detection  $x_{th} = 0.0$ . If  $x(t)$  is smaller than  $x_{th}$ , we replace  $x(t)$  by the value of the fix point  $x_f$ . For  $x(t) \geq x_{th}$ , we use the original value of  $x(t)$ . This replacement is used only for the calculation of the  $Q_{th}$  parameter and not for the simulation of the original time series with the Heun method. The filtered time series are also plotted in Fig. 7 by the dashed line. In Figs. 8–10 (excitable regime, at the bifurcation point, and oscillatory regime, respectively) the dependencies of the quality of the information transport (represented by the  $Q_{th}$  parameter

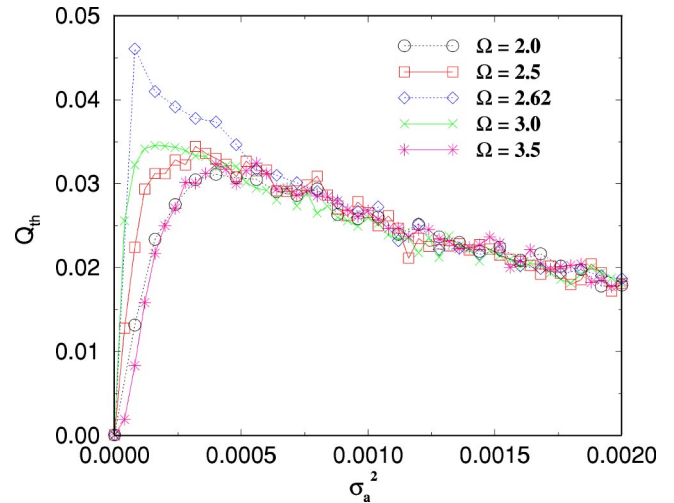


FIG. 9. Signal processing at the low-frequency ( $\omega$ ) input signal versus the noise intensity for various frequencies of the high-frequency input signals  $\Omega$  for the FHN system at the bifurcation point. Parameters:  $a = 1.0$ ,  $b = 0.01$ ,  $C = 0.02$ , and  $\omega = 0.251$ . The Canard-resonance frequency is  $\Omega_C = 2.62$ , see Fig. 5.

at the low frequency  $\omega$ ) on the noise intensity  $\sigma_a^2$  are depicted for different frequencies of the high-frequency driving force.

All three cases have in common that without noise ( $\sigma_a^2 = 0$ ) we observe no information transport, because  $Q_{th}$  is zero. That means that the FHN system does not show a spiking behavior. These figures demonstrate the bell shaped form of  $Q_{th}$ , well-known SR effect [1], for all different high frequencies. In the range of lower noise, it can be clearly seen that for the HF part of the signal being in resonance with Canard frequency, the SR effect at the low frequency  $\omega$  is significantly enhanced. In this region there is a significant difference in the  $Q_{th}$  parameter between the forcing at the

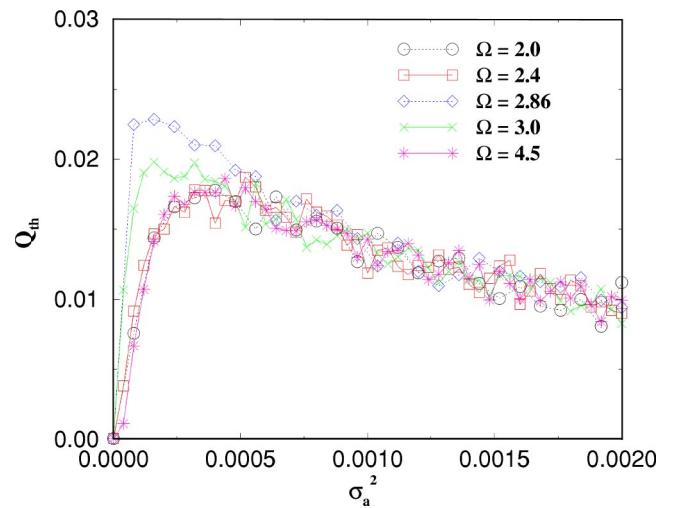


FIG. 10. Signal processing at the low-frequency ( $\omega$ ) input signal versus the noise intensity for various frequencies of the high-frequency input signals  $\Omega$  for the FHN system in the oscillatory regime. Parameters:  $a = 0.998$ ,  $b = 0.005$ ,  $C = 0.01$ , and  $\omega = 0.251$ . The Canard-resonance frequency is  $\Omega_C = 2.86$ , see Fig. 6.

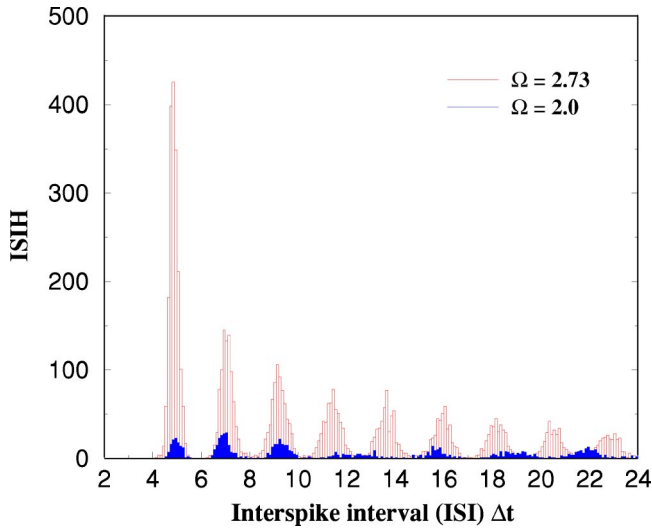


FIG. 11. ISI histogram by forcing of the excitable FHN system in ( $\Omega = 2.73 = \Omega_C$ ) and out of the Canard resonance ( $\Omega = 2.0 \neq \Omega_C$ ).

Canard-resonance frequency ( $\Omega = \Omega_C$ ) and the forcing out of the Canard resonance ( $\Omega \neq \Omega_C$ ). The difference in the  $Q_{th}$  parameter is caused only by a change of the frequency  $\Omega$  of the HF signal because the amplitudes are the same within one figure. This effect can be understood as the coexistence of two resonances. The first resonance happens between the high frequency of a signal and the frequency of Canard oscillations. If these two frequencies are similar, this resonance amplifies the conventional SR for a signal with low frequency.

The demonstration of signal enhancement may be presented also in the form of interspike interval histograms. In Fig. 11 the ISIH is depicted for the same parameters ( $\omega = 0.251$ ) which are used for both the time series in Figs. 7(a) and 7(b). Both ISIHs were calculated with the same length of 100 000 time units for the underlying time series in Canard resonance ( $\Omega = 2.73 = \Omega_C$ ) and out of resonance ( $\Omega = 2.0 \neq \Omega_C$ ). In the resonant case, much more spikes occur, and hence, the peaks of ISIH have higher values. The first maximum in the ISIH for both time series is between  $\Delta t = 4.8$  and  $4.9$  and corresponds exactly to the resonance frequency of the spikes with period  $T = 4.83$ . The time of the first maximum is the minimal time between two adjacent spikes when one spike follows the other one without any waiting time, i.e., without any small Canard oscillation.

For the Canard-resonant case, we observe the expected multimodal structure with peaks located at multiples of the period length of the Canard oscillations or high-frequency force at  $T = 2.3$  ( $\Omega = 2.73$ ). This modulation is very regular. By forcing out of Canard resonance with  $\Omega = 2.0$  or  $T = 3.14$ , the first three peaks are approximately at the same position as in the resonant case. Although we force out of the Canard frequency, one or two Canard periods can occur be-

tween two adjacent spikes. Except for these three peaks in the ISIH, the multimodal structure with the period of the Canard period is suppressed. For higher interspike intervals, a modulation with the period of  $T \approx 3$  can be observed, which corresponds to the high-frequency input signal. In this case the Canard oscillation can succeed only for two periods and lose the competition with the high-frequency forcing after this time, and the waiting time will be dominated now by integer numbers of the high-frequency period.

#### IV. SUMMARY

In conclusion, we have considered a signal processing in the noisy system which possesses both oscillatory and excitable properties under the action of an additional HF signal. This system was represented by the FHN model with a stiffness between pure excitable and oscillatory regime. We have demonstrated the possibility to amplify the SR effect in such systems using the Canard oscillations. In this effect the HF signal that is in resonance with the frequency of Canard oscillations strongly improves signal processing of the low-frequency signal. The effect shows a frequency selectivity and disappears in the region out of resonance with the Canard frequency.

For supercritical Hopf bifurcation in FHN-like models, this phenomenon is relevant for biology if the stiffness of the system (a degree of excitability) is limited by the interval  $\varepsilon \in [0.2 - 0.01]$  in order to get the observable periods of noise-induced Canard-like orbits. In this interval very small noise is necessary for a significant improvement of signal processing. It means, e.g., for neurons, the possibility of a new regulation of signal processing which, in addition to the choice of the value of the bifurcation parameter, can control the signal transmission under a small noisy environment.

We hope that these theoretical findings will stimulate experimental work to find new possibilities of signal receiving and propagation in systems, which demonstrate Canard-like oscillations, especially in nonlinear chemical systems [44] or in biophysical models [23,24]. Moreover, the dynamical systems, which have some specific regime between excitable and oscillatory states, are not limited by the FHN with Canard phenomenon. Recently, it has been shown that the modified Oregonator equations have three steady states and excitation occurs via resonance between damped HF oscillations around the stable fixed point and periodic perturbations with an appropriate tuning frequency [45]. A similar SR enhancement by HF signal may also be expected in this chemical system with low excitability.

#### ACKNOWLEDGMENTS

E.V. and J.K. acknowledge financial support from SFB 555 (Germany), E.U. from the International MP Research School on Biomimetic Systems, and A.Z. from the Microgravity Application Program/Biotechnology of the European Space Agency.

- [1] L. Gammaitoni, P. Hänggi, P. Jung, and F. Marchesoni, *Rev. Mod. Phys.* **70**, 223 (1998).
- [2] R. Benzi, A. Sutera, and A. Vulpiani, *J. Phys. A* **14**, L453 (1981).
- [3] P. Hänggi, *Chem. Phys.* **3**, 285 (2002).
- [4] A. Zaikin, J. Kurths, and L. Schimansky-Geier, *Phys. Rev. Lett.* **85**, 227 (2000).
- [5] K. Wiesenfeld *et al.*, *Phys. Rev. Lett.* **72**, 2125 (1994).
- [6] R. Rozenfeld, J.A. Freund, A. Neiman, and L. Schimansky-Geier, *Phys. Rev. E* **64**, 051107 (2001).
- [7] J. Douglas, L. Wilkens, and L. Pantazelou, *Nature (London)* **365**, 337 (1993).
- [8] T. Mori and S. Kai, *Phys. Rev. Lett.* **88**, 218101 (2002).
- [9] D. Russel, L. Wilkens, and F. Moss, *Nature (London)* **402**, 291 (1999).
- [10] J. Lindner *et al.*, *Phys. Rev. Lett.* **75**, 3 (1995).
- [11] S. Kádár, J. Wang, and K. Showalter, *Nature (London)* **391**, 770 (1998).
- [12] A. Zaikin, J. García-Ojalvo, L. Schimansky-Geier, and J. Kurths, *Phys. Rev. Lett.* **88**, 010601 (2002).
- [13] R. Reigada, A. Sarmiento, and K. Lindenberg, *Phys. Rev. E* **63**, 066113 (2001).
- [14] J.F. Lindner, B.K. Meadows, W.L. Ditto, M.E. Inchiosa, and A.R. Bulsara, *Phys. Rev. Lett.* **75**, 3 (1995).
- [15] J. Lindner *et al.*, *Phys. Rev. E* **63**, 041107 (2001).
- [16] J. Lindner *et al.*, *Phys. Rev. E* **53**, 2081 (1996).
- [17] F. Marchesoni, L. Gammaitoni, and A.R. Bulsara, *Phys. Rev. Lett.* **76**, 2609 (1996); J.M.G. Vilar and J.M. Rubí, *ibid.* **78**, 2886 (1997).
- [18] H.S. Wio, *Phys. Rev. E* **54**, R3075 (1996); S. Bouzat and H.S. Wio, *ibid.* **59**, 5142 (1999).
- [19] A. Neiman and W. Sung, *Phys. Lett. A* **223**, 341 (1996).
- [20] A. Pikovsky and J. Kurths, *Phys. Rev. Lett.* **78**, 775 (1997).
- [21] C. Heneghan *et al.*, *Phys. Rev. E* **54**, 2228 (1996).
- [22] V.A. Makarov, V.I. Nekorkin, and M.G. Velarde, *Phys. Rev. Lett.* **86**, 3431 (2001).
- [23] S. Baer and T. Erneux, *SIAM (Soc. Ind. Appl. Math.) J. Appl. Math.* **46**, 721 (1986).
- [24] S. Schuster and M. Marhl, *J. Biol. Systems* **9**, 291 (2001).
- [25] P. Glendinning, *Stability, Instability, and Chaos: An Introduction to the Theory of Nonlinear Differential Equations* (Cambridge University Press, Cambridge, 1994).
- [26] F. Dumortier and R. Roussarie, *Mem. Am. Math. Soc.* **577**, 1 (1996).
- [27] L. Alfonsi, L. Gammaitoni, S. Santucci, and A. Bulsara, *Phys. Rev. E* **62**, 299 (2000).
- [28] S.R. Massanes and C.P. Vicente, *Phys. Rev. E* **59**, 4490 (1999).
- [29] M. Inchiosa *et al.*, *Phys. Rev. E* **63**, 066114 (2001).
- [30] J. Acebrón, W. Rappel, and A. Bulsara, *Phys. Rev. E* **67**, 016210 (2003).
- [31] V. Mironov and V. Sokolov, *Radiotekh. Elektron. (Moscow)* **41**, 1501 (1996).
- [32] J. Victor and M. Conte, *Visual Neurosci.* **17**, 959 (2000).
- [33] D. Su, M. Chiu, and C. Chen, *Precis. Eng.* **18**, 161 (1996).
- [34] A. Maksimov, *Ultrasonics* **35**, 79 (1997).
- [35] C. Cho *et al.*, *Pharmacol. Res.* **19**, 1123 (2002).
- [36] J. Karnes and H.W. Burton, *Arch. Phys. Med. Rehabil.* **83**, 1 (2002).
- [37] O. Schlafer *et al.*, *Ultrasonics* **40**, 25 (2002).
- [38] E. Ullner, A. Zaikin, R. Bascones, J. García-Ojalvo, and J. Kurths, *Phys. Lett. A* **312**, 348 (2003).
- [39] J. Das and H. Busse, *Biophys. J.* **60**, 369 (1991).
- [40] S. Girard *et al.*, *Biophys. J.* **61**, 509 (1992).
- [41] H. Mahara, T. Yamaguchi, and Y. Amagishi, *Chem. Phys. Lett.* **317**, 23 (2000).
- [42] P. Parmananda, C.H. Mena, and G. Baier, *Phys. Rev. E* **66**, 047202 (2002).
- [43] E.M. Izhikevich, *Neural Networks* **14**, 883 (2001).
- [44] M. Brons and J. Sturis, *Phys. Rev. E* **64**, 026209 (2001).
- [45] P. Parmananda, H. Mahara, T. Amemiya, and T. Yamaguchi, *Phys. Rev. Lett.* **87**, 238302 (2001).



# Appendix D

## Frequency-dependent stochastic resonance in inhibitory coupled excitable systems

E.I. VOLKOV, E. ULLNER, A.A. ZAIKIN AND J. KURTHS, Frequency-dependent stochastic resonance in inhibitory coupled excitable systems. *Physical Review E* 68, 2003, 061112.

DOI: [10.1103/PhysRevE.68.061112](https://doi.org/10.1103/PhysRevE.68.061112)



**Frequency-dependent stochastic resonance in inhibitory coupled excitable systems**E. I. Volkov,<sup>1</sup> E. Ullner,<sup>2</sup> A. A. Zaikin,<sup>3</sup> and J. Kurths<sup>2</sup><sup>1</sup>*Department of Theoretical Physics, Lebedev Physical Institute, Leninskii 53, Russia*<sup>2</sup>*Institut für Physik, Potsdam Universität, Am Neuen Palais 10, D-14469 Potsdam, Germany*<sup>3</sup>*Institut für Biochemie, Charité, Humboldt Universität, Hessische Strasse 3-4, 10115 Berlin, Germany*

(Received 4 September 2003; published 31 December 2003)

We study frequency selectivity in noise-induced subthreshold signal processing in a system with many noise-supported stochastic attractors which are created due to slow variable diffusion between identical excitable elements. Such a coupling provides coexisting of several average periods distinct from that of an isolated oscillator and several phase relations between elements. We show that the response of the coupled elements under different noise levels can be significantly enhanced or reduced by forcing some elements in resonance with these new frequencies which correspond to appropriate phase relations.

DOI: 10.1103/PhysRevE.68.061112

PACS number(s): 05.40.Ca, 05.45.-a

**I. INTRODUCTION**

The signal processing in an excitable system of oscillators or networks is a key element of information exchange in neural networks. By the investigation of such processes several unexpected phenomena have been found. One of the most interesting and counterintuitive effect is stochastic resonance (SR) [1], initially found in bistable systems [2], and later studied in a large variety of physical [1] or biological systems [3], including also noise-induced structures [4] or excitable systems [5,6]. SR consists in an improvement of the system response to an input signal due to an optimal noise intensity acting upon the system. In SR a part of the noise energy is used for constructive purposes, to cause a form of synchronization between input and output signals [7]. Several investigations have been performed to find possibilities for the amplification of this SR effect. Array-enhanced SR has been considered in Refs. [8,9], where it has been shown that embedding of the processing element in a network of elements with optimal coupling and noisy strength [10] can improve the signal. This effect is closely connected and sometimes conceptually indistinguishable from spatiotemporal SR [11] or SR in extended bistable systems [12]. Another possibility to amplify the SR effect has been exploited in Ref. [9] by application of noninvasive control of SR. In this case, the external feedback has enhanced the response of a noisy system to a monochromatic signal. Finally, there were investigations, which have shown that with internal colored noise the SR effect can be enhanced in systems with a large memory time [13].

In isolated excitable systems, SR has been usually investigated for the paradigmatic FitzHugh Nagumo (FHN) model [5,6,14,15], as well as array-enhanced SR has been considered for FHN oscillators coupled via diffusion of their fast variables. Recently it has been shown that a frequency and phase locking in an ensemble of noise stimulated excitable oscillators can be enhanced by an optimal number of coupled elements [16,17]. Typically, studies of SR do not demonstrate a sensitive dependence on the frequency of the forcing. Partially this is caused by using an adiabatic approximation which is applied to get analytic results about SR. There are only some investigations in which the frequency of the signal

is the essential parameter. Gang *et al.* [18] have shown that SR in specifically globally coupled large bistable systems with two series of cells demonstrates the bell-shaped dependence on the signal frequency. Lindner *et al.* [19] have shown the amplification of the spectral power at particular frequencies in small arrays of underdamped monostable oscillators. To our knowledge, the role of the signal frequency for *excitable* systems has been studied in Refs. [15,17,20–23] for isolated FHN, when the characteristic time of the system, defined by an external period providing the maximal level of synchronization, practically coincides with the excursion time of an excitable element, and this time is the single natural reference point for time scale. Such a form of frequency selectivity can be also important for biological membranes in enzymatic systems [24]. In other studies the frequency sensitivity in weak signal processing results from a resonance between small oscillations around steady state and a signal [25–28]. Hence, despite different excitation mechanisms, the oscillation frequency is defined by the parameters of isolated elements. On the other hand, our mechanism is based on the appearing of new resonance frequencies due to special phase relations in an inhibitor coupled array.

In this paper we investigate the influence of a signal frequency in SR effects in a system of excitable oscillators, coupled via the inhibitory variable. This form of coupling between oscillators may provide a broad spectrum of additional frequencies in the system's behavior. Oscillatory media with inhibitory coupling have very rich dynamics and have been reported to be important in numerous physical [29], electrical [30], and chemical systems [31,32]. To be particular, the inhibitory form of coupling is used to explain morphogenesis in Hydra regeneration and animal coat pattern formation [33], or to provide the understanding of pattern formation in an electron-hole plasma and low-temperature plasma [29]. In chemistry, the effective increase of inhibitor diffusion by reducing of activator diffusivity via the complexation of iodide (activator) with the macromolecules of starch results in a Turing structure formation [34]. It has been shown that the dominance of such a coupling between identical oscillators results in the generation of many stable limit cycles with different periods and phase relations [35,36]. This type of diffusion is referred to the

class of “dephasing” interaction because there is a large area of the phase space where the phase points repel each other due to this interaction. Dephasing is a source of multirhythmicity, which was observed in different systems [37–40]. For excitable noisy elements the dephasing interaction of stochastic limit cycles (instead of deterministic ones) may provide coexistence of spatiotemporal regimes which are selectively sensitive with respect to the period of external signals. In these systems noise plays two roles, at least: (i) it stimulates firings of stable elements and, consequently, their interaction during return excursion and (ii) it stimulates transitions between coupling-dependent attractors if they occur and have visible lifetimes.

The paper is structured as follows. After the explanation of the model equations and the method, used to estimate signal processing, we review the classical SR effect in an isolated excitable oscillator to emphasize the difference with the selective SR in a coupled system. Then we study a chain of two identical inhibitory coupled excitable oscillators. In this situation the phase relation becomes important for the resonance frequency and the antiphase motion exhibits another resonance frequency than that of an isolated oscillator. In contrast to an isolated oscillator, the ensemble reacts very sensitively upon the new resonance frequency of the antiphase attractor. This new frequency selectivity can be used for an enhancement of the signal processing and information transport in the SR effect at this new resonance frequency. After that, we study a chain of three coupled elements with a richer spectrum of the phase relations and the frequencies. Beside the antiphase motion (two in-phase oscillators are in antiphase with the third one), this system demonstrates the so-called dynamic trap regime in which the middle element does not produce spikes because of antiphase motion of neighbors. This additional resonance frequency of the ensemble enables to demonstrate a frequency selective modifications of the signal processing.

## II. MODEL

We study several rather simple small arrays of inhibitory diffusively coupled stationary but very strongly excitable FitzHugh Nagumo models (FHN) under the action of white additive noise and subthreshold periodic signal which is applied to one of the elements. The FHN model is a paradigmatic model describing the behavior of firing spikes in neural activity [41], and in general the activator-inhibitor dynamics of excitable media [42]. We show that for some values of the signal period the dependence of SR measures on the noise level has a second maximum and the dependence of SR on the values of the signal period under some fixed noise resembles the conventional resonance.

In order to get the reference frame for further comparisons, we begin with the study of the dependence of classical SR on the signal period in the simplest version of FHN model. The previous investigation [21] was very limited in relation to the value of the periods studied. The model is given by the following equations:

$$\frac{dx}{dt} = A - y + \xi + A_s \sin\left(\frac{2\pi}{T_s} t\right), \quad (1)$$

$$\varepsilon \frac{dy}{dt} = x - \frac{y^3}{3} + y, \quad (2)$$

where, in a neural context,  $y(t)$  represents the membrane potential of the neuron and  $x(t)$  is related to the time-dependent conductance of the potassium channels in the membrane [41]. The dynamics of the activator variable  $y$  is much faster than that of the inhibitor  $x$ , as indicated by the small time-scale-ratio parameter  $\varepsilon$ . It is well known that for  $|A| > 1$  the only attractor is a stable fixed point. For  $|A| < 1$ , the limit cycle generates a periodic sequence of spikes. We fix  $A$  close to the bifurcation in the interval  $[1.01, 1.03]$  in order not to use high-level noise to excite oscillations and thereby to avoid masking of the fine structure of the interspike intervals histograms. Here  $\varepsilon$  is in the range  $[0.0001, 0.001]$ , which is significantly smaller compared to those that are commonly used. Such a stiff excitation is needed to provide a fast jumping between the attractors. The stochastic forcing is represented by Gaussian white noise  $\xi$  with zero mean and intensity  $\sigma_a^2$ ,  $\langle \xi(t)\xi(t+\tau) \rangle = \sigma_a^2 \delta(\tau)$ . The harmonic signal is subthreshold,  $A_s < A - 1.0$ . To evaluate the amplitude of the input frequency in the output signal, we calculated the linear response at the input frequency  $\omega = 2\pi/T_s$  [1],

$$Q_{\sin} = \frac{\omega}{2n\pi} \int_0^{2\pi n/\omega} 2y(t) \sin(\omega t) dt,$$

$$Q_{\cos} = \frac{\omega}{2n\pi} \int_0^{2\pi n/\omega} 2y(t) \cos(\omega t) dt,$$

$$Q = \sqrt{Q_{\sin}^2 + Q_{\cos}^2},$$

when  $n$  is the number of periods  $T_s$ , covered by the integration time.

## III. CLASSIC SR IN AN ISOLATED FHN

Figure 1 shows the dependence of the linear response  $Q$  on the noise amplitude for different values of the signal period. For the numerical integration of the model we have used here and below the Heun’s algorithm [43]. All curves demonstrate standard SR behavior, but the influence of the period is not weak especially for  $T_s = 3.2$  which corresponds to the duration of excursion time after firing  $T_{\text{exc}}$ . For this period the optimal signal amplification takes place in a broad range of noise amplitude. Furtheron, the resonance frequency depends on the noise intensity  $\sigma_a^2$  and hence the driving period  $T_s$  can be in resonance only at a suitable range of  $\sigma_a^2$  and not overall [Fig. 1(b)]. This explains the appearance of the additional maximum in the dependence for  $T_s = 3.2$ . A detailed investigation of the resonant forcing of an isolated FHN can be found in Ref. [21]. Under strong noise, the realizations of stochastic cycles are very similar to corresponding noisy limit cycle (e.g., with  $A = 0.99$ ) and the de-

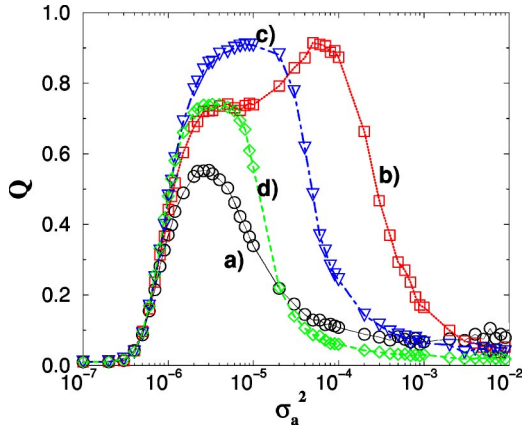


FIG. 1. The linear response  $Q$  for an isolated FHN [Eqs. (1) and (2)] as function of the noise intensity  $\sigma_a^2$  for different signal periods  $T_s=2.8$  (a), 3.2 (b), 3.4 (c), and 4.0 (d). Other parameters are  $A=1.02$ ,  $\varepsilon=0.0001$ ,  $A_s=0.01$ .

pendence of  $Q$  on the period under fixed large noise contains the conventional main resonance and secondary resonances at  $T=1.6, 1.08$ , at least (Fig. 2). A conventional resonance occurs when the time moments of the end of phase point excursions coincide with “negative” phase of the signal which significantly facilitates the next firing ( $A$  is shifted closer to 1.0). Figure 2 illustrates that if the signal period is one half or one third of the excursion time  $T_{exc}$  then the secondary resonances occur.

#### IV. FREQUENCY-DEPENDENT SR IN TWO COUPLED OSCILLATORS

Now we consider two identical and coupled elements and introduce the diffusion of the inhibitory variables,

$$\frac{dx_{1,2}}{dt} = A - y_{1,2} + \xi_{1,2} + A_{s,1,2} \sin\left(\frac{2\pi}{T_s} t\right) + C(x_{2,1} - x_{1,2}), \quad (3)$$

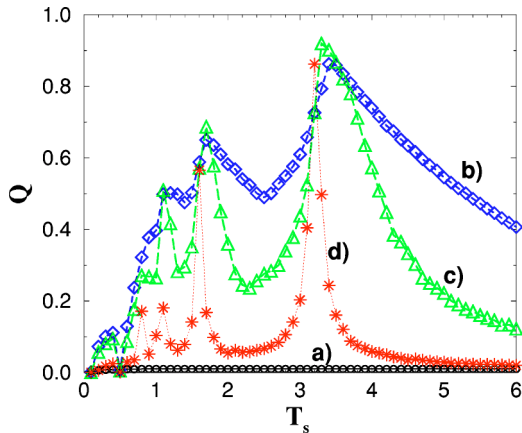


FIG. 2. The dependence of the linear response  $Q$  for an isolated FHN [Eqs. (1) and (2)] on the signal period  $T_s$  for several values of the noise level  $\sigma_a^2=0.0$  (a),  $3 \times 10^{-6}$  (b),  $1 \times 10^{-5}$  (c),  $1 \times 10^{-4}$  (d).

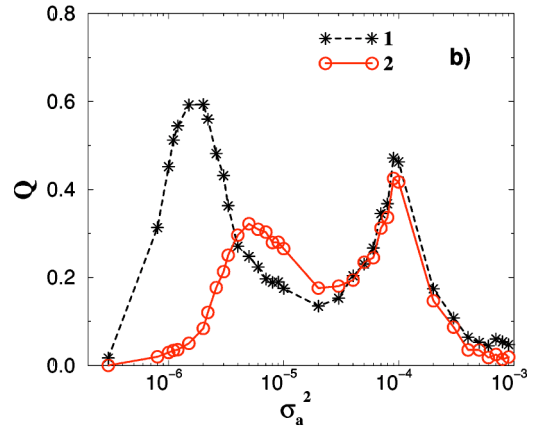
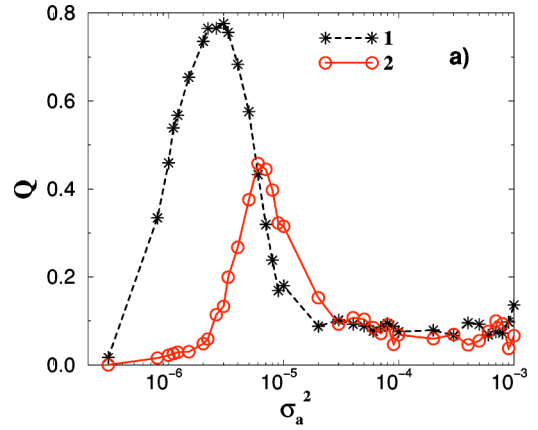


FIG. 3. The linear response  $Q$  for two inhibitor coupled FHN [Eqs. (3) and (4)] as function of the noise intensity for signal periods  $T_s=3.2$  (a) and  $T_s=4.2$  (b).  $A=1.02$ ,  $\varepsilon=0.0001$ ,  $A_{s,1}=0.01$ ,  $A_{s,2}=0.0$ ,  $C=0.1$ .

$$\varepsilon \frac{dy_{1,2}}{dt} = x_{1,2} - \frac{y_{1,2}^3}{3} + y_{1,2}, \quad (4)$$

where the signal is applied only to the first element ( $A_{s,1}=0.01$  and  $A_{s,2}=0.0$ ), and  $\langle \xi_i(t) \xi_j(t+\tau) \rangle = \sigma_a^2 \delta(\tau) \delta_{i,j}$ .

We investigate the dynamics of Eqs. (3) and (4) in the same region of the signal periods and noise levels as in Figs. 1 and 2 and select the most typical results. Figure 3 presents the dependence of  $Q$  on the noise intensity for (a)  $T_s=3.2$  and (b)  $T_s=4.2$ .

Under the action of weak noise the first element shows SR at any  $T_s$  and the transmission of the signal to the second element is observed starting from the SR-optimal noise. For standard SR a further evolution of  $Q$  with noise for both element should be a continuous decreasing of  $Q$ . The same is true for the elements coupled via their fast variables, but the inhibitory coupled relaxation excitable elements demonstrate a large second peak [Fig. 3(b)] for some interval of  $T_s=4.2-4.5$ . The nature of this peak is the noise-induced antiphase stochastic cycle in the presence of the coupling. It has been shown recently that in a broad interval of noise amplitudes the antiphase cycle dominates and results in a new type of coherence resonance [44]. The period of this cycle depends on the coupling strength and the noise ampli-

tude which define the position of the second peak on the curve  $Q(\sigma_a^2)$  in Fig. 3(b). The influence of the stiffness is also essential because for  $\varepsilon > 0.001$  the second peak cannot be clearly observed (data not shown), but the rate of  $Q(\sigma_a^2)$  decreasing is less than that for standard SR (Fig. 1). A similar double maximum in the power spectral amplitude at the forcing frequency as a function of the noise intensity has been found recently but for an underdamped bistable system where two maxima are linked with two noise-induced motions: intrawell and interwell [45]. These results show that we can use inhibitory coupled oscillators for frequency selection in stochastic resonance. Notably, a multipeak *coherence* resonance also has been observed in coupled FHN models [46].

### V. FREQUENCY-DEPENDENT SR IN A CHAIN OF THREE OSCILLATORS

Three identical coupled elements can demonstrate a richer set of regimes which depend on the configuration

$$\frac{dx_1}{dt} = A - y_1 + \xi_1 + A_s \sin\left(\frac{2\pi}{T_s} t\right) + C(x_2 - x_1), \quad (5)$$

$$\frac{dx_2}{dt} = A - y_2 + \xi_2 + A_s \sin\left(\frac{2\pi}{T_s} t\right) + C(x_1 - x_2) + C(x_3 - x_2), \quad (6)$$

$$\frac{dx_3}{dt} = A - y_3 + \xi_3 + C(x_2 - x_3), \quad (7)$$

$$\varepsilon \frac{dy_{1,2,3}}{dt} = x_{1,2,3} - \frac{y_{1,2,3}^3}{3} + y_{1,2,3}, \quad (8)$$

where  $\langle \xi_i(t) \xi_j(t + \tau) \rangle = \sigma_a^2 \delta(\tau) \delta_{i,j}$ .

Let us analyze possible attractors in the autonomous system of three inhibitory coupled identical oscillators. For a linear chain of oscillators whose bifurcation parameters are close to Hopf bifurcation, three main types of stable attractors occur [47]. The first is in antiphase regime in which oscillators at the ends move in antiphase with the middle one. The second type was called “dynamic trap” because the antiphase motion of the end’s oscillators does not permit the firing of the middle one. The third type is not a single attractor but a family of attractors which may be designated as  $n/2/n$ , where  $n=3,5,7,\dots$ . The value of  $n$  depends on the coupling strength and the distance of  $A$  from the bifurcation value. The closer the  $A$  to 1.0 (for FHN model) the larger is the value  $n$  and the stronger is the crowding of attractors. If the elements do not oscillate deterministically but are excited by noise, then the observed stochastic collective modes only partially resemble these types of regimes due to noise-dependent perturbations of trajectories. The attractors  $n/2/n$  will be practically corrupted by noise. This type of multimodal distributions is not model specific and was observed for autooscillating [48] and excitable [49] electronic arrays with dephasing (inhibitory) interactions.

Figure 4 shows the distribution of interspike intervals (ISIs) for three coupled excitable elements without an exter-

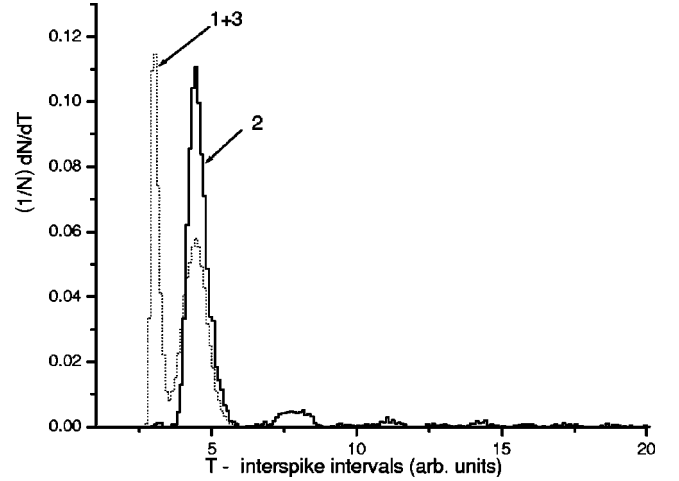


FIG. 4. The ISI distributions for a chain of three coupled excitable elements [Eqs. (5)–(8)] and no signal ( $A_s = 0.0$ ). The ISI distributions of first and the third (1+3) oscillators are denoted by a dashed line and the second one (2) by a solid line. The other parameters are  $A = 1.02$ ,  $C = 0.1$ ,  $\sigma_a^2 = 10^{-4}$ , and  $\varepsilon = 0.0001$ .

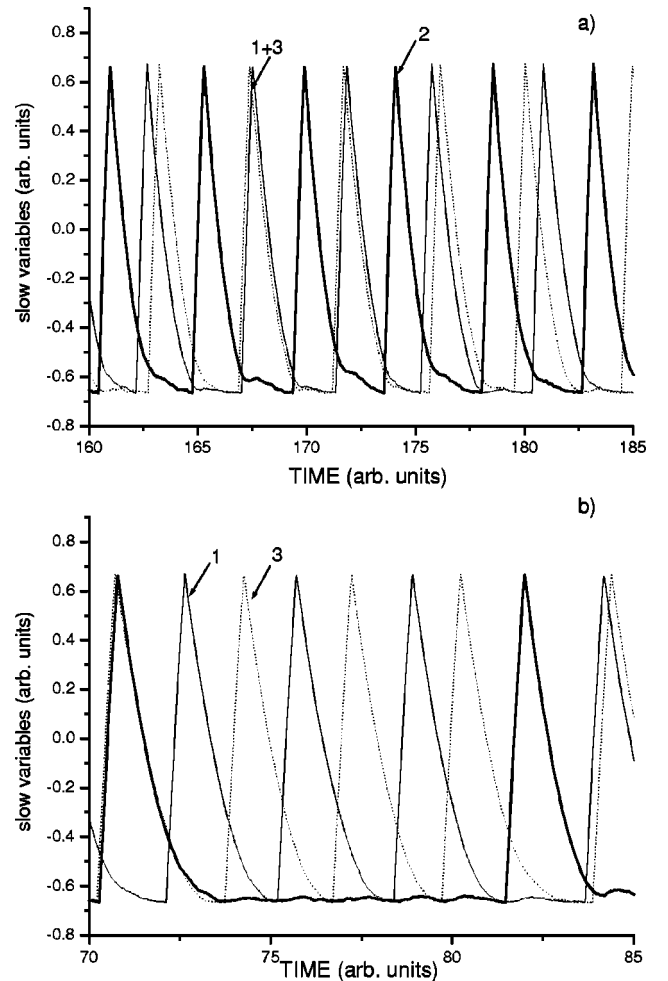


FIG. 5. The time-series intervals selected from trajectory giving ISI distribution of Fig. 4. They present the antiphase regime (a) and dynamic trap (b).

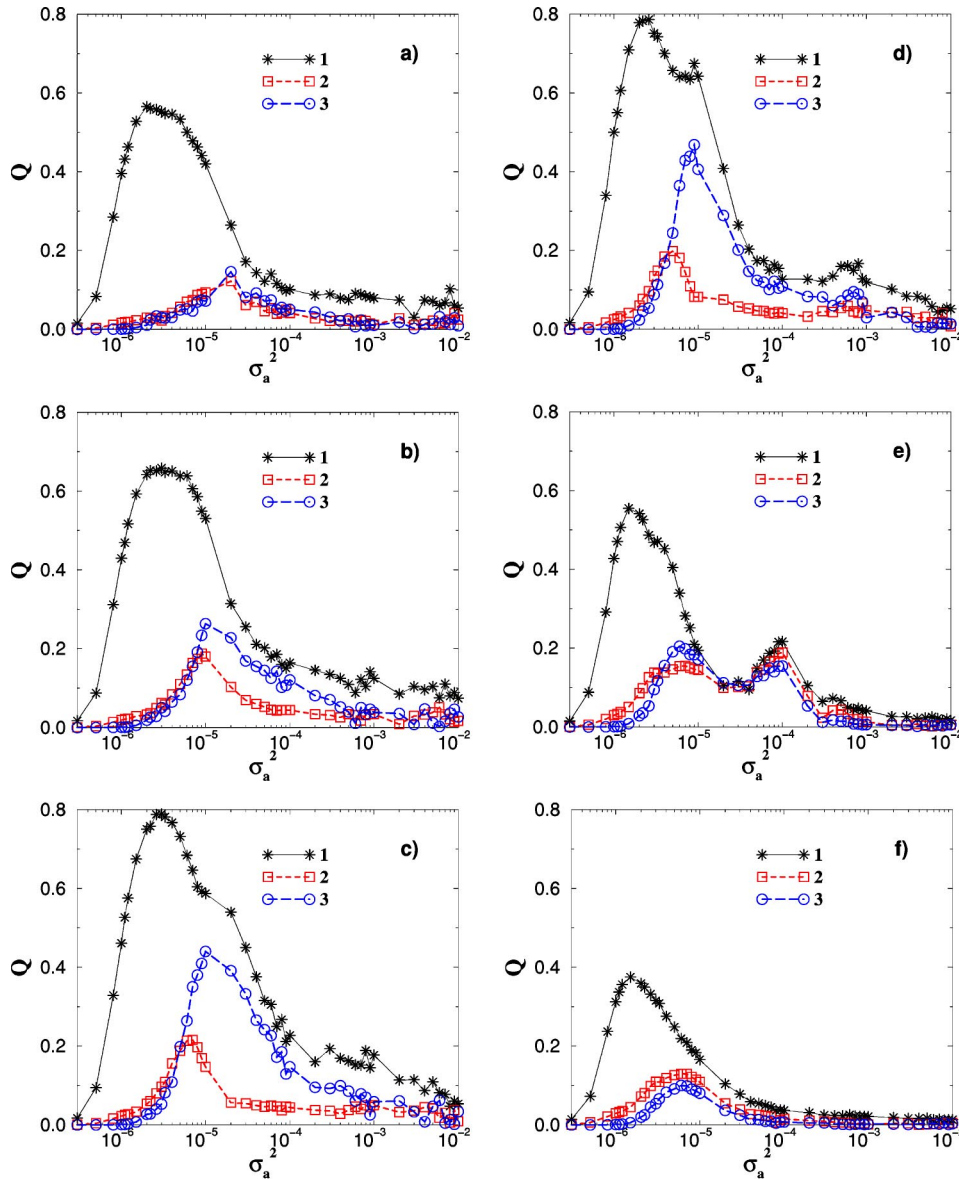


FIG. 6. The dependencies of the linear response  $Q$  for a chain of three elements [Eqs. (5)–(8)] as a function of the noise intensity for different signal periods:  $T_s = 2.8$  (a), 3.0 (b), 3.2 (c), 3.4 (d), 4.5 (e), 6.0 (f);  $A = 1.02$ ,  $\varepsilon = 0.0001$ ,  $C = 0.1$ . The signal of the amplitude  $A_{s1} = 0.01$  is applied to the first oscillator only ( $A_{s2} = 0.0$ ).

nal signal. It can be clearly seen that only two stochastic attractors are really manifested in the ISI distributions. In the dynamic trap, in which the first and the third oscillators are moved in average in antiphase, their interspike intervals are around  $T \approx 3.0$  that is very close to  $T_{exc} = 3.2$ . Since the system is symmetric, the ISI histograms of the first and third elements are identical. In this regime the ISI distribution for the middle element is very broad and polymodal. There are only infrequent realizations with very large ISI for the second element. In the antiphase regime, in which the first and the third oscillators are moving in average in-phase but in antiphase with middle oscillators, they all have the same average period about  $T_{anti} \approx 4.2$  under the given set of the other parameters. Figure 5 shows typical selected time series of the inhibitor variables  $x(t)$  of the three coupled oscillators related to the two main phase regimes antiphase motion Fig. 5(a) and of dynamic trap Fig. 5(b).

The lifetimes and periods of attractors depend on the coupling strength and noise values, which may be adjusted to

enhance (or to inhibit) the acceptance of a sinusoidal signal of a given period. To check this possibility, we calculate  $Q(\sigma_a^2)$  for different signal periods and present results which clearly reflect the specific modification of signal acceptance. We consider two cases.

*Case 1.* The harmonic signal with  $A_{s1} = 0.01$  is applied only to the first oscillator ( $A_{s2} = 0.0$ ). The corresponding dependencies of the linear response, measured for all three oscillators are shown in Fig. 6 for different periods of the external signal  $T_s$ . As discussed above, we have in this system two noise-supported attractors: a dynamical trap ( $T = 3.0-3.6$ ) and an antiphase attractor ( $T \approx 4.2$ ). These two time scales demonstrate itself also in the frequency selectivity by signal processing. If the signal period  $T_s < 3.0$  (e.g.,  $T_s = 2.8$ ) or  $T_s > 5.5$ , the behavior of  $Q_1(\sigma_a^2)$  is quite similar to that of isolated FHN and  $Q_2 \approx Q_3$  have only one peak as in the classical SR [Figs. 6(a) and 6(f)]. If the signal period is in the interval  $T_s = [3.0, 3.4]$  then  $Q_1$  sharply declines in com-

parison with Fig. 1 but  $Q_3$  dramatically increases for noise amplitudes in the interval  $[10^{-5}, 5 \times 10^{-5}]$  [Figs. 6(b)–6(d)], i.e., the signals with these periods easily penetrate through the middle element and are selectively manifested in the time series of the third oscillator. For  $T_s > 3.6$   $Q_3$  decreases again [Fig. 6(e)]. The reason for this phenomenon is the coincidence of the signal period with the average values of the interspike intervals of the stochastic dynamic trap [Fig. 5(b)]. In this regime the average ISI of the first and the third elements are equal and their interspike distributions are significantly narrower than that of the second element. Therefore, the signal manifestation in the behavior of the second oscillator is small enough for this interval of the signal period.

If the noise amplitude is larger than  $5 \times 10^{-6}$ , the average activation time of excitation is small and several stochastic attractors may occur, but the harmonic signal supports those which has a similar value of average period. The next stochastic attractor which has a noticeable lifetime (not very sensitive to noise) under stronger noise is the antiphase oscillation with the average period  $T_{anti} \approx 4.2$ . The second peak on the curves  $Q_i(\sigma_a^2)$  at  $T_s = 4.0$ – $4.5$  at about  $\sigma_a^2 \approx 2 \times 10^{-4}$  is realized for all oscillators [Fig. 6(e)], because the average ISIs are the same for all elements in this regime [Fig. 5(a)]. All the three oscillators generate a similar spike sequences and hence perform with nearly the same linear response  $Q$ . For the current model and the given set of other parameters, the distance between ISIs is not large (Fig. 4) and the selectivity of signal enhancement is limited by noise-induced transitions between these regimes.

*Case 2.* The harmonic signal is applied only to the middle element ( $A_{s1} = 0.0$  and  $A_{s2} = 0.015$ ). This example of the selective enlargement of  $Q(\sigma_a^2)$  is presented in Fig. 7(a) and 7(b). For  $T_s = 3.2$ , which corresponds to the maximal manifestation of the signal in the behavior of an isolated oscillator up to noise amplitude  $10^{-4}$  (see Fig. 1), the function  $Q_2$  dramatically decreases if the noise is around  $10^{-5}$ . Such a behavior reflects the absence of small ISIs in the time series of the second element after this noise value. The increase of signal period up to  $T_s = 4.0$  results in the appearance of the second peak on all curves  $Q_{1,2,3}(\sigma_a^2)$  and that is similar to Fig. 6(e) except for here  $Q_2$  is larger than  $Q_{1,3}$  because the signal is applied to the middle element of the chain.

Thus, the presence of a double resonant peak structure of  $Q(\sigma_a^2)$  is caused by the coexistence of two stochastic limit cycles which share the phase space due to the inhibitor exchange. In our model the distances between average periods of attractors are not large and therefore the amplitudes of the second peaks in Figs. 3, 6, and 7 are noticeable but not so pronounced as compared with the standard SR peak which, however, is almost the same for any values of the external periods.

The attractors not only differ by the periods but by the phase relations as well, which means (opens) the possibility for additional checking of our explanation by the simultaneous applications of two harmonic subthreshold signals with appropriate phase shift. For instance, the second peak on the  $Q_{1,2,3}$  has a larger height if two signals are applied to

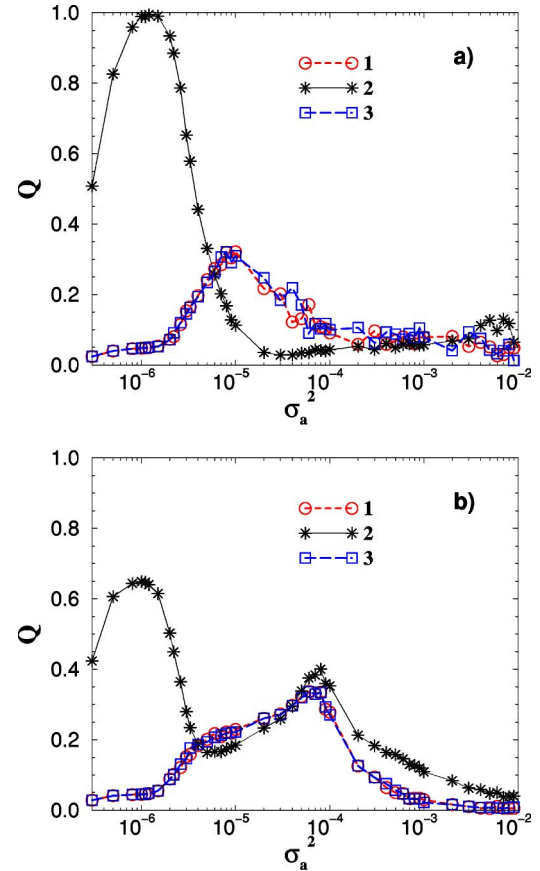


FIG. 7. The linear response  $Q$  as a function of the noise intensity for signal periods  $T_s = 3.2$  (a) and  $T_s = 4.5$  (b).  $A = 1.02$ ,  $\varepsilon = 0.0001$ ,  $C = 0.1$ . The periodic signal  $A_{s2} = 0.015$  is applied only to the middle oscillator ( $A_{s1} = 0.0$ ).

the end's oscillators in phase but  $Q_{1,2,3}$  is almost negligible if the same signals are in antiphase each other (data not shown).

The manifestation of the described effects depends not only on the stiffness but on the other model parameters too: the coupling strength and the proximity of  $A$  to the bifurcation value. Our studies have shown that the results are retained under a two-fold changing of coupling and the difference ( $A - 1.0$ ).

## VI. CONCLUSION

In summary, we have demonstrated the frequency selective response and information propagation in a noisy system which consists of inhibitory coupled excitable units and is driven by a subthreshold harmonic signal. The signals with periods from some intervals (e.g.,  $T_s = 4.0$ – $4.2$ ) may be enhanced not only for small but also for larger noise which are typically ineffective for standard SR. The signals with shorter periods (e.g.,  $T_s = 3.0$ – $3.2$ ), which are the most effective for SR, may be strongly inhibited under some noise levels in comparison with Fig. 1. The background of the selectivity is the multirhythmicity generated by the inhibitory coupling in combination with the high stiffness of elements

which provides the fast transitions between stochastic attractors.

The mechanism of this selectivity can be explained by the appearance of new resonance frequencies of the coupled system which are caused by different phase relations of the oscillators and differ from the resonance frequency of an isolated FHN. Especially the resonance frequencies of the antiphase and dynamic trap regime exhibit stable attractors in a noisy environment. By forcing one element of the network in resonance with these coupling-dependent resonance frequencies, we observe an additional resonance peak in the SR curve besides the typical bell-shaped curve of standard SR. Another interesting phenomenon, which we have explained, is the masking of the information flow in the dynamic trap regime. In this effect, the last oscillator in the row shows a much better response at the signal frequency, which was fed at the first oscillator of the row, than the middle one. We believe that the study of the frequency selective SR and the masking of information flow in an array due to inhibitory coupling can be useful for understanding of multifrequency information exchange mechanisms in neural networks. Because of the generality of these effects for diffusive coupled

activator-inhibitor oscillator arrays and not only to FHN systems, we expect that the findings can be applied also in other fields, e.g., in chemistry or biology.

It is important to note that these results contribute also to the study of fundamental synchronization phenomena [50]. In frames of this study SR can be considered as a synchronizationlike phenomenon, in which optimal noise induces phase synchronization between output and input signals. In Ref. [51] it has been shown that in deterministic systems of coupled elements, synchronization can happen through the asynchronized region. The effect, considered here, demonstrates a synchronizationlike behavior through the dynamical trap, and can be considered as a stochastic analog of this kind of a phase synchronization in deterministic systems.

#### ACKNOWLEDGMENTS

E.V. and J.K. acknowledge financial support from SFB 555 (Germany), E.U. from the International MP Research School on Biomimetic systems, A.Z. from DFG project No. 472/6-2.

- 
- [1] L. Gamaitoni, P. Hänggi, P. Jung, and F. Marchesoni, *Rev. Mod. Phys.* **70**, 223 (1998).
- [2] R. Benzi, A. Sutera, and A. Vulpiani, *J. Phys. A* **14**, L453 (1981).
- [3] P. Hänggi, *ChemPhysChem* **3**, 285 (2002).
- [4] A. Zaikin, J. Kurths, and L. Schimansky-Geier, *Phys. Rev. Lett.* **85**, 227 (2000).
- [5] F. Moss *et al.*, *Ann. N.Y. Acad. Sci.* **706**, 26 (1993).
- [6] K. Wiesenfeld *et al.*, *Phys. Rev. Lett.* **72**, 2125 (1994).
- [7] R. Rozenfeld, J.A. Freund, A. Neiman, and L. Schimansky-Geier, *Phys. Rev. E* **64**, 051107 (2001).
- [8] J.F. Lindner, B.K. Meadows, W.L. Ditto, M.E. Inchiosa, and A.R. Bulsara, *Phys. Rev. Lett.* **75**, 3 (1995).
- [9] J. Lindner *et al.*, *Phys. Rev. E* **63**, 041107 (2001).
- [10] J. Lindner *et al.*, *Phys. Rev. E* **53**, 2081 (1996).
- [11] F. Marchesoni, L. Gamaitoni, and A.R. Bulsara, *Phys. Rev. Lett.* **76**, 2609 (1996); J.M.G. Vilar and J.M. Rubí, *ibid.* **78**, 2886 (1997).
- [12] H.S. Wio, *Phys. Rev. E* **54**, R3075 (1996); S. Bouzat and H.S. Wio, *ibid.* **59**, 5142 (1999).
- [13] A. Neiman and W. Sung, *Phys. Lett. A* **223**, 341 (1996).
- [14] D.R. Chialvo, A. Longtin, and J. Müller-Gerking, *Phys. Rev. E* **55**, 1798 (1997).
- [15] B. Lindner and L. Schimansky-Geier, *Phys. Rev. E* **61**, 6103 (2000).
- [16] C. Zhou, J. Kurths, and B. Hu, *Phys. Rev. Lett.* **87**, 098101 (2001).
- [17] C. Zhou, J. Kurths, and B. Hu, *Phys. Rev. E* **67**, 030101 (2003).
- [18] H. Gang, H. Haken, and X. Fagen, *Phys. Rev. Lett.* **77**, 1925 (1996).
- [19] J.F. Lindner *et al.*, *Phys. Rev. E* **63**, 051107 (2001).
- [20] A. Longtin and D.R. Chialvo, *Phys. Rev. Lett.* **81**, 4012 (1998).
- [21] S.R. Massanés and C.J.P. Vicente, *Phys. Rev. E* **59**, 4490 (1999).
- [22] T. Kanamaru, T. Horita, and Y. Okabe, *Phys. Lett. A* **255**, 23 (1999).
- [23] H.E. Plesser and T. Geisel, *Phys. Rev. E* **59**, 7008 (1999).
- [24] A. Fuliński, *Phys. Rev. Lett.* **79**, 4926 (1997).
- [25] E.M. Izhikevich, *Neural Networks* **14**, 883 (2001).
- [26] P. Parmananda, H. Mahara, T. Amemiya, and T. Yamaguchi, *Phys. Rev. Lett.* **87**, 238302 (2001).
- [27] F. Liu, J. Wang, and W. Wang, *Phys. Rev. E* **59**, 3453 (1999).
- [28] E. Volkov, E. Ullner, A. Zaikin, and J. Kurths, *Phys. Rev. E* **68**, 026214 (2003).
- [29] B. Kerner and V. Osipov, *Usp. Fiz. Nauk* **160**, 1 (1990) [*Sov. Phys. Usp.* **33**, 679 (1990)].
- [30] D. Ruwisch, M. Bode, D. Volkov, and E.I. Volkov, *Int. J. Bifurcation Chaos Appl. Sci. Eng.* **9**, 1969 (1999).
- [31] V. Vanag *et al.*, *Nature (London)* **406**, 389 (2000).
- [32] V. Castets, E. Dulos, J. Boissonade, and P.D. Kepper, *Phys. Rev. Lett.* **64**, 2953 (1990).
- [33] H. Meinhardt, *Models of Biological Pattern Formation* (Academic, New York, 1982).
- [34] I. Lengyel and I. Epstein, *Science* **251**, 650 (1990).
- [35] E.I. Volkov and M.N. Stolyarov, *Phys. Lett. A* **159**, 61 (1991).
- [36] E.I. Volkov and M.N. Stolyarov, *Biol. Cybern.* **71**, 451 (1994).
- [37] V.V. Astakhov, B.P. Bezruchko, E.N. Erastova, and E.P. Seleznev, *J. Tekh. Fiz.* **60**, 19 (1990) [*Sov. J. Tech. Phys.* **35**, 1122 (1990)].
- [38] A. Sherman and J. Rinzel, *Proc. Natl. Acad. Sci. U.S.A.* **89**, 2471 (1992).
- [39] G.S. Cymbalyuk, E.V. Nikolaev, and R.M. Borisjuk, *Biol. Cybern.* **71**, 153 (1994).
- [40] D. Postnov, S.K. Han, and H. Kook, *Phys. Rev. E* **60**, 2799 (1999).
- [41] J. Keener and J. Snyder, *Mathematical Physiology* (Springer, New York, 1998).

- [42] A.S. Mikhailov, *Foundations of Synergetics*, 2nd ed. (Springer, Berlin, 1994).
- [43] J. García-Ojalvo and J.M. Sancho, *Noise in Spatially Extended Systems* (Springer, New York, 1999).
- [44] E. Volkov, M. Stolyarov, A. Zaikin, and J. Kurths, Phys. Rev. E **67**, 066202 (2003).
- [45] L. Alfonsi, L. Gammaitoni, S. Santucci, and A.R. Bulsara, Phys. Rev. E **62**, 299 (2000).
- [46] Y. Horikawa, Phys. Rev. E **64**, 031905 (2001).
- [47] E.I. Volkov and M.N. Stolyarov, J. Biol. Systems **3**, 63 (1995).
- [48] E.I. Volkov and D.V. Volkov, Phys. Rev. E **65**, 046232 (2002).
- [49] D.E. Postnov, O.V. Sosnovtseva, S.K. Han, and W.S. Kim, Phys. Rev. E **66**, 016205 (2002).
- [50] A. Pikovsky, M. Rosenblum, and J. Kurths, *Synchronization. A Universal Concept in Nonlinear Sciences* (Cambridge University Press, Cambridge, 2001).
- [51] Z. Zheng, G. Hu, and B. Hu, Phys. Rev. Lett. **81**, 5318 (1998).